UNIVERSITAT DE BARCELONA

Effects of some mixing flows on diffusion-controlled reactions

Efectes d'alguns fluxes de mescla en reaccions controlades per difusió

Ramon Reigada Sanz

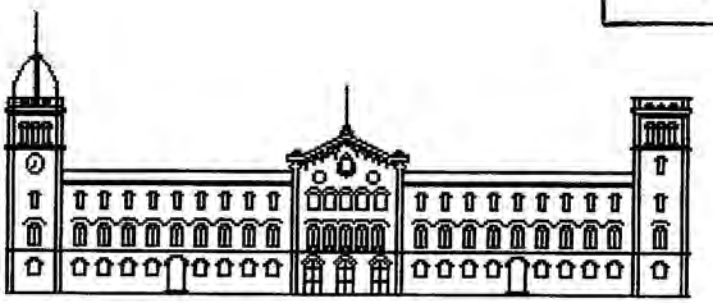

UNIVERSITAT DE BARCELONA

Departament de Química-Física

EFFECTS OF SOME MIXING FLOWS ON DIFFUSION-CONTROLLED REACTIONS.

EFECTES D'ALGUNS FLUXES DE MESCLA EN REACCIONS CONTROLADES PER DIFUSIO.

NOVEMBRE 1997

Memòria de la Tesi presentada per Ramon Reigada Sanz per optar al grau de Doctor en Ciències Químiques

FRANCESC SAGUÉS MESTRE, Professor Titular del Departament de Química-Física de la Universitat de Barcelona,

i

JOSE MARIA SANCHO HERRERO, Catedràtic del departament d'Estructura i Constituents de la Matèria de la Universitat de Barcelona,

CERTIFIQUEN: que aquesta Memòria titulada 'Efecte d'alguns Fluxes de Mescla en Reaccions Controlades per Difusió. ', presentada per Ramon Reigada Sanz per optar al grau de Doctor en Ciències Químiques corresponent al programa de doctorat de Química Fonamental: Química-Física (bieni 1993-95) s'ha realitzat sota la seva direcció.

Francesc Sagués Mestre

José María Sancho Herrero

Membres del Tribunal

President: Dr. M. Arturo López Quintela
Catedràtic d'Universitat
Departamento de Química Física
Universidade de Santiago de Compostela.

Vocals: Dr. Igor Sokolov
Professor Assistent
Institut für Theoretische Polymerphysik
Universität von Freiburg.

Dr. Jaume Masoliver García
Professor Titular
Departament de Física Fonamental
Universitat de Barcelona.

Dra. Ana Lacasta Palacio
Professora Associada
Departament de Física Aplicada
Universitat Politècnica de Catalunya.

Secretàri: Dr. Francesc Mas Pujadas
Professor Titular
Departament de Química Física
Universitat de Barcelona.

Suplents: Dr. Antonio Aguilar Navarro
Catedràtic d'Universitat
Departament de Química Física
Universitat de Barcelona.

Dr. Eudald Vilaseca Font
Professor Titular
Departament de Química Física
Universitat de Barcelona.

-AGRAIMENTS-

En aquest full voldria deixar constància del meu agraïment a totes aquelles persones que han contribuit d'una forma o altra a la realització d'aquesta Tesi.

En primer lloc als meus directors, els professors Francesc Sagués i José María Sancho que han guiat amb decisió i saviesa tot el treball realitzat durants aquests anys. Especialment voldria destacar la generositat i l'enorme esforç amb la que en Francesc Sagués s'ha dedicat a la meva formació com a investigador. Professionalment, tot el que soc li dec a ell.

Com a importantíssima he de calificar l'ajuda rebuda durant els últims dos anys per part de l'Igor Sokolov; la seva col.laboració va suposar l'empenta definitiva que el meu treball requeria. Agrair també a tots els components del Theoretische Polymerphysik Institut de Freiburg, comandat per l'Alex Blumen, per la seva hospitalitat i ajuda durant les múltiples estades que he realitzat en aquesta bonica ciutat alemana.

També he d'agrair l'ajuda científica rebuda en diversos aspectes per companys tant del Departament de Química-Física (Agustí Careta, Jordi Mach, Heiner Lehr,...) com del Departament d'Estructura i Constituents de la Matèria (Ana Lacasta, Arturo Martí,...).

En general a tots els companys del Departament de Química-Física. Als professors que he tingut durant la carrera. Als companys de grup com en Josep Claret, la Rosa Albalat, en Francesc Mas, l'Eudald Vilaseca i en especial amb els que comparteixo despatx: el Dani, la Marta, el Heiner i la Rosa. 'A pesar' de que siguin d'altres grups, també he d'agrair-los les estones d'oci i conversa, en absolut científica, a la Mercè, la Maite i la Pilar.

En cap cas podria oblidar-me dels meus companys de promoció, i especialment aquells amb els quals el contacte ha sigut més intens inclús un cop acabada la Llicenciatura: el Sergi Vizoso, el Luis Rodriguez, el Jesus Hijazo i el Marc Planas. Les estones i anècdotes viscudes amb ells des de que vam començar el quart curs de carrera fins el moment es mereixen un agraïment especial. A tots quatre els hi desitjo un futur ple de felicitat.

Agrair també l'ajuda en forma de Beca per la Formació d'Investigadors per part de la CIRIT.

Abans d'acabar m'agradaria fer un petit recordatori per alguns ex-companys del Departament que malgrat treballar dura i eficientment han hagut de seguir els seus destins professionals fora de la Universitat. L'Agustí Careta, el Pedro Pablo Trigueros, la Laura Lopez, el Jordi Mach, el Jordi Casanovas i tants d'altres ens han de recordar forçosament que la nostra Universitat no és ni molt menys perfecta i que encara queden moltes coses per les que tots hem de lluitar.

A tots els amics i familiars que durant tot aquest temps m'han demostrat una estima i un recolçament importantíssims. En especial als meus pares, sense l'esforç dels quals jo no hauria pogut tenir la formació acadèmica i humana que m'han permès escriure aquesta Tesi.

Dedico aquesta Tesi als meus pares i a les meves dues germanes.

Efectes d'alguns Fluxes de Mescla en Reaccions Controlades per Difusió

1-Introducció:

Aquesta Tesi està dividida en dues parts ben diferenciades. Per un costat, l'estudi detallat d'un sistema de reacció-difusió, en concret pel sistema binari reactiu A+B->0, on el control cinètic del mateix recau en el procés difusiu i les inhomogeneïtats locals inicials. Per un altre, la implementació en aquest mateix sistema d'un segon procés de transport en forma d'un flux advectiu que donarà lloc a l'aparició de diversos comportaments cinètics i a formes peculiars d'autorganització espacio-temporal dels reactius.

En aquesta primera secció del resum pretenem donar una idea global de cadascuna de les dues temàtiques a fi de contextualitzar el treball i continguts de la present Tesi.

1.1-Fluctuacions Espacials en Reaccions Controlades per Difusió:

Ens proposem abordar l'estudi d'un procés reactiu extremadament simple en el seu plantejament però que dóna com a resultat tot un seguit de comportaments que podriem qualificar d'anòmals o no clàssics. El sistema considerat està format per dues espècies, que anomenarem A i B, inicialment distribuides estequiomètricament de manera aleatòria i que reaccionen segons el procés binari A+B->0. De fet, el '0' significa que no estem interessats en el o els productes de reacció, considerant doncs aquelles situacions on aquests no intervinguin en la reacció ni en la dinàmica global del sistema. Queda doncs, descartada la reversibilitat en el procés reactiu, si be en alguns treballs aquesta possibilitat és contemplada obtenint resultats qualitativament similars a aquells a que ens referirem en tota aquesta Tesi.

El tractament que clàssicament es dóna al problema es fonamenta en la hipòtesi d'homogeneïtat total en el sistema reactiu, la qual cosa simplifica la resolució de les equacions cinètiques de forma evident. Segons aquest plantejament el comportament temporal ve descrit per l'equació $dc_A/dt=dc_B/dt=-Kc_Ac_B$ on K seria la constant cinètica global i $c_{A,B}$ les concentracions globals respectives dels reactius. Integrant aquesta simple equació diferencial obtenim l'anomenat comportament cinètic clàssic: $1/c(t)=(1/c(0))+Kt$, llei que a temps grans esdevindrà $c(t)\sim(Kt)^{-1}$. En condicions estequiomètriques s'enten que $c(t)\equiv c_A(t)=c_B(t)$. Durant el

transcurs de la reacció, el sistema aniria disminuint la seva concentració de forma uniforme a tots els punts del mateix, conservant l'homogeneïtat espacial. El control cinètic, en aquest cas, recau exclusivament en el procés reactiu.

Abans de seguir, cal fer un petit comentari sobre el que hem qualificat com control per part del procés reactiu. Ens referim d'aquesta manera a aquella situació prototípica en que el sistema es suposa que conserva estrictament la seva homogeneïtat espacial, la qual cosa justifica de fet, el poder-se referir a una constant del procés reactiu denotada anteriorment com a K. La majoria de vegades identificarem aquesta constant amb la pròpiament dita constant de reacció química, entenent que el procés reactiu vindrà descrit fonamentalment pel procés de col.lisió molecular (llei d'Arrhenius). Altrament podem considerar situacions en que el control per part del procés reactiu vingui determinat pel procés d'autodifusió molecular local dels reactius previ a l'etapa de col.lisió, aquesta darrera suposada infinitament ràpida. En aquest cas i malgrat considerar que el sistema a gran escala continua essent homogeni espacialment, parlarem d'un control reactiu per difusió. De fet, i seguint la teoria de Smoluchowski [Smo17, Osh94] referida a aquesta darrera situació, només en el cas tridimensional i de forma asimptòtica es pot considerar aquesta constant com a independent del temps i per tant només en aquest cas el control reactiu del procés es traduirà en la llei cinètica clàssica $c(t) \sim (Kt)^{-1}$. Fins i tot en aquesta darrera situació hi podriem englobar casos de control mixte, és a dir per col.lisió i difusió molecular.

El plantejament clàssic anterior, malgrat ser el que de forma estàndard s'accepta com a vàlid, no deixa de ser necessàriament idealitzat. En efecte, el sistema pot estar incialment distribuit de forma homogènia en el sentit

global, però a escales més petites és ben probable que poguem observar inhomogeneïtats, és a dir, excessos de la concentració d'una espècie respecte de l'altre distribuides aleatòriament. De quina manera afecta això al tractament anterior?. Si considerem que el procés difusiu és capaç de mesclar aquestes fluctuacions de forma eficient durant el transcurs de la reacció podrem acceptar com a vàlida la resolució clàssica comentada anteriorment, però que succeix si no és així?. Es obvi que aquesta qüestió és especialment rellevant en processos controlats per difusió de forma que per a aquests darrers casos tot el tractament clàssic pot quedar invalidat desde la seva mateixa hipòtesi inicial.

La dinàmica d'aquests sistemes, si es vol ser estricte, vindrà determinada pels dos processos que hi tenen lloc: la reacció química i la difusió. El primer estarà quantitativament descrit per la constant de reacció química, mentre que el segon ho serà pel coeficient de difusió molecular. L'existència de les inevitables inhomogeneïtats inicials tindrà una importància cabdal en el desenvolupament futur del sistema en el cas de que el procés de transport, en aquest cas el de difusió, sigui incapaç d'anular-les abans que el procés reactiu les amplifiqui. D'una forma esquemàtica i suposant una constant de reacció infinita, ens podem imaginar aquesta situació de la següent forma. Fixant-nos en una zona molt petita del nostre sistema just a l'inici de la reacció, ens adonarem que ràpidament, i abans de que les partícules puguin entrar o sortir significativament d'aquesta zona per difusió, les partícules en excés hauran eliminat totalment a les de l'altre espècie. Ha començat en aquest moment la formació de incipients dominis de cadascuna de les dues espècies reactives que anomenarem 'clusters'. Si la reacció és suficientment ràpida com per a que qualsevol partícula d'una espècie reaccioni, i per tant desapareixi, al intentar entrar en un d'aquests dominis de l'espècie contrària, cadascun dels 'clusters' estarà destinat a

créixer en tamany de forma progressiva. Els dominis d'una mateixa espècie cooperaran per aniquilar els de l'altra, de manera que cada cop tindrem menys 'clusters' però més grans. Aquest fenomen portarà a la segregació del sistema en forma de regions en les quals només un tipus de partícula estarà present.

Es evident doncs que si la difusió és poc eficient, i això és lògic pensar també que dependrà de la dimensionalitat del sistema, la reacció quedarà confinada a les zones de frontera, també anomenades zones de reacció, entre els diferents dominis i per tant és d'esperar un alentiment de la cinètica respecte al tractament clàssic on la reacció tenia lloc en gairebé tot el sistema. A aquest nou comportament el qualificarem de regim dominat per fluctuacions espacials en reaccions controlades per difusió. En aquesta Tesi, seguint la majoria de treballs sobre el tema, s'empra majoritàriament l'expressió de control difusiu ('diffusion-controlled'), en el que podria ser un abús de llenguatge tenint en compte com s'ha dit abans que no ens referirem precissament a un control tipus Smoluchowski al qual hom s'hi refereix com a control per difusió. En altres treballs i fins a cert punt d'una manera més específica, s'utilitza la terminologia de cinètica dominada per fluctuacions ('fluctuation-dominated kinetics'). En qualsevol cas, i si no es diu el contrari, quan parlem de control difusiu o control per les fluctuacions inicials ens referirem a l'efecte de les inhomogeneïtats inicials en sistemes de reacció-difusió on la difusió és l'etapa limitant.

Un simple argument d'escala ens permetrà extreure la nova llei cinètica que resultarà del procés de segregació esmentat anteriorment. Si considerem que la distribució inicial d'ambdós reactants correspon a una disposició aleatòria de les partícules en el sistema, per exemple la típica distribució poissoniana, és ben conegut que l'excés inicial de partícules d'un tipus respecte a l'altre (n_{ex}) en un volum V serà de l'ordre de l'arrel

quadrada del nombre total de partícules dins aquest volum, $n_{ex} \sim \sqrt{c(0)V}$, on c(0) és la concentració global inicial. Si considerem que el nostre sistema té dimensionalitat d, podrem escriure el volum V com l_D^d, essent l_D el tamany lineal d'aquest volum. Tenint en compte que una partícula comportant-se difusivament recorre un espai lineal de l'ordre de $l_D \sim \sqrt{Dt}$ i que per tant es pot considerar que totes les inhomogeneïtats a una escala inferior de l_D desapareixeran, mentre que les d'escala superior sobreviuran, es pot escriure que $n_{ex}(t) \sim c(0)^{1/2}(Dt)^{d/4}$. Si dividim aquesta quantitat pel volum i considerem que el sistema està totalment segregat ($c(t)=c_{ex}(t)$), obtenim la següent estimació per a l'evolució temporal de la concentració d'ambdós espècies: $c(t) \sim c(0)^{1/2}(Dt)^{-d/4}$. Observem clarament que per d<4 el ritme del decaiment de la concentració és més lent que pel cas clàssic. Aquests arguments d'escala van ser primerament reportats a la literatura per Ovchinnikov i Zeldovich pel cas tridimensional [Ovc78] per després extendre's a sistemes d-dimensionals [Tou83, Kan84].

Cal destacar que en tots els arguments anteriors ens hem basat en un fet particular: el procés difusiu no és el suficientment ràpid (com a mínim respecte al procés reactiu) com per a mesclar les inhomogeneïtats inicials i impedir que aquestes formin dominis que creixeran i segregaran el sistema, alentint el ritme de reacció. L'exponent -d/4 ens diu també, que l'efecte del control difusiu sobre el ritme de reacció serà més important en dimensions petites, com s'intuia anteriorment, on la difusió tindrà topològicament més problemes per a mesclar els reactants. De fet, en tot allò que segueix estudiarem les anòmalies cinètiques en sistemes controlats per difusió per d<4 i en condicions d'inhomogeneïtats locals inicials.

De totes formes, s'ha de tenir present que el règim difusiu no s'aconsegueix d'immediat. Ambdós comportaments, el clàssic i el controlat

per les fluctuacions inicials, representen dos comportaments extrems entre els quals evoluciona el nostre sistema. A temps inicials, el sistema seguirà un comportament cinètic pràcticament clàssic degut a la reacció dels parells propers d'espècies diferents, mentre que a mida que la reacció vagi avançant la ineficàcia de la difusió anirà segregant el sistema. L'evidència cinètica d'aquest canvi la trobarem en observar l'exponent α, $c \sim t^{\alpha}$, des del valor -1 al $-d/4$ que s'assolirà de forma asimptòtica per a temps suficientment grans. El pas entre el control per reacció i el control per difusió-fluctuacions dependrà exclussivament dels valors dels parametres de reacció i difusió.

La influència que tenen les fluctuacions inicials en el futur desenvolupament de la cinètica en aquest tipus de sistemes ha obert les portes a la comprensió de gran quantitat de fenomens físics i químics en els quals l'ineficiència del procés difusiu en determina el comportament. No només experiments en cinètica química [Pri97], sino també fenomens de la física de matèria condensada, de fotoconductivitat i inclús estudis sobre el comportament de monopols superpesants en una primitiva etapa de la formació de l'univers, tenen la seva explicació en el comportament de processos reactius controlats per difusió sota l'efecte de fluctuacions inicials.

A part del sistema A+B->0 existeixen multitut d'altres sistemes reactius que també mostren de diferentes maneres un comportament cinètic peculiar sota control difusiu. Podriem enumerar per exemple, els sistemes A+A->0, A+B->B, també amb les versions de B immòbil ('trapping problem') o A immòbil ('target problem'), A+B↔C, etc... Dins el mateix problema A+B->0 o les variants recentment esmentades també hi ha una gran varietat de possibilitats a estudiar, com per exemple al considerar situacions no estequiomètriques, disposicions inicials fractals, mobilitats diferents per les dues espècies, sistemes amb fonts de reactius, etc... Algunes d'elles han estat

tractades en aquesta Tesi, i les que no, com a mínim estan referenciades per si n'interessa el seu estudi [Zum85, Sok88, San96].

Un aspecte d'enorme interès en aquest tipus de sistemes, a banda del cinètic ja esmentat, consisteix en l'estudi dels 'clusters' en que s'organitzen els reactius. Donada la naturalesa gausiana del procés difusiu, que de fet és el que governa el nostre sistema, es dedueix fàcilment que els 'clusters' de cadascuna de les espècies creixeran amb $\sqrt{Dt}$. També s'analitzen en aquest treball altres variables estructurals com els tamanys de zones de reacció, les funcions de correlació espacial per reactius o de les seves zones de reacció, les distribucions de probabilitat de tamany de 'cluster', etc... Aquests estudis morfològics van ser iniciats per models de tipus discret o també anomenats Monte Carlo [Ley91], on els reactius estan simbolitzats per partícules, i en els últims temps per models continus de reacció-difusió [Sok86], on es treballa amb variables continues que representen les concentracions de reactius.

La inclusió de models continus en aquest tipus de problema ha suposat un enorme avanç en l'estudi dels processos controlats per difusió, i en concret pel nostre sistema binari. Desde el punt de vista numèric, el model continu ens permet extreure resultats de més qualitat en menys temps de càlcul. Pel que fa a l'exploració analítica, i en particular pel cas on les mobilitats d'ambdues espècies són la mateixa, les equacions deterministes de camp mig, reservant el paper aleatori a la distribució inicial dels reactius, permeten obtenir expressions sobre variables tant cinètiques com morfològiques que amb models discrets serian inabastables. A tot això s'ha d'afegir la dificultat que tenen els models de partícules per a descriure matemàticament un 'cluster', sobretot en dues i tres dimensions.

1.2-Processos de Mescla:

La mescla de substancies és un procés molt extès tant en la vida quotidiana com en aplicacions industrials. Accions de la vida normal com ensucrar un cafè, passant per complexos processos industrials de tipus químic, petroquímic i farmacèutic necessiten normalment posar en contacte dos o més reactius mitjançant diferents mecanismes de mescla. L'estudi d'aquests processos permet també, la comprensió de multitut de fenomens químics, físics o biològics que tenen lloc sota la influència de fluxes hidrodinàmics.

En el nostre cas particular l'interès pels processos de mescla resideix en la possibilitat que ens proporcionen de prevenir el procés de segregació a que ens hem referit anteriorment i que té lloc en els sistemes de tipus A+B->0 controlats per difusió. La idea consisteix en afegir un procés d'advecció en forma de flux hidrodinàmic al nostre problema de reacció-difusió, de forma que aquest segon fenomen de transport ajudi a homogenitzar el sistema. Per un costat ens interessa estudiar les diferents lleis cinètiques i organitzacións espacials que en resulten, i per un altre aquest estudi pot també interpretar-se com adreçat a comprobar el grau d'eficàcia de diferents mecanismes de mescla, basant-nos precisament en el comportament d'aquest sistema binari tan simple i alhora tan sensible a la distribució espacial dels reactius.

Es ben sabut que els fluids poden comportar-se de dues formes extremes. Per un costat tenim els fluids laminars que flueixen de forma suau i regular [Mon75, Sok91a], i per un altre, els fluids turbulents en els quals la velocitat, la pressió i altres magnituts canvien ràpidament en l'espai i en el temps de forma pràcticament caòtica [Bat70, Mon75].

O. Reynolds [Rey1894] va estudiar la transició entre fluids laminars i turbulents, destacant la importància de l'anomenat nombre de Reynolds, $Re=UL/\nu$, on L i U representen la longitut característica i la velocitat del flux respectivament, i ν és la viscositat cinemàtica. Aquest paràmetre correspon a una relació dinàmica entre les forces inercials, que transfereixen energia de escales grans a escales petites formant les inhomogeneïtats característiques de la turbulència, i les forces viscoses que, mitjançant la disipació de l'energia, tendeixen a l'homogenització del sistema. Per valors grans de Re, el flux es comportarà de forma turbulenta, mentre que per valors petits ho farà de manera laminar.

Un dels principals objectius dels mecanismes d'advecció és que siguin realment eficients, és a dir, que mesclin el màxim possible. Un mecanisme de mescla eficient estalviarà temps i energia, però la clau del problema no està tant en la intensitat del flux sino en la forma en que aquest mescla. El concepte de mescla eficient està íntimament relacionat amb el de caos, i és per això que l'estudi de la formació de zones caòtiques en un sistema agitat està molt lligada a l'anàlisi de fluxes de mescla eficient. Les característiques caòtiques d'un flux de mescla s'originen en els mecanismes elementals d'estirament i plegament ('stretching and folding') del fluid [Ott88, Sok91a, Ott92], constituint un procés global que aconsegueix ampliar indefinidament la zona de contacte entre els diferents components del fluid. Serà impossible obtenir zones caòtiques amb fluxes estacionaris bidimensionals, ja que aquests estaran caracteritzats per línies de flux tancades, seguint les quals el fluid es mourà indefinidament sense mesclar, com a mínim de forma indefinida que és el que es preten. Una condició necessària per a aconseguir el concepte d'estirament i plegament és el creuament de línies de flux a temps arbitraris, i això es pot aconseguir, per exemple, amb fluxes bidimensionals adequadament periòdics en el temps.

A banda dels models de flux o de mescla que volguem imaginar, experimentalment hi ha una gran quantitat de mecanismes d'advecció que mostren comportament caòtic. De totes formes també és ampliament reconegut que qualsevol d'aquests processos de mescla, per molt eficient que sigui, no aconseguirà extendre el caos a tot el sistema [Ott88, Ott92]. En general, zones caòtiques de mescla eficient coexistiran amb regions de mescla molt poc eficient, també anomenades illes coherents del flux. El fluid dins d'aquestes illes mai podrà escapar-ne i el de l'exterior mai hi podrà entrar. La ruptura d'aquestes illes significa un pas endavant en la consecució d'una mescla perfecta [Lam96] i el seu estudi és, per tant, de gran importància pel món de la indústria química.

S'han implementat multitut de models destinats a simular processos de mescla, i en concret per simular fluxes turbulents. Com hem comentat amb anterioritat, un flux turbulent es pot definir com aquell que es comporta de manera no determinista i les magnituts del qual, com la velocitat, varien en el temps i en l'espai de forma desordenada. En un primer intent es podria pensar en modelar aquests fluxes directament mitjançant l'equació de Navier-Stokes però en la pràctica aquest procediment resulta extremadament complicat. Una primera alternativa consisteix en modelar-los en forma de fluxes estocàstics amb una sèrie de propietats estadístiques determinades. Aquestes propietats seran l'espectre d'energies, la intensitat i les escales de temps i longitut. D'aquest plantejament se'n diu 'cinemàtic' o 'sintètic' i un exemple específic que de fet s'utilitzarà en tot el que segueix el trobem a [Car93b, Mar97]. Una segona alternativa seguida per J. Klafter consisteix en combinar una visió lagrangiana del problema amb l'implementació dels anomenats 'Levy flights' [Kla96].

En el nostre treball s'estudiaran dos tipus de flux. Un de tipus determinista i estacionari que ens demostrarà la importància que té la topologia de les línies de flux a l'hora de formar els 'clusters' en que es segrega el nostre sistema. El segon tipus correspon a un fluxe turbulent modelat de forma sintètica i que a pesar del seu caràcter espacio-temporal aleatori, no aconseguirà mesclar el nostre sistema de forma indefinida. De fet comprovem com els sistemes controlats per difusió constituiran una dura prova de cara a testar l'eficiència de mecanismes de mescla, ja que tenen una tendència indefinida a segregar-se.

2-Continguts de la Tesi:

En aquesta secció resumirem els continguts generals del treball desenvolupat a la Tesi mitjançant la presentació de la metodologia emprada i dels resultats més significatius. Cadascuna de les següents subseccions correspondrà a un capitol de la Tesi.

2.1-La Reacció A+B->0 Controlada per Difusió [Rei96a]:

El nostre primer objectiu en aquest treball consisteix en l'estudi exhaustiu de la reacció A+B->0 sota condicions de control difusiu, que com hem dit anteriorment són aquelles condicions en les que sota els efectes d'inhomogeneïtats inicials es troben comportaments cinètics i d'organització dels reactius diferents als clàssics.

L'estudi d'aquesta reacció s'ha subdividit en tres parts ben diferenciades. En primer lloc, la presentació del model amb el qual desenvolupem tots els càlculs, tant els numèrics com els analítics. En segon lloc, una exploració extensa de les lleis cinètiques anòmales que aquests sistemes mostren, en funció de la seva dimensionalitat, dels coeficients de difusió i de les condicions inicials dels reactius. Per últim, realitzarem un estudi morfològic de com s'organitzen en l'espai les diferents espècies en aquest tipus de reaccions. En tot moment es consideraran condicions estequiomètriques ($c_A(0)=c_B(0)$).

2.1.a-Model:

El punt de partida inicial de tot el nostre treball consisteix en l'adopció d'un parell d'equacions de reacció-difusió apropiades al sistema reactiu considerat. Treballarem amb un model continu, amb concentracions i no amb partícules, seguint l'aproximació de camp mig pel terme reactiu. Les equacions corresponents són:

$$\frac{\partial c_A(\vec{r},t)}{\partial t}=D_A\nabla^2 c_A(\vec{r},t)-Kc_A(\vec{r},t)c_B(\vec{r},t) \qquad (0\text{–}1)$$

i

$$\frac{\partial c_B(\vec{r},t)}{\partial t}=D_B\nabla^2 c_B(\vec{r},t)-Kc_A(\vec{r},t)c_B(\vec{r},t) \qquad (0\text{–}2)$$

on $D_A=D_B$ són els coeficients de difusió, K la constant local de reacció i c_i les concentracions locals en cada moment.

El primer punt que estem obligats a resoldre abans de continuar endavant és el referent a considerar K com a constant en el sentit temporal

de la paraula, en els termes quadràtics de les equacions anteriors. La teoria de Smoluchowski [Smo17] argumenta que la definció d'aquesta K s'ha de fer en principi en termes de K(t). Mitjançant la solució del problema per a una partícula dins un medi continu de l'espècie contrària arriba a la conclusió de que asimptòticament K és una constant únicament per tres dimensions, mentre que no es pot considerar així per una i dues dimensions.

De totes formes, la consideració de K com constant no serà excessiu problema degut a que treballem en un contexte on el control del procés recau en mans de la difusió a gran escala, degut a la formació de 'clusters', i no del procés de col.lisió pur ni del transport difusiu a nivell local [Ric85, Zum91, Kot96]. La segregació del sistema degut a les inhomogeneïtats inicials i al control difusiu controlaran la cinètica del sistema en major mesura que el procés de difusió local. En altres paraules, si utilitzéssim per una i dues dimensions les expressions de K(t) de la teoria de Smoluchowski sense tenir en compte els termes difusius a les Eqs. 0-1 i 0-2, obtindriem lleis cinètiques més ràpides que les que trobem amb el control difusiu. Per tant, i per la majoria de resultats d'aquesta Tesi, considerarem vàlida l'aproximació de K constant.

La utilització d'aquest model continu i de camp mig ens permetrà un estudi, tant analític com numèric, molt més extens que el que ens permetien fins el moment els models discrets o de partícules. Analíticament, i sobretot pel cas on els coeficients de difusió són iguals per ambdues espècies, podrem arribar a extreure fàcilment les lleis cinètiques i inclús expressions per la distribució de tamanys de 'cluster' i funcions de correlació. Numèricament, l'avanç tant en qualitat com en quantitat de resultats és més que evident. Podem obtenir millors resultats en menys temps de càlcul.

El cas on $D_A=D_B$ permet la descripció del sistema en funció d'aquestes dues noves equacions:

$$\frac{\partial q(\vec{r},t)}{\partial t} = D\nabla^2 q(\vec{r},t) \qquad (0\text{–}3)$$

i

$$\frac{\partial s(\vec{r},t)}{\partial t} = D\nabla^2 s(\vec{r},t) - K(s^2(\vec{r},t) - q^2(\vec{r},t)) \qquad (0\text{–}4)$$

on hem definit $q(\vec{r},t)$ com la funció semidiferència de les concentracions i $s(\vec{r},t)$ com la funció semisuma de les concentracions.

Amb aquestes dues noves equacions estem en disposició d'explorar analíticament el problema amb relativa facilitat. En primer lloc, mitjançant la funció de Green corresponent resolem l'equació (0-3) en funció de les condicions inicials ($q(\vec{r},0)$). La condició d'homogeneïtat estadística, la naturalesa gaussiana de la funció de Green solució de l'Eq. (0-3) i la hipòtesi de reacció molt ràpida ($K\to\infty$) ens permeten arribar a la següent relació a temps grans:

$$\langle s(t)\rangle = c(t) \sim \sqrt{\langle q^2(t)\rangle} \qquad (0\text{–}5)$$

Descrivim la disposició inicial d'A i B segons la funció d'estructura, $\Gamma(k)$, definida com la transformada de Fourier de la funció de correlació de la funció diferència a t=0. En el cas en que poguem escriure aquesta funció d'estructura en la forma $\Gamma(k)\sim |k|^{\beta}$, i seguint tot el procés de resolució de l'Eq. (0-3) trobem que

$$c(t) \sim t^{-(d+\beta)/4} \qquad (0\text{–}6)$$

Pel cas on la distribució inicial és totalment aleatòria, per exemple condicions inicials poissonianes, $\beta=0$, i per tant

$$c(t) \sim t^{-d/4} \quad (0\text{–}7)$$

que representa, com ja haviem previst, un alentiment del ritme de la reacció respecte a allò que clàssicament es prediu. Aquesta llei és l'anomenada llei cinètica de Zeldovich i cal recordar que és vàlida únicament a temps grans i sota condicions de reacció molt ràpida.

Pel que fa a la resolució numèrica, treballem directament amb la discretització de les Eqs. (0-1 i 0-2) utilitzant un model explícit de primer ordre en el temps, derivades centrades pel terme laplacià i condicions de contorn periòdiques.

Abans de l'explotació numèrica d'aquest model es treballa per a la correcta assignació dels valors dels increments de temps i espai utilitzats en la discretització per tal d'assegurar la convergència del mètode. S'escolleixen també els valors adequats de les variables D i K per tal d'observar els règims anòmals en el rang de temps idoni. En general treballarem amb valors grans per K i petits per D, si be els valors concrets dependran de la dimensionalitat del sistema.

2.1.b-Lleis Cinètiques:

En termes generals, realitzem tres tipus de simulació numèrica: en funció de la dimensionalitat del sistema, variant els coeficients de difusió i experimentant amb diferents condicions inicials.

Pel que fa a la primera sèrie de simulacions, fixem els coeficients de difusió al mateix valor per ambdues espècies, distribuim inicialment els reactants de forma aleatòria i simulem en d=1, 2 i 3. En els tres casos reproduim asimptòticament la llei cinètica de Zeldovich i el seu exponent -d/4. S'ha de destacar però, que pels models discrets, tant analítica com numèricament, s'obté per d=1 un transitori amb exponent -1/2. Aquest règim té lloc a temps curts, un cop els parells propers de partícules diferents han reaccionat i les 'supervivents' senten un buit al seu voltant que provoca aquest alentiment de la reacció. Obviament, dins el nostre contexte continu, on no hi ha partícules que desapareixin, és impossible reproduir aquest transitori.

El mateix tipus de simulació es realitza també per espècies amb mobilitat diferent, obtenint els mateixos exponents de Zeldovich en tots els casos. Unicament s'aprecien diferències en el temps que necessiten els sistemes en assolir el règim difusiu. En general, a mida que reduim la mobilitat d'una de les espècies, s'observa abans el comportament controlat per difusió. Aquest tipus de simulacions amb difusions diferents són més interessants però en l'apartat d'organització espacial com es comentarà més endavant.

Finalment, simulem una sèrie de sistemes amb mobilitats iguals per ambdós reactius però considerant diferents distribucions incials. Una d'elles és una condició inicial estadísticament fractal amb una funció d'estructura $\Gamma(k) \sim |k|^{-D_f}$, on D_f és la dimensió fractal de la distribució original, que condueix a la llei cinètica $c \sim t^{-(d-D_f)/4}$ predita teòricament [San96].

També experimentem amb distribucions inicials de tipus lamelar en una i dues dimensions. Per aquestes condicions cal distingir dues possibilitats: les distribucions lamelars de longitut o àrea, segons treballem en una o dues dimensions, de tipus aleatori, per a les quals s'obté un comportament $c \sim t^{-d/4}$, i aquelles distribucions de lameles amb longitut o àrea fixes per a les que s'observa un decaiment exponencial. Ambdós resultats concorden amb els obtinguts de forma analítica.

2.1.c-Organització Espacial:

Les lleis cinètiques anòmales que obtenim per la reacció A+B->0 són la manifestació directa de la segregació que es produeix en el sistema si aquest està controlat pel procés difusiu. Com hem comentat anteriorment, l'existència d'inhomogeneïtats en la disposició inicial dels reactius, i en aquest apartat parlarem únicament de distribucions inicials aleatòries, marca el futur desenvolupament topològic del sistema. La ineficàcia de la difusió fa que aquestes inhomogeneïtats, enlloc de suavitzar-se, s'amplifiquin formant dominis de les diferents espècies ('clusters'). L'estudi d'aquests 'clusters' ens facilitarà la comprensió de com es comporten cinèticament aquests sistemes.

Una primera mesura que ens ajudarà a entendre com s'organitza el sistema són les anomenades funcions de correlació de densitat a temps iguals. Podem definir dues d'aquestes funcions de correlació: les d'espècies iguals, que correspondrà a la correlació entre la concentració d'una espècie a dos punts diferents del sistema, i les d'espècies diferents, corresponent a la correlació entre la concentració d'una espècie amb la de l'altre espècie en un altre punt del sistema. Si el sistema està totalment homogenitzat el valor per les funcions de correlació és 1, mentre que si està segregat, val 1 únicament per distàncies grans, però s'allunya d'aquest valor per distàncies curtes. En

aquest últim cas, podriem dir que les funcions de correlació 's'obren': la correlació entre espècies iguals augmenta de valor i la d'espècies diferents disminueix, a mida que ens acostem a distància nul.la.

L'observació de les funcions de correlació per les simulacions realitzades amb mobilitats iguals ens mostren clarament com el sistema es segrega i els 'clusters' creixen. Comprovem com les funcions de correlació escalen amb $\sqrt{Dt}$, el que demostra que els 'clusters' creixen difusivament, com no podria ser d'una altra forma tenint en compte la naturalesa gaussiana de la funció $q(\vec{r},t)$. Mitjançant la funció de correlació de la variable diferència a dos punts, sempre per $D_A=D_B$, obtenim unes expressions analítiques per les funcions de correlació a les quals s'ajusten correctament els resultats numèrics. S'ha de destacar que aquestes expressions teòriques són universals, és a dir, que no depenen de la dimensionalitat del sistema.

Una anàlisi paral.lela es realitza amb l'anomenada distribució de probabilitat de tamanys de 'cluster'. Aquesta funció s'obté de la següent forma: en el sistema d-dimensional i per cada temps considerat es tracen diferentes rectes i sobre cadascuna d'elles es mira les vegades que la funció $q(\vec{r},t)$ canvia de signe. La distància entre dos 'ceros' de la funció diferència pot ser considerada com el tamany del 'cluster', i l'estadística d'aquests valors em donarà la distribució de tamanys buscada.

Per les simulacions amb mobilitat igual, l'aspecte d'aquestes distribucions de probabilitat mostra com els 'clusters' creixen amb $\sqrt{Dt}$ de forma coherent amb els resultats obtinguts amb les funcions de correlació. Mitjançant l'estudi analític basat en la distribució de 'ceros' en una funció gaussiana aconseguim una expressió, també universal, per la distribució de tamanys de 'cluster' que coincideix amb els resultats numèrics.

Un cas apart el proporcionen els sistemes on les mobilitats de les espècies són diferents. Amb aquestes condicions les Eqs. (0-1 i 0-2) perden la simetria que permetia treballar fàcilment amb les funcions $q(\vec{r},t)$ i $s(\vec{r},t)$. Estem, doncs, davant la impossibilitat d'extreure expressions analítiques per a les funcions de correlació i per a les distribucions de tamany de 'clusters'. Els resultats numèrics ens mostren un trencament de la universalitat de les funcions anteriors, si be es segueix mantenint el creixement difusiu, $t^{1/2}$, dels 'clusters' en totes les simulacions on cap de les dues espècies està absolutament estàtica.

Pels casos on una de les espècies està totalment immobilitzada, arribem a dues conclusions importants. La primera d'elles és que en el nostre esquema continu, és impossible que els 'clusters' de l'espècie immòbil creixin, mentre que sí que ho fan en la descripció dels models discrets. La rao d'això és que en els models discrets un 'cluster' d'una espècie es defineix com el volum, àrea o segment de l'espai on no hi ha cap partícula de l'altre espècie. Amb aquesta definició els models discrets poden 'fer' que una espècie immòbil formi 'clusters' i que aquests creixin degut a la desaparició de les partícules de l'espècie contrària. Obviament, el nostre esquema continu no dóna lloc a 'curiositats' d'aquest tipus. En segon lloc, els 'clusters' de l'espècie mòbil creixen també de forma difusiva a excepció dels sistemes monodimensionals. En una dimensió, i en el nostre esquema continu, es pot produir un efecte d'estancament d'agregats de l'espècie mòbil entre 'parets' de l'espècie immòbil. Aquest efecte fa, que en aquesta situació, els agregats creixin a un ritme inferior de l'esperat. Es una de les particularitats de treballar amb un model continu.

2.2-Aplicació de Camps de Velocitat [Rei96b,Rei97a,Rei97b]:

Un cop considerada exhaustivament la reacció A+B->0 sota condicions de control difusiu, passarem al segon objectiu del nostre treball. Aquest consisteix en la implementació d'un segon procés de transport en forma de camp de velocitats o flux hidrodinàmic. Com hem comentat anteriorment, és de suposar que aquest procés advectiu col.labori amb la difusió per tal d'evitar la segregació del sistema i restablir el comportament cinètic clàssic. Veurem en el nostre cas com això només és possible en una certa mesura.

Aquest estudi s'ha subdividit també en tres parts. En la primera s'introduiran els models pels dos tipus d'advecció que reprodueixen les condicions de mescla del sistema, així com la forma en que els implementem en el nostre esquema continu. La incorporació dels processos d'advecció al nostre problema ens reporta una gran quantitat de nous règims cinètics que estudiem en la segona subsecció. Per últim, es realitza un estudi detallat de la distribució espacial de reactius pels sistemes subjectes a flux turbulent. En aquesta segona part de la Tesi es consideraran únicament sistemes bidimensionals, amb mobilitats iguals per ambdues espècies i distribucions inicials aleatòries.

2.2.a-Models de Flux:

La incorporació d'un flux hidrodinàmic al nostre problema consistirà simplement en la inclusió en les equacions de reacció-difusió que ja teniem d'un terme advectiu:

$$\frac{\partial c_A(\vec{r},t)}{\partial t} + \vec{v}\cdot\vec{\nabla}c_A(\vec{r},t) = D\nabla^2 c_A(\vec{r},t) - Kc_A(\vec{r},t)c_B(\vec{r},t) \qquad (0\text{–}8)$$

i

$$\frac{\partial c_B(\vec{r},t)}{\partial t} + \vec{v}\cdot\vec{\nabla}c_B(\vec{r},t) = D\nabla^2 c_B(\vec{r},t) - Kc_A(\vec{r},t)c_B(\vec{r},t) \qquad (0\text{–}9)$$

En aquest treball experimentem amb dos tipus de fluxes bidimensionals i incompressibles. El primer d'ells consisteix en una disposició de remolins fixa en el temps i periòdica espacialment descrita segons

$$v_x(x,y) = 2u_0 \cos(\frac{n\pi x}{L})\sin(\frac{n\pi y}{L}) \qquad (0\text{–}10)$$

i

$$v_y(x,y) = -2u_0 \sin(\frac{n\pi x}{L})\cos(\frac{n\pi y}{L}) \qquad (0\text{–}11)$$

on la intensitat del flux vindrà donada per u_0, nxn serà el nombre de remolins repartits pel sistema i LxL l'àrea del mateix. Per conservar les condicions de contorn periòdiques també pel flux n ha de ser necessàriament un nombre parell. L'aplicació d'aquest flux determinista ens permetra observar tota una sèrie de règims cinètics que un cop estudiats en detall ens demostraran la importància de l'existència de línies de flux tancades a l'hora de parlar de processos de mescla poc eficients.

Per un altre costat, estem interessats en la construcció d'un camp de velocitats turbulent, estadísticament estacionari, homogeni i isòtrop del que poguem controlar les seves propietats estadístiques més importants. Aquestes són en particular, l'espectre d'energies, la intensitat, el temps de correlació i la longitut de correlació. El camp de velocitats $\vec{v}(\vec{r},t)$ pel flux turbulent s'obté a partir d'una funció de corrent $\eta(x,y)$ de la següent manera

$$\vec{v}(\vec{r},t) = \left(-\frac{\partial \eta}{\partial y}, \frac{\partial \eta}{\partial x}\right) \qquad (0\text{–}12)$$

de forma que assegurem la imcompressibilitat del camp, així com transferim totes les propietats estadístiques del camp escalar $\eta(x,y)$ al flux $\vec{v}(\vec{r},t)$.

L'evolució temporal de la funció de corrent vindrà determinada per la següent equació de Langevin

$$\frac{\partial \eta(\vec{r},t)}{\partial t} = \nu \nabla^2 \eta(\vec{r},t) + Q(\lambda^2 \nabla^2) \vec{\nabla} \cdot \vec{\xi}(\vec{r},t) \qquad (0\text{–}13)$$

on ν és la viscositat cinemàtica, i $\vec{\xi}(\vec{r},t)$ és un vector de components de soroll blanc gaussià, de mitja nul.la i correlació

$$\langle \xi_i(\vec{r_1},t_1) \xi_j(\vec{r_2},t_2) \rangle = 2\varepsilon\nu\delta(t_1-t_2)\delta(\vec{r_1}-\vec{r_2})\delta_{ij} \qquad (0\text{–}14)$$

El conjunt de parametres ε, λ i ν determinaran la intensitat i el temps i longitut de correlació del flux turbulent respectivament. L'operador Q vindrà determinat pel tipus d'espectre d'energies que volguem fer servir. En el treball desenvolupat en la segona part d'aquesta Tesi utilitzarem l'anomenat espectre d'energies de Kraichnan [Kra70].

La manipulació numèrica del flux turbulent requereix un tractament especial. L'evolució temporal de l'equació de Langevin, Eq. (0-13) discretitzada és més senzilla si treballem en l'espai de Fourier. D'aquesta forma aconseguim desacoplar les equacions diferencials per cada punt de la xarxa i es pot integrar de forma exacta [Car93b,Mar97]

2.2.b-Lleis Cinètiques:

a) Disposició de Remolins:

Aquest flux mostra una gran varietat de règims cinètics que estan directament relacionats amb la topologia del camp de velocitats. En primer lloc, i per temps molt petits, el flux encara no mescla el sistema i tenim per tant, el típic règim difusiu $c \sim t^{-1/2}$. Un cop l'advecció mescla el sistema el ritme de reacció s'incrementa fins observar la llei cinètica clàssica, $c \sim t^{-1}$. Aquest règim de mescla, però, no dura indefinidament. S'observa la formació de dominis d'ambdues espècies amb forma circular i seguint les línies de flux tancades dins de cada remolí. Quan el sistema queda disposat definitivament d'aquesta forma, el flux deixa, obviament, de mesclar i l'únic procés de transport efectiu del sistema passa a ser la difusió en direcció transversal als 'clusters'. Degut a això, el ritme de la reacció decau fins assolir el règim de Zeldovich però per una dimensio, $c \sim t^{-1/4}$. Un cop la reacció ha eliminat l'excés de cada espècie dins de cada remolí, el sistema es comporta com un sistema 2D-lamelar aproximadament periòdic. Això suposa un decaiment transitoriament exponencial de la concentració fins que s'assoleix finalment altre cop el règim difusiu $c \sim t^{-1/2}$. En aquest règim, els 'clusters' apareixen com grans agrupacions de remolins.

El que resulta més destacable de tots aquests resultats és l'esgotament del règim de mescla degut a la formació de dominis concèntrics i paral.lels a les línies de flux tancades del camp de velocitats. Per tal d'estudiar més detalladament aquest fenomen fem servir un model advectiu més senzill basat en un flux de cisalla ('shear-flow') i que està definit sobre la superfície d'un cilindre disposat en la direcció z i on $v_x = \alpha z$. Amb aquest model observem de forma clara el pas desde el primer règim difusiu al règim de

mescla, així com la progressiva formació de 'clusters' en la direcció x que ens portarà finalment al règim difusiu unidimensional.

La simplicitat d'aquest camp de velocitats ens permet aproximar de forma senzilla la solució analítica per a les Eqs. (0-8 i 0-9) mitjançant les funcions q(r,t) i s(r,t). El procés a seguir és anàleg al que vem utilitzar en el model sense flux, però ara amb una funció de Green diferent i lleugerament més complicada. D'aquesta forma podem preveure els tres règims cinètics anteriors i fer una estimació dels temps de pas d'uns als altres.

b) Flux Turbulent:

El fet de que el flux turbulent sigui aleatori i que, per tant, no existeixin línies de flux tancades de forma estacionària, faria pensar en que podrem aconseguir un règim de mescla indefinit. Els resultats, però, ens demostren el contrari. Igualment que en el cas anterior, comencem amb el típic règim difusiu, $c \sim t^{-1/2}$, per després passar al de mescla, $c \sim t^{-1}$. El flux turbulent no és prou eficient com per mantenir aquest règim i per temps suficientment grans el sistema, però, torna a segregar-se i recuperem el comportament difusiu, $c \sim t^{-1/2}$.

Un estudi detallat d'aquesta última etapa ens demostra com el sistema, efectivament, està controlat per la difusió però amb un coeficient de difusió diferent i que anomenarem efectiu (D_{ef}). Per calcular D_{ef} utilitzarem sistemes subjectes a flux turbulent on es dispersa un únic camp escalar. Quan aquests sistemes es comporten difusivament, és a dir a temps grans, el segon moment de la variable posició creix linealment amb el temps i la constant de proporcionalitat determina D_{ef}. Sobre aquest tema hi ha estudis més extensos en altres treballs [Car93a, Car94]. Nosaltres ens limitem al

càlcul dels valors de D_{ef} pels camps de velocitats que imposem als nostres sistemes A+B->0. Comparem els resultats per sistemes amb reacció sense flux i amb el coeficient de difusió normal, amb els de sense flux però amb D_{ef}. Observem com el règim de mescla corresponent al sistema amb advecció connecta perfectament els comportaments difusius d'aquests dos sistemes.

La durada dels tres règims cinètics que mostra el flux turbulent depen en gran mesura dels paràmetres del camp de velocitats. El primer règim difusiu desapareix abans per fluxes intensos mentre que el règim de mescla té una durada més gran per fluxes amb temps i longituts de correlació elevats. El règim de difusió efectiva es veu afavorit per fluxes amb temps i longituts de correlació petits.

2.2.c-Organització Espacial per a Fluxes Turbulents:

Realitzem un estudi més detallat dels sistemes subjectes a flux turbulent i en especial fixant-nos en el període de règim de mescla. Ens interessa especialment la disposició espacial del sistema quan la llei cinètica correspon al comportament clàssic i per tant, tothom esperaria la completa homogenització del sistema. Sense fer encara cap conjectura, resulta evident que si el sistema acaba segregant-se, és impossible que en una etapa anterior estigui totalment homogenitzat. Aquest fet el constatem mitjançant les funcions de correlació de densitat i una nova funció anomenada de correlació de productes. Aquesta nova funció correspon a la correlació entre diferents punts del sistema pel producte local de les concentracions d'espècies diferents. L'anàlisi d'aquesta funció ens permet determinar l'amplada de les zones de reacció, així com un càlcul estimatiu del volum del sistema on coexisteixen ambdós reactius. Els conceptes de segregació i

homogenització queden bastant més clars amb l'observació d'aquesta nova funció.

Pels casos on la intensitat del flux i/o el coeficient de difusió són grans, i durant el règim de mescla, el sistema està molt homogenitzat i el control cinètic recau en el procés de reacció; estem parlant d'un règim estrictament clàssic. En canvi, per intensitats i/o coeficients de difusió petits, el sistema encara està segregat malgrat mostrar una llei cinètica clàssica. En aquest cas el control del sistema està en mans del flux i podriem parlar d'un règim 'pseudo-clàssic'. De totes formes, estem definint dues situacions extremes. Podem dir que un sistema es comporta més o menys clàssicament, però en tot cas el que queda clar és que en major o menor mesura el procés de segregació segueix latent inclús en aquells moments en que el sistema mostra un comportament cinètic clàssic. D'aquí la ineficàcia del flux turbulent per a mesclar indefinidament el nostre sistema.

3-Resultats Originals:

De tot el treball realitzat en aquesta Tesi cal mencionar els resultats obtinguts considerats com a més rellevants d'acord amb la contextualització del tema que s'ha fet en aquesta introducció. Estan llistats a continuació com a resultats originals d'aquesta Tesi:

-) Reacció A+B->0 segons un model continu de l'esquema de reacció-difusió.

-) Resolució numèrica.

-) Simulacions generals, on els coeficients de difusió són iguals per ambdues espècies i les condicions inicials són aleatòries de tipus poissonià. Simulem en una, dues i tres dimensions. Desde el punt de vista

cinètic reproduim l'exponent -d/4 corresponent al comportament controlat per difusió. Estructuralment analitzem les funcions de correlació i les distribucions de tamany de 'cluster', observant-se per ambdues la segregació del sistema i el creixement difusiu dels 'clusters'. Trobem comportaments d'escala universals, és a dir independents de la dimensió del sistema i dels coeficients de difusió, que s'ajusten a les previsions teòriques.

-) Simulacions per diferents condicions inicials entre les que destaquen les de tipus lamelar, per una i dues dimensions, i les de tipus fractals, amb $1<D_f<2$. Reproduim en ambdós casos les lleis cinètiques previstes teòricament.

-) Simulacions per diferents coeficients de difusió, i en especial el cas on una de les espècies és immòbil. Pel que fa a les lleis cinètiques no observem en els resultats numèrics cap canvi significatiu. Respecte a l'organització dels reactants, seguim observant segregació tant pel que fa a les funcions de correlació com per la distribució de tamanys de 'cluster', però perdem, en canvi, la universalitat que trobavem per aquestes funcions en el cas d'espècies amb la mateixa mobilitat.

-) Resolució analítica. Realitzem una exploració analítica de les equacions de reacció-difusió pel cas on els coeficients de difusió són iguals per ambdues espècies.

-) Hem obtingut una formulació analítica que permet obtenir la llei cinètica $c \sim t^{-(d+\beta)/4}$ pels sistemes sota control difusiu, i per qualsevol distribució inicial que es pugui descriure amb la funció d'estructura de la seva variable diferència com $\Gamma(k) \sim |k|^{\beta}$.

-) Obtenim expressions universals per a les funcions de correlació per espècies iguals i espècies diferents que s'ajusten correctament als resultats numèrics obtinguts.

-) Obtenim una expressió universal per a la distribució de tamanys de 'cluster' que coincideix amb els resultats numèrics.

-) Reacció A+B->0 en presència de fluxes advectius.

-) Flux en forma de xarxa de remolins.

-) Obtenim una gran varietat de règims. En primer lloc recuperem la llei cinètica clàssica, $c \sim t^{-1}$, si be només de forma momentània, fins la formació d'estructures circulars dins de cada remolí que fan disminuir dràsticament el ritme de reacció, $c \sim t^{-1/4}$ abans d'assolir l'inevitable règim difusiu, $c \sim t^{-1/2}$.

-) Per tal d'estudiar detalladament el règim $c \sim t^{-1/4}$ explorem analítica i numèricament un model de flux anomenat 'shear-flow' sobre la superfície tancada d'un cilindre.

-) Flux turbulent.

-) Obtenim decaiments de la concentració que comencen amb el règim de control difusiu normal, per passar després per un transitori de mescla, $c \sim t^{-1}$, assolint finalment un règim difusiu amb un coeficient de difusió efectiu.

-) Estudiem la influència dels paràmetres del flux en la duració dels diferents règims cinètics.

-) Fem càlculs numèrics de la difusió turbulenta d'escalars per tal d'obtenir el coeficient de difusió efectiu.

-) Comprovem com el règim de mescla per un sistema subjecte a flux turbulent connecta el comportament difusiu corresponent al mateix sistema sense flux amb el règim difusiu amb coeficient de difusió efectiu.

-) Estudiem detalladament l'organització espacial del sistema mitjançant les funcions de correlació de densitat i les funcions de correlació de productes. L'estudi d'aquestes funcions ens demostra la possibilitat de l'existència de dos tipus de control diferent pel mateix comportament cinètic $c \sim t^{-1}$.

Tot el treball original d'aquesta Tesi ha donat lloc a la publicació dels següents sis articles: [Rei96a, Rei96b, Sok96, San96, Rei97a i Rei97b].

-BIBLIOGRAFIA BASICA-

[Bat70] G.K. Batchelor, 'The theory of homogeneous turbulence'. Cambridge University, Cambridge, (1970).

[Car93a] A. Careta, F. Sagués, L. Ramirez-Piscina i J.M. Sancho. 'Effective diffusion in a stochastic velocity field', J. Stat. Phys. **71**, 235 (1996).

[Car93b] A. Careta, F. Sagués i J.M. Sancho. 'Generation of homogeneous isotropic turbulence with well-defined spectra', Phys. Rev. E **48**,2279 (1993).

[Car94] A. Careta, F. Sagués i J.M. Sancho. 'Diffusion of passive scalar under stochastic convection', Phys. Fluids **6**, 349 (1994).

[Kan84] K. Kang i S. Redner. 'Scaling approach for the kinetics of recombination processes', Phys. Rev. Lett. **52**, 955 (1984).

[Kla96] J. Klafter, M.F. Shlesinger i G. Zumofen. 'Beyond brownian motion', Physics Today (Feb. 1996), 33.

[Kra70] R.H. Kraichnan. 'Diffusion by a random velocity field', Phys. Fluids **13**, 22 (1970).

[Kot96] E. Kotomin i V. Kuzovkov. 'Modern aspects of diffusion-controlled reactions. Cooperative phenomena in bimolecular processes'. Comprehensive Chemical Kinetics, Vol. 34. Ed. Elsevier (1996).

[Lam96] D.J. Lamberto, F.J. Muzzio, P.D. Swanson i A.L. Tonkovich. 'Using time-dependent RPM to enhance mixing in stirred vessels', Chem. Eng. Sci. **51**, 733 (1996).

[Ley91] F. Leyvraz i S. Redner. 'Spatial organization in the two-species annihilation reaction A+B->0', Phys. Rev. Lett. **66**, 2168 (1991).

[Mar97] A.C. Marti, J.M. Sancho, F. Sagués i A. Careta, 'Langevin approach to generate synthetic turbulent flows', Phys. Fluids **9**, 1078 (1997).

[Mon75] A.S. Monin i A.M. Yaglom. 'Statistical Fluids Mechanics', MIT Press, Cambridge, MA, (1975).

[Osh94] G. Oshanin, M. Moreau i S. Burlatsky. 'Models of chemical reactions with participation of polymers', Advances in Colloid and Interface Science **49**, 1 (1994).

[Ott88] J.M. Ottino, C.W. Leong, H. Rising i P.D. Swanson. 'Morphological structures produced by mixing in chaotic flows', Nature **333**, 419 (1988).

[Ott92] J.M. Ottino, F.J. Muzzio, M. Tjahjadi, J.G. Franjione, S.C. Jana i H.A. Kusch. 'Chaos, symmetry, and self-similarity: exploiting order and disorder in mixing processes', Science **257**, 754 (1992).

[Ovc78] A.A. Ovchinnikov i Ya.B. Zeldovich. 'Role of density fluctuations in bimolecular reaction kinetics', Chem. Phys. **28**, 215 (1978).

[Pri97] V. Privman. 'Non-equilibrium statistical mechanics in one dimension', Capítol I per R. Kopelman i A.L. Lin. Cambridge University Press, Cambridge (1997).

[Rei96a] R. Reigada, F. Sagués, I.M. Sokolov, J.M. Sancho i A. Blumen. 'Spatial correlations and cross sections of clusters in the A+B->0 reaction', Phys. Rev. E **53**, 3167 (1996).

[Rei96b] R. Reigada, F. Sagués, I.M. Sokolov, J.M. Sancho i A. Blumen. 'Kinetics of the A+B->0 reaction under steady and turbulent flows', J. Chem. Phys. **105**, 10925 (1996).

[Rei97a] R. Reigada, F. Sagués, I.M. Sokolov, J.M. Sancho i A. Blumen. 'Fluctuation-dominated kinetics under stirring', Phys. Rev. Lett. **78**, 741 (1997).

[Rei97b] R. Reigada, F. Sagués, I.M. Sokolov, J.M. Sancho i A. Blumen. 'Spatial organization in the A+B->0 reaction under confined-scale mixing', J. Chem. Phys. **107**, 843 (1997).

[Rey1894] O. Reynolds. Nature **50**, 161 (1894).

[Ric85] S.A. Rice. 'Diffusion-limited reactions' Comprehensive Chemical Kinetics, Vol. 25. Ed. Elsevier (1985).

[San96] J.M. Sancho, A.H. Romero, K. Lindenberg, F. Sagués, R. Reigada i A.M. Lacasta. 'A+B->0 reaction with different initial patterns', J. Phys. Chem. **100**, 19066 (1996).

[Smo17] M. Smoluchowski. 'Mathematical theory of the kinetics of the coagulation of colloidal solutions', Z. Phys. Chem. **92**, 129 (1917).

[Sok86] I.M. Sokolov. 'Spatial and temporal asymptotic behavior of annihilation reactions', JETP Lett. **44**, 67 (1986).

[Sok88] I.M. Sokolov. 'Stochastic aggregation and subsequent recombination of particles generated by pulsed excitation in fractal and homogeneous systems', Sov. Phys. JETP **67**, 1846 (1988).

[Sok91a] I.M. Sokolov i A. Blumen. 'Mixing in reaction-diffusion problems', Int. J. Mod. Phys. B **5**, 3127 (1991).

[Sok96] I.M. Sokolov, R. Reigada, F. Sagues, J.M. Sancho i A. Blumen. 'Fluctuation-dominated kinetics under regular and turbulent flows' al llibre del CFIC96 cel.lebrat a Roma el Setembre de 1996 (per publicar).

[Tou83] D. Toussaint i F. Wilczek. 'Particle-antiparticle annihilation in diffusive motion', J. Chem. Phys. **78**, 2642 (1983).

[Zum85] G. Zumofen, A. Blumen i J. Klafter. 'Concentration fluctuations in reaction kinetics', J. Chem. Phys. **82**, 3198 (1985).

[Zum91] G. Zumofen, J. Klafter i A. Blumen. 'Stochastic and deterministic analysis of reactions: the fractal case', Phys. Rev. A **44**, 8390 (1991).

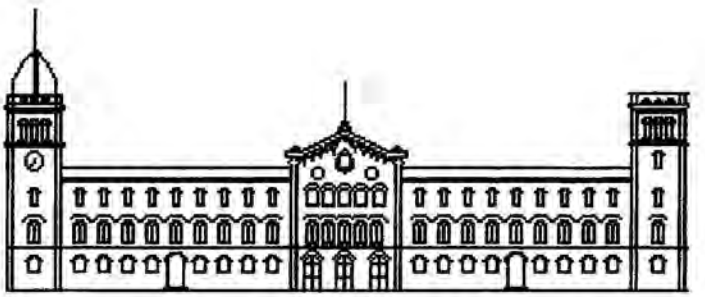

UNIVERSITAT DE BARCELONA

Departament de Química-Física

EFFECTS OF SOME MIXING FLOWS ON DIFFUSION-CONTROLLED REACTIONS.

EFECTES D'ALGUNS FLUXES DE MESCLA EN REACCIONS CONTROLADES PER DIFUSIO.

NOVEMBRE 1997

Memòria de la Tesi presentada per Ramon Reigada Sanz per optar al grau de Doctor en Ciències Químiques

Contents

PART 1- THE A+B->0 DIFFUSION-CONTROLLED REACTION.

PART 2- MIXING FLOW EFFECTS

PART 1

-THE A+B->0 DIFFUSION-CONTROLLED REACTION-

Introduction

Diffusion-controlled reactions in low-dimensional geometries are well-known to exhibit 'anomalous' kinetics in the sense that the rate laws for global concentrations do not follow the behavior expected from standard law-of-mass-action arguments. In the present work we are going to study an example of this anomalous behavior: the diffusion-limited irreversible reaction A+B->0. The '0' means that we are only considering those binary reactions whose products do not affect to the evolution of the system. All numerical and analytical results will be obtained for the case of stoichiometrical conditions.

For an initial randomly distributed system, the formal treatment of the problem is based on the total homogeneity hypothesis. This assumption allows to easily solve the problem. If the distribution of each reactant is considered spatially homogeneous, the rate laws for the global reactant concentrations $c_A(t)$ and $c_B(t)$ are expected to be $dc_A/dt=dc_B/dt=-Kc_Ac_B$, where K is a constant global rate coefficient. If $c_A(0)=c_B(0)=c_0$, then the global concentration of the two species are equal at all times, $c_A(t)=c_B(t)=c(t)$, and the notation can be simplified by writing $dc/dt=-Kc^2$. In the integrated form $c^{-1}(t)=(1/c_0)+Kt$; at long times $c\sim(Kt)^{-1}$. We call this behavior classical.

According to this kinetic law the local concentration value will be the same for both species in all points of the whole system. As reaction proceeds this value will decrease but always preserving the homogeneity of the concentrations. Thus, it is clear that only the reaction process (K) is responsible of the kinetic control of the system.

Before going ahead, some details are to be explained on what respects to what we call K-controlled processes. If we assume that diffusion is fast enough to keep the initial homogeneity of the system we can consider that K is really a chemical reaction constant that only depends on the activation energy of the collision process (Arrhenius expression). On the other hand, if the collision process does not need a lot of energy to make A and B react, the local diffusion transport can be the slowest stage in the global reaction process. In this case, studied by Smoluchowsky [Smo17], the K is controlled by the local diffusion of the particles and depends on time. Actually, only in the three dimensional case one can obtain a constant value of K for asymptotic times [Smo17, Osh94]. Nevertheless, in both cases the kinetics of the system is controlled by the global reaction process (K).

The actual asymptotic rate law in an infinite volume in Euclidean dimensions d<4 for an initially random distribution of reactants is instead slower than the classical one. The physical origin of this anomaly is in general clearly understood. The usual laws of mass action assume a spatially homogeneous mixture of reactants, but the mechanism for this homogenization or mixing is usually not specified. In low dimensions, diffusion, quantified with its corresponding diffusion coefficient D, is not an efficient mixing mechanism and may be incapable of smoothing out reactant concentration inhomogeneities that are created by its initial fluctuations.

Consider, for example, the A+B->0 reaction starting from an initially random distribution of A and B. Such a distribution exhibits local concentration inhomogeneities; that is, certain regions of the system are relatively rich in species A while others are relatively rich in species B. By 'efficient' mixing we mean mixing that is rapid relative to the local reaction rate. Thus, if efficient mixing -by whatever mechanism- occurs, such local inhomogeneities are rapidly suppressed; while perhaps reappearing elsewhere, but being rapidly suppressed there again. If mixing is not efficient as, for example, in a diffusion-limited reaction in low dimensions, then the reaction will cause the local minority species to be eliminated extremely rapidly by the local majority species, and diffusion is not able to homogenize the system. Very quickly we observe an evolution of domains (clusters) in which essentially only one of the species is present, and any attempt of the other species to diffuse into this region leads to its rapid disappearance by reaction. The reaction in fact only takes place then at the interfaces of clusters of different species. As time proceeds and the concentrations of reactants decrease, the regions in space that are occupied by reactants of only one species grow in size, and the total interface region at which the reaction takes place decreases. This leads to even more effective spatial segregation of

the species and an associated slowing down of the reaction relative to its rate in a homogeneous mixture.

We can obtain the corresponding diffusion-limited kinetic law through a simple dimensional argument, see figure. It is well-known that for a random distribution of reactants, for example the poissonian distribution used in this Thesis, the fluctuations of concentrations are tipically on the order of the square root of the average local concentrations. A particle that behaves diffusively travel an average distance defined by the diffusion length $l_D=(Dt)^{1/2}$. Concentration fluctuations on a length scale shorter than l_D have had time to die out, but fluctuations on longer scales are still present. In a volume of linear size l_D, the initial difference between A and B numbers is on the order of $(c_0 l_D^d)^{1/2}$. This corresponds to an excess concentration $c_{ex}\sim c_0^{1/2}(Dt)^{-d/4}$ for this segregated volume. If we consider that the system is going to be totally segregated in an asymptotical way, we have $c(t)\sim c_{ex}(t)$ and thus, $c(t)\sim t^{-d/4}$.

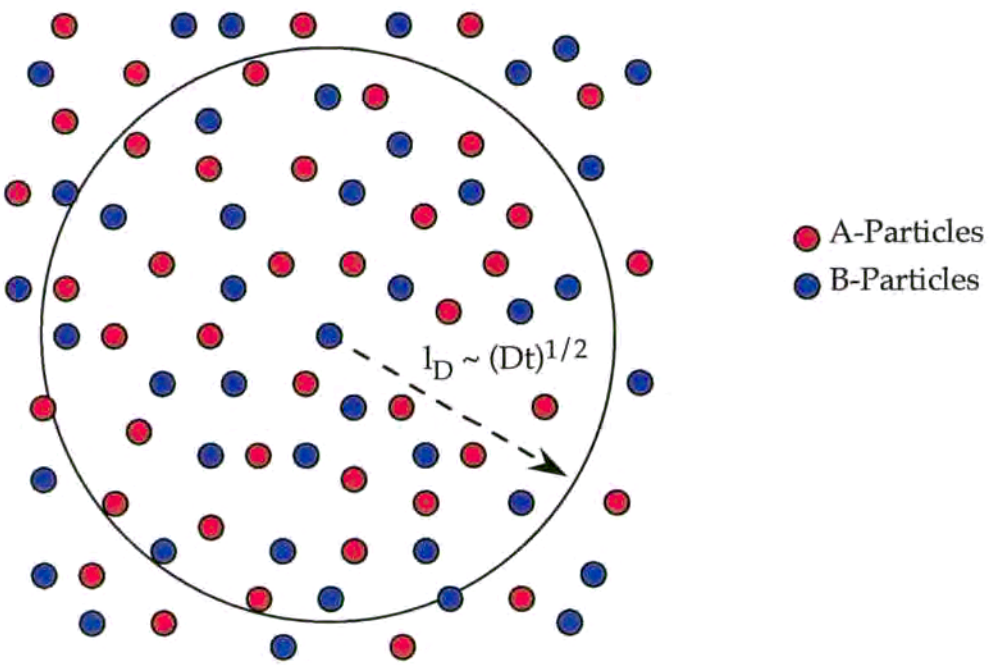

This is the fluctuation-dominated or also the diffusion-limited kinetic regime for initial randomly distributed binary systems. This law was first deduced by Ovchinnikov and Zeldovich for three dimensions [Ovc78], and extended for the general d-dimensional case in other works [Tou83, Kan84]. Contrarily to the classic situation, now the system is controlled by the diffusion process and the initial inhomogeneities. The critical dimension for this anomalous behavior is d=4. We can also see from the exponent -d/4 that the slowing down of the reaction rate is more evident in low-dimensional systems since the diffusion transport has more topological difficulties to mix the reactants. On what follows we will use indistinctly the expressions 'fluctuation-dominated' and 'diffusion-controlled' to refer to the effect of initial inhomogeneities in reaction-diffusion systems where the diffusion transport is the slow process.

However, the fluctuation-dominated law corresponds in fact, to an asymptotic behavior. First the system will behave as a classical one because of the reaction of very-close-different-species pairs. After this, the first clusters emerge, the system becomes more and more segregated and thus, the reaction rhythm slows down to attain the diffusion-limited kinetic law $c \sim t^{-d/4}$. The segregation process will be evidenced by the change of the exponent of $c \sim t^{\alpha}$ from $\alpha=-1$ to $-d/4$ which is the asymptotic value. The crossover between both regimes will depend on how fast are the reaction and the diffusion processes and thus, on the prescribed values of K and D.

The importance of the initial fluctuations for the long-time behavior of this kind of systems has been the key for the understanding of a lot of diffusion-controlled chemical and physical phenomena. One example on solid state physics is the recombination kinetics of Frenkel defects in crystals [Kuz84]. As is well known, irradiation of most crystals produces Frenkel

pairs of defects (vacancies and interstitials) that can be treated as the A and B particles in our diffusion-limited problem. Another application consists on explaining the unusual electronic properties of amorphous semiconductors [Hva80, Var80, Mor80, Ore81, Kir82]. Electron-hole pairs are created in these amorphous semiconductors by pulsed optical excitation, and the following fotoconductivity behavior by recombination of these pairs is also governed by diffusion-limited laws. The diffusion-limited problem also came to our attention in thinking about the fate of superheavy magnetic monopoles produced in the very early universe [Pol74, Hoo74, Zel78, Pre79]. These monopoles are topological singularities which may disappear only through annihilation with an antimonopole, thus, our A+B->0 model can be applied for this study. Also, some artificial laboratory experiments have been designed to reproduce the fluctuation-dominated behavior, for example in the triplet exciton homofusion in naphthalene isotopic mixed crystals [Kly82, Kop86, Kop88a]. Other chemical experiments on this topic have been reported in [Pri97] and references therein.

Obviously, diffusion-limited behaviors can emerge from a lot of systems and situations. The A+A->0 has been extensively studied [Kan85, Zum85, Kuz88, Arg93] and also shows anomalous kinetics in the so-called 'depletion zone regime'. Also the system A+B->B has been studied in its two versions: the target problem, where A remains immobile [Blu86], and the trapping problem, where B is immobile [Bal74, Don75, Anl84]. Some attempts have been done to study the reversible version of the binary problem (A+B↔C) [Kan85], the coagulation-annihilation recombination ($A_n+B_m->A_{n-m}$) [Sok94c], etc.

Even the A+B->0 problem can show different interesting situations. For example the corresponding situation for open systems, where particle

sources lead to some steady-state behaviors [Lin88, Kuz88, Sok94a]. Studies on non-euclidean but fractal systems have been developed in a lot of works [Ana87, Kop88b, Cle90, Lin91, Sok91g, Zum91] and even more complicated systems with combination of sources and fractal support [Sok88, Sok89a, Sok89b, Cle89]. Different results are obtained in the case where the particles move under short-range interaction forces [Blu91, Sok93a, Sok93c, Sok94b] and interesting studies have been developed for the non-stoichiometrical case [Zum85, Kuz88, Sch90, Sok92a]. Obviously, the fact that this kind of systems are controlled by their initial distribution motivated a lot of works reporting on the corresponding kinetic laws for different initial distributions of reactants. We will specifically mention here the case of a fractal distribution [San96] or the lamellar one [Sok91d].

On what respects to the different approaches developed until now for the A+B->0 system we can distinguish two different ways of dealing with the problem. Initially, discrete models, also called Monte Carlo or particle models, were studied. They consider an idealized model in which an amount of A and B particles are distributed at random on a d-dimensional lattice. Particles are allowed to jump to a randomly chosen nearest-neighbor site. If an attempted move is to a site occupied by a particle of the opposite species, then both particles are removed from the system. After each move attempt, the time is incremented by the inverse of the number of particles, thus, in each step of time all the particles are moved. Almost the majority of the works that contain numerical results and that were referenced before use this discrete approach. From this kind of simulations you can obtain concentration decay patterns by counting at each time the number of 'surviver' particles. This model also allows some topological explorations like studying the statistics and the scaling behavior of the nearest-neighbor distance between like and unlike particles, the domain size, etc... [Ley91].

Nevertheless, discrete models have some limitations. First of all, when dealing with this kind of models you are not abble to easily modify the diffusion and the reaction parameters. Diffusion has been modeled by one-site jumps and reaction occurs always that A and B coincide in the same site. These limitations could be more or less overcamed by allowing random jumps not only to the nearest-neighbor sites and by fixing a finite probability of reaction when A and B coincide in the same site, but the implementation of these variants have not been pursued at all. Second, we need a large amount of particles to obtain the diffusion-limited asymptotic behavior, and thus, large enough systems. This is not a computational problem in one dimension but simulations in two and three dimensions became unaffordable. Moreover, it is not easy to observe directly in the time-reactant-patterns from particle simulations how the system segregates. Finally, there are also obvious difficulties in defining the morphological variables that we introduced before, like cluster size, in two and three dimensions for discrete systems [Ley92]. Due to these limitations the continuum models have been recently applied to our binary diffusion-controlled system.

A continuum model is based on the deterministic reaction-diffusion equations for both species. Normally, a mean-field approach for the reaction term is considered in order to simplify the numerical and analytical procedures. Smoluchowski theory [Smo17] allows the mean-field approach with a constant value for the local reaction rate (K) only for three-dimensional systems where the asymptotic value of K could be considered constant [Ric85, Kot96]. On the other hand, in one and two dimensions this value depends on time. Nevertheless, if we are interested in the study of the diffusion-limited case, i.e. when the local reaction process does not control the kinetic behavior of the system, the constant-K approximation will be

valid [Zum91]. Obviously, some intermediate kinetic behaviors like the 'depletion zone regime' [Arg93] found for our binary system in d=1 and 2 with the discrete approach can not be reproduced with the continuum scheme.

The big advantatge of the continuum models concerns to the analytical approaches they possibilitate. From such schemes we can obtain analytical expressions for the initially random distribution of reactants and, in general, for other initial conditions through the resolution of the diffusion equation for the semi-difference function [Sok86, Vit88]. However, this is only possible for the case where the diffusion coefficients for both reactants are the same, otherwise only the numerical procedure is available [Sok91f, Rei96a]. Contrarily to the discrete models, the continuum scheme provides an easy way to deal with morphological variables like the size of clusters [Sok91e, Rei96a], the width of the reaction zones [Sok86] and the density correlation functions [Vit88, Rei96a]. For all these variables the continuum approach obtains analytic and universal expressions, i.e. non-depending on the dimension of the system, that can be tested with the numerical results.

The corresponding numerical procedure consists on the discretization of the main reaction-diffusion equations generally by taking a centered form for the diffusion term, with periodic boundary conditions and a forward first-order difference on time. Numerical results are improved with this scheme, since they need less CPU time and memory than the discrete simulations. Contrarily to the particle description, with the continuum model there is the possibility of varying the reaction and the diffusion processes only by changing the values of K and D used in the deterministic equations. We can also obtain a good enough representation of the system

that provides us with the possibility of directly observing the segregation process.

In this Thesis we are going to work with the reaction-diffusion continuum model because we really think that it is the best way for the study of the A+B->0 diffusion-limited reaction.

From our continuum model simulations we can represent the reactive system at different times as we show in Figures 0. The whole segregation process explained before is clearly observed in these figures. On what follows two different representations will be used to display the spatial organization of the system resulting from our simulations: the distribution of reactants and of the reaction zones. In the reactants picture, Fig. 0a, we paint the zones where $c_A(i,j)>c_B(i,j)$ from white to blue (proportional to $c_A(i,j)$), and the zones where $c_B(i,j)>c_A(i,j)$ from white to red (proportional to $c_B(i,j)$). For each cell of the system we have assigned a blue or a red color, depending on which c_A or c_B respectively is larger, and normalized according to the maximum value of c_i for each corresponding time-pattern. Therefore the clusters of A will appear in blue and the clusters of B will be drawn in red. In the reaction zones pictures, Fig. 0b, one can see how strong is the system segregated since we draw from white to black the value of the product $c_A(i,j)c_B(i,j)$ also normalizing with the maximum value of this variable at each time. The clusters, of A and B, will appear in white, meanwhile the dark zones will correspond to the areas of the system where the reaction takes place. These two representations are complementary and both are needed to exactly describe the system. Turning to Figs. 0 you can note from them that the strong segregation makes the reaction zones be less space filling with time and therefore the decay of reactants concentrations will be slowed down.

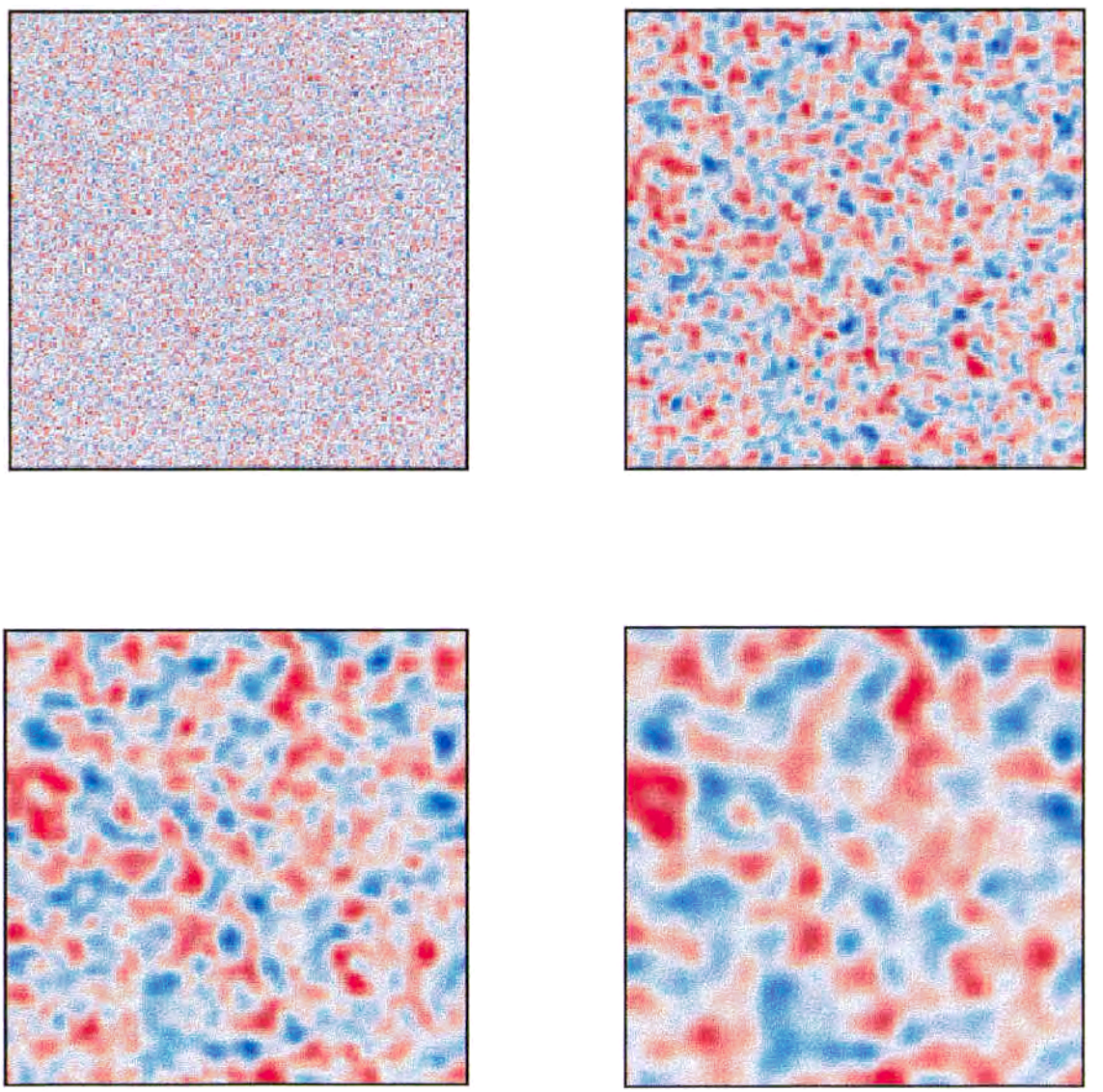

Fig. 0- a) Patterns corresponding to the time evolution of the reactants for a fluctuation-dominated binary reaction in two dimensions.

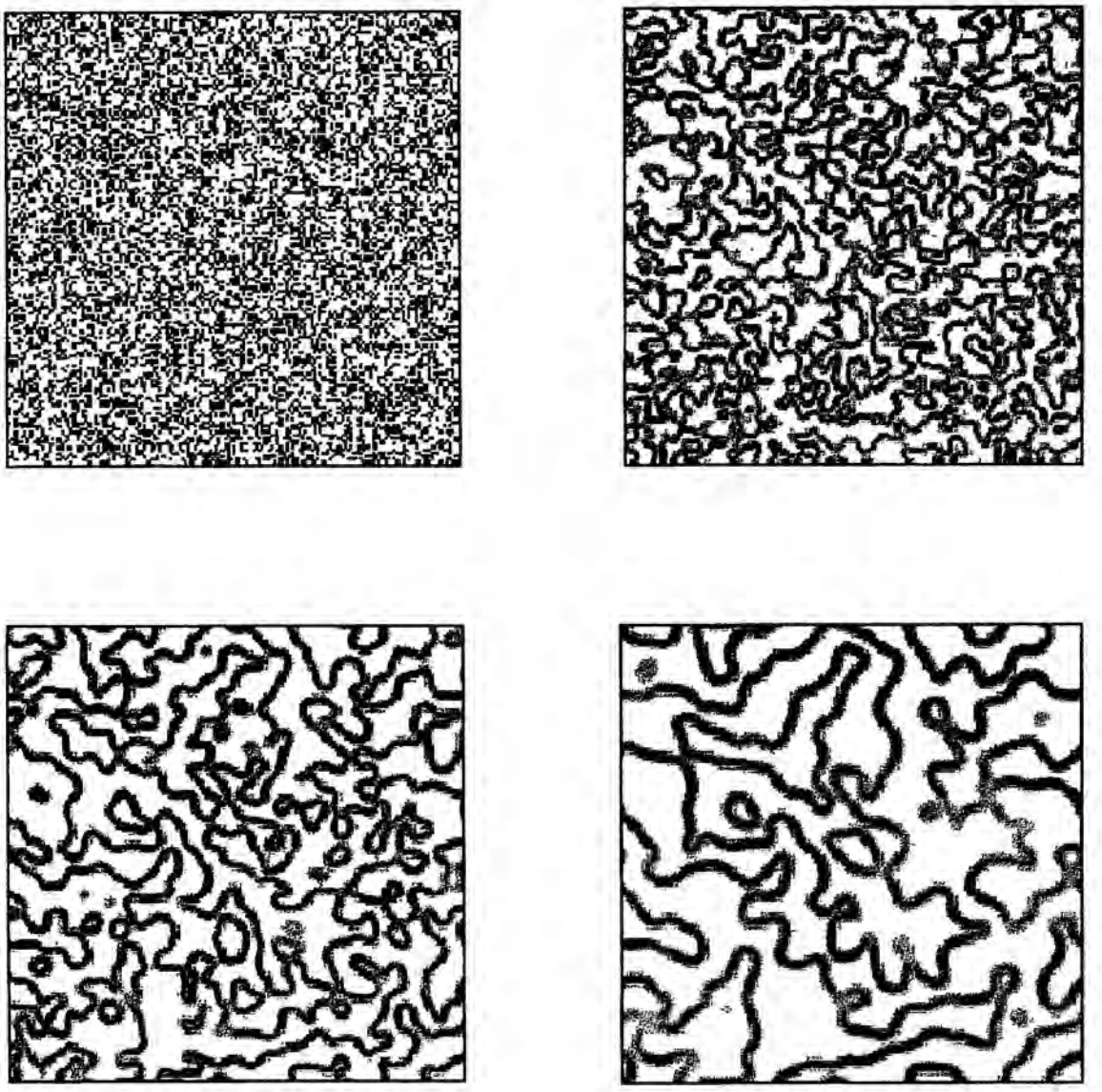

Fig. 0- b) Plots of the structure of the reaction zones for the system of Fig. 0a.

We have seen that the A+B->0 diffusion-limited reaction will display anomalous kinetic behavior closely related to a very specific spatial self-organization of the reactants. In the Part I of this Thesis both aspects will be studied for the stoichiometrical case. First, Chapter I summarizes the continuum model and the analytic and numerical tools used for solving the reaction-diffusion system. In Chapter II different kinetic aspects are studied. In the first section, the so-called Zeldovich regime for random initial distributions of reactants is analyzed. Other initial conditions and their kinetic behaviors are also studied in the second section of this chapter. In Chapter III we concentrate on a precise characterization of the spatially segregated domains through the determination of the density-density correlation functions and of the distributions of clusters' cross sections. Much interest will be focussed on the spatial structure of these clusters and especially on their scaling properties. Finally, Chapter IV is a concluding and summarizing section.

CHAPTER I

-Model Equations. Analytic and Numerical Procedures-

This chapter introduces the different tools that we are going to use in the study of the diffusion-controlled A+B->0 reactions.

In the first section the continuum, mean-field like scheme for this reaction-diffusion system is presented. Some discussions and comparisons with the most-commonly used discrete schemes are reported.

In the second section the equations that govern the reaction-diffusion system are explored analytically by defining the sum and the difference functions of the concentration variables and using the Green's function technique appropriate to the diffusion equation. As it will become clear in that section, the initial distribution of reactants will completely determine the all-time kinetics of the reaction.

Finally, the third section contains the numerical procedures that are used in our simulations.

SECTION I-1 -Model Equations-

The reaction kinetics is modeled in terms of the usual deterministic and mean-field like reaction-diffusion equations for the local concentrations $c_{A,B}(\vec{r},t)$:

$$\frac{\partial c_A(\vec{r},t)}{\partial t}=D_A\nabla^2 c_A(\vec{r},t)-Kc_A(\vec{r},t)c_B(\vec{r},t) \qquad (I-1)$$

and

$$\frac{\partial c_B(\vec{r},t)}{\partial t}=D_B\nabla^2 c_B(\vec{r},t)-Kc_A(\vec{r},t)c_B(\vec{r},t) \qquad (I-2)$$

where K is a time-independent rate coefficient, and D_A and D_B are the diffusion coefficients of the reactants.

According to the Smoluchowski theory for diffusion-controlled reactions [Smo17, Ric85, Osh94, Kot96] the main characteristics of this deterministic scheme is the existence of K as a constant rate which is included in the quadratic terms of Eqs. (I-1) and (I-2). The Smoluchowski theory uses the solution of a pair problem for the non-solvable exactly kinetics in many-particle systems. He considered an ensemble of particles A with density $c_A(r,t)$ surrounding a single sink with radius r_0 with one particle B at the origin. The kinetics of this system is governed by the normal diffusion equation with a coefficient of relative diffusion $D=D_A+D_B$.

Solution of this problem could be easily obtained with the following initial and boundary conditions: $c_A(r>r_0,0) = c_A(\infty,t) = c_A^0$. The flux of particles A falling at the sink B will be proportional to $(\partial c_A(r,t)/\partial r)_{r=r_0}$ and therefore the value of K(t) will depen on the time evolution of $c_A(r,t)$. For any dimension the behavior of $c_A(r,t)$ shows a depletion zone around the sink due to the fact the diffusion process is not efficient enough to homogenize the system. Nevertheless, for d=3 and after a transient stage, the $c_A(r,t)$ profile tends to an assymptotic shape giving a constant value for K equal to $K(\infty)=4\pi Dr_0$. For d=1 and d=2 the $c_A(r,t)$ profile shows a non-stop growing depletion zone. In these cases K(t) is non-stationary and always decays in time never reaching the steady-state value.

Thus, the definition of K independent of time is strictly valid only for three dimensions. Nevertheless, for d=2 and even for d=1 the behavior of K(t) will give us a faster kinetics than those ones corresponding to the fluctuation-dominated regimes. For this reason, the approach of K independent of time can be also used in low dimensions at least on what respects to obtainig the assymptotic fluctuation-dominated behavior.

Anyway, some differences between discrete models and our continuum approach will be found in Chapter II and III mainly concerning some kinetic transient regime and the spatial organization of the 1D-systems. In some sense, the monodimensional formulation of a continuum model allows for matter interpenetration, whereas a Monte-Carlo model does not. In spite of this anomaly most of the results which are obtained by discrete models even in one dimension will be reproduced here. Quantitatively, however, care must be exercised [Zum91].

When $D_A=D_B$ holds, the system described by Eqs. (I-1) and (I-2) can be explored to a large extent analytically. This is due to the prevailing high symmetry of the problem. Contrarily for $D_A \neq D_B$ most of the results can only be obtained numerically.

SECTION I-2 -Analytic Formulation-

A starting point in the analytic solution of reaction-diffusion Eqs. (I-1) and (I-2) for the case $D_A=D_B=D$ is to introduce the semi-sum and semi-difference variables $s(\vec{r},t) \equiv \frac{c_A(\vec{r},t)+c_B(\vec{r},t)}{2}$ and $q(\vec{r},t) \equiv \frac{c_A(\vec{r},t)-c_B(\vec{r},t)}{2}$. The equations for these new variables read

$$\frac{\partial q(\vec{r},t)}{\partial t} = D\nabla^2 q(\vec{r},t) \qquad \text{(I-3)}$$

and

$$\frac{\partial s(\vec{r},t)}{\partial t} = D\nabla^2 s(\vec{r},t) - K(s^2(\vec{r},t) - q^2(\vec{r},t)) \qquad \text{(I-4)}$$

where the first equation is a linear partial differential equation (PDE) for the variable q only, and the second one contains q as a parameter. The first one of these equations can be formally solved using Green's function, *vide infra*. Actually, the relevant quantities from a kinetic point of view are the averages over spatial coordinates and initial fluctuations of the variables defined above. The spatial averaging ($\langle\,\rangle_{\vec{r}}$) of the Eq. (I-4) gives

$$\frac{\partial \langle s(\vec{r},t)\rangle_{\vec{r}}}{\partial t} = -K(\langle s^2(\vec{r},t)\rangle_{\vec{r}} - \langle q^2(\vec{r},t)\rangle_{\vec{r}}) \qquad \text{(I-5)}$$

where we have noted that $\nabla^2\langle s(\vec{r},t)\rangle_{\vec{r}} = 0$ since $\langle s(\vec{r},t)\rangle_{\vec{r}}$ is independent of $\vec{r}$.

In the limiting case of very fast reactions, where $K \to \infty$, the solution of Eq.(I-5) obeys locally $s(\vec{r},t) \approx |q(\vec{r},t)|$, so that for the stoichiometric case

$$c_A(t) = c_B(t) = \langle s(\vec{r},t) \rangle_{\vec{r}} = \langle | q(\vec{r},t) | \rangle_{\vec{r}} \qquad \text{(I–6)}$$

holds. This gives us an exact lower bound for the concentration's decay.

In the case of small local reaction rates K a closure for Eq. (I-5) is necessary. The simplest aproximation here is to take $\langle s(\vec{r},t) \rangle_{\vec{r}} = \langle s^2(\vec{r},t) \rangle_{\vec{r}}^{1/2}$. Substituting this equality and the corresponding expression of $\langle q^2(\vec{r},t) \rangle_{\vec{r}}$, containing all the dependence on the initial distribution of reactants, into Eq. (I-5) transform this last one into a Riccatti form. The solution of this Riccatti equation for long enough times is very similar to the case with $K \to \infty$; see Sect. 3.4 of Ref. [Sok91a]. Nevertheless, in this Thesis we concentrate ourselves on very fast reactions. This implies $K \to \infty$ for the analytical procedures and $K \gg 1$ for the numerical simulations.

The formal solution of Eq. (I-3) reads

$$q(\vec{r},t) = \int d\vec{r}' q(\vec{r}',0) G(\vec{r},\vec{r}',t) \qquad \text{(I–7)}$$

where $G(\vec{r},\vec{r}',t)$ is the Green's function of the diffusion equation. Therefore,

$$\begin{aligned} \langle q^2(\vec{r},t) \rangle &= \left\langle \int \int d\vec{r}' d\vec{r}'' q(\vec{r}',0) G(\vec{r},\vec{r}',t) \cdot q(\vec{r}'',0) G(\vec{r},\vec{r}'',t) \right\rangle = \\ &= \int \int d\vec{r}' d\vec{r}'' \langle q(\vec{r}',0) q(\vec{r}'',0) \rangle \cdot G(\vec{r},\vec{r}',t) G(\vec{r},\vec{r}'',t) \end{aligned} \qquad \text{(I–8)}$$

where the average is here understood as taken over statistically different initial conditions. In fact, we are interested in the overall behavior of this

quantity, that is the complete average $\langle\langle q^2(\vec{r},t)\rangle\rangle_{\vec{r}}$. Moreover, due to the fact that the averaged initial conditions are homogeneous, the ensemble average $\langle q^2(\vec{r},t)\rangle$ does not depend on the coordinate $\vec{r}$, so we can take $\langle q^2(t)\rangle \equiv \langle q^2(0,t)\rangle = \langle q^2(\vec{r},t)\rangle$. On all what follows we shall consider that the spatial averaging is equivalent to the averaging over different initial distributions. In Eq. (I-8) integration and averaging have been interchanged because the Green's function is a nonrandom quantity which does not depend on the particular realization of the initial conditions.

Eq. (I-8) will be the starting point in the analytic studies developed in the following sections. Its resolution will depend on the $\langle q(\vec{r}',0)q(\vec{r}'',0)\rangle$ function, determined by the initial distribution of reactants. First, in the next section Eq. (I-8) will be explored taking random, and non-correlated, initial distributions for the q function. This assumption will lead to the fluctuation-dominated kinetic regime. Meanwhile, in the last section we will work with Eq. (I-8) taking a generic initial distribution.

Independently of the initial distribution of reactants the Green's function for diffusion is the solution of the equation

$$\frac{\partial G}{\partial t} = D\nabla^2 G \qquad \text{(I–9)}$$

under the initial condition $G(\vec{r},\vec{r}',0) = \delta(\vec{r}-\vec{r}')$. This solution reads

$$G(\vec{r},\vec{r}',t) = (4\pi Dt)^{-d/2} e^{-|\vec{r}-\vec{r}'|^2/4Dt} \qquad \text{(I–10)}$$

Turning now to consider the very fast reaction case, Eq. (I-6) implies

$$c_A(t)=2\langle q(\vec{r},t)\theta(q(\vec{r},t))\rangle \qquad \text{(I–11)}$$

and

$$c_B(t)=2\langle q(\vec{r},t)\theta(-q(\vec{r},t))\rangle \qquad \text{(I-12)}$$

with $\theta(x)$ being the Heaviside function. The ensemble average can be performed taking into account the Gaussian nature of the q variable. As is well known, the Green's function Eq. (I-10) is bell-like, with a characteristic width $\sqrt{Dt}$ and height $1/\sqrt{Dt}$. Due to this fact and according to the central limit theorem, for long enough times the integral in Eq. (I-7) represents a sum over many independent random variables corresponding to the initial values of q in different spatial domains. One has therefore

$$s(t)=c(t)=2\int_0^\infty q\frac{1}{\sqrt{2\pi}\sigma(t)}\exp(-\frac{(q-\bar{q}(t))^2}{2\sigma^2(t)})dq=\frac{2}{\sqrt{2\pi}}\sigma(t) \;\Rightarrow\; c(t)\sim\sqrt{\langle q^2(t)\rangle} \qquad \text{(I-13)}$$

where $\sigma(t)=\langle q^2(t)\rangle^{1/2}$ and $\bar{q}(t)=\langle q(\vec{r},t)\rangle_{\vec{r}}$. Here, note that $\bar{q}(t)=0$ under stoichiometrical conditions.

Thus, one can obtain the concentration decay for very fast reactions by solving Eq. (I-8) for the corresponding initial condition $\langle q(\vec{r}',0)q(\vec{r}'',0)\rangle$ and replacing $\langle q^2(t)\rangle$ in Eq. (I-13).

SECTION I-3 -Numerical Procedure-

We numerically solve the coupled partial differential equations (PDE's), Eqs. (I-1) and (I-2), by using a standard discrete scheme with a centered form for the Laplacian operator with periodic boundary conditions and a forward first-order difference in time. Simple lattices of sidelength L and spatial dimension d are taken. For dimensions d=2 and d=3 the handling of the numerical code is largely improved by vectorizing the corresponding lattices into a one-dimensional array. Time and space are discretized by increments of Δt and Δx, thus, the number N of cells of the system is equal to $(L/\Delta x)^d$. For most of the simulations $\Delta t=0.01$ and $\Delta x=1$. This last choice guarantees that the scheme is numerically stable and convergent for the values of $c_{A,B}$, K and $D_{A,B}$ used here. The simulations will never exceed a maximum time denoted t_{max}, long enough to capture the asymptotic behaviors that we want to analyze here.

In all this Thesis we will work under stoichiometrical conditions, and thus $\langle c_A(\vec{r},t)\rangle=\langle c_B(\vec{r},t)\rangle=c_A(t)=c_B(t)$, where the average is taken over all sites $\vec{r}$. In the following the used notation will be: $c(t)\equiv c_A(t)=c_B(t)$. $c_0\equiv c(t=0)=1.0$ is fixed for all the simulations presented in this work but we will be able to choose the initial distribution of reactants among several possibilities. Normally random and completely uncorrelated distributions of the concentrations are chosen. The standard example is the poissonian distribution which is the most commonly used throughout this work. It consists on distributing the whole amount of each reactant $M=c_0 \cdot V$ according to $p(k)=\mu^k \cdot e^{-\mu}/k!$, where $\mu=M/N$ and p(k) is the probability that a given cell

contains k 'particles'. Note that in this case we are initially discretizing the concentration values to $c_i(\vec{r},0)=k_{\vec{r}}/(\Delta x)^d$ because of the discrete form of the Poisson probability distribution.

Other random conditions that will be analyzed correspond to the so-called premixed and non-premixed random distributions. In both cases a given amount of A, equal to $2c_0$, is placed in randomly choosen $N/2$ cells of our system. The reactant B is distributed analogously. In the first case we do not care if one cell contains A and B, but in the second case we allow each cell to contain either A or B. Periodic and fractal initial distributions are also used in some sections of the following chapter.

On what respects to the values of K, $D_{A,B}$, L and t_{max}, the way we choose them here will depend on different factors. First, the core memory of our computers will determine $L=10^4$-10^5 for d=1, L=150-300 for d=2 and L=50-75 for d=3. Secondly, to detect the anomalous kinetic behaviors we have to work with fast reaction conditions, that implies large K. On the other hand, the value of K should also preserve the convergence limit of the prescribed discretization scheme. Note that we are working with parabolic differential equations with an additional non-lineal term. One can easily demonstrate that for this case the numerical convergence is guaranteed if $\frac{D\cdot\Delta t}{(\Delta x)^2}+K\Delta t<\frac{1}{2}$ [Smi85]. Consistently with this criterium, in our simulations K will be fixed to a maximum value of 10.

The reaction-diffusion equations will be integrated with periodic boundary conditions. This means that we have to be aware of the constraints imposed by a finite system size. Thus, although we will try to obtain behaviors that would be expected to persist forever in an infinite system, in the simulations they will persist only up to the time when the finite-size

effects appear. In practice, we will control these finite-size effects by never letting the linear mean cluster size exceed 0.2L. Taking into account that the mean cluster size will be equal to $2\pi\sqrt{Dt}$, t_{max} is determined according to $2\pi\sqrt{Dt_{max}} \leq 0.2L$; see Chapter III.

Finally, the value of $D_{A,B}$ will be fixed in such a way that the diffusion-limited behavior, on what respects to kinetics and spatial organization, will appear as robust as possible. This supposes to guarantee some kind of exponent-consistency that can be achieved by fixing the correct values of the diffusion coefficients according to the values of K and t_{max}. In order to reproduce the fluctuation-dominated behavior $D_{A,B} << K$ is fixed. Thus the diffusion transport will indeed be the limiting process in our diffusion-reaction system, but the exact values will depend on the dimensionality of the problem. In low dimensions the diffusion transport is less effective than in high dimensions due to the geometrical properties of the system; therefore we will need larger values of D for d=1 than for d=3. Normally, D=0.01 for d=3, D=0.1 for d=2 and D=1 for d=1 will be fixed.

The code was written in FORTRAN-77 and the calculation performed on the CRAY Y-MP/232 of Centre de Supercomputació de Catalunya (CESCA), on a HewlettPackard 720 Apollo workstation and on a Power Indigo-2 SiliconGraphics workstation. Graphic outputs of these simulations were performed by some C-software rutines that have been developed in the SiliconGraphics computer.

CHAPTER II

-Kinetic Laws: Analytic and Numerical Results-

This chapter containts a review of the analytic and numerical results concerning the kinetics of the A+B->0 diffusion-limited reaction.

In the fisrt section the systems with uncorrelated and random initial distributions of reactants that lead to the asymptotic $t^{-d/4}$ decay have been widely treated. This exponent has been obtained analytically for the case $D_A=D_B$ and it is also supported by the numerical results even in the cases with $D_A \neq D_B$. Different kinetic regimes that appear in some time scales before and after the fluctuation-dominated one have been also studied.

In the second section specific interest is focussed on the effect of other initial conditions, in particular those corresponding to random but correlated distributions. We have stressed that the initial pattern determines the future kinetics of the problem as if the system had some kind of 'memory'. This idea is once more verified here by analyzing both analytically and numerically the fractal and lamellar initial conditions.

SECTION II-1 -Random Initial Distributions-

II-1-a Theoretical Framework

For a random and non-correlated initial distribution of reactants one has under stoichiometrical conditions

$$\langle q(\vec{r}',0)q(\vec{r}'',0)\rangle = c_0\delta(\vec{r}'-\vec{r}'') \qquad \text{(II–1)}$$

so that Eq. (I-8) now reads

$$\langle q^2(t)\rangle = c_0\int\int d\vec{r}'d\vec{r}''\delta(\vec{r}'-\vec{r}'')G(0,\vec{r}',t)G(0,\vec{r}'',t) = c_0\int d\vec{r}'G^2(0,\vec{r}',t) \qquad \text{(II–2)}$$

Substitution of the expression of the Greens' function given by Eq. (I-10) into Eq. (II-2) leads to the following expression for $\langle q^2(t)\rangle$:

$$\langle q^2(t)\rangle = \frac{c_0}{4}\cdot(2\pi Dt)^{-d/2} \qquad \text{(II–3)}$$

Replacing $\langle q^2(t)\rangle$ given by Eq. (II-3) into Eq. (I-13) one obtains the Zeldovich behavior for diffusion-limited reactions:

$$c(t\to\infty) = \sqrt{\frac{c_0}{2\pi}}\cdot(2\pi Dt)^{-d/4} \quad \Rightarrow \boxed{c \sim t^{-d/4}} \text{ (for } d\leq 4) \qquad \text{(II–4)}$$

Thus, as we anticipated, the initial non-correlated inhomogeneities on diffusion-controlled systems lead to an anomalous kinetic regime whose long-time behavior is fluctuation-dominated. It is worth remarking here again that in this Thesis we use indistinctly the expressions 'fluctuation-dominated' and 'diffusion-controlled' referring to the effect of initial inhomogeneities on diffusion-controlled systems.

To emphasize this anomalous feature let's recall that the classical law can be obtained by solving Eqs. (I-1) and (I-2) under completely homogeneous conditions. This leads to:

$$c(t) = \frac{c_0}{1+c_0 K t} \qquad \text{(II–5)}$$

The overall behavior of the diffusion-controlled systems shows both regimes: before segregation occurs the reaction experiences a fast initial stage, due to the initial mixed distribution, obeying the classical law $c \sim t^{-1}$ as given by Eq. (II-5). After this transient regime, the reaction follows a slow kinetics, $c \sim t^{-d/4}$, due to the poor mixing efficiency of the diffusion transport and the subsequent clusterization of both reactants.

The crossover from the classical time behavior described by Eq. (II-5) to the long time one given by Zeldovich law in Eq. (II-4) occurs at times of the order of the segregation time t_s which will depend on the values of K, D and d. A qualitative estimation of this quantity can be obtained by making the curves $c_{zel}(t_s)$, Eq. (II-5), and $c_{clas}(t_s)$, Eq. (II-4) intersect at long times.

In Figure II-1a we have drawn generic curves of $c_{clas}(t)$ for two different values of K and asymptotic curves $c_{zel}(t)$ in d=2 for two different values of D. One can easily deduce from Eq. (II-4) that for a given d, $c_{zel}(t;D_1)$

> $c_{zel}(t;D_2)$ if $D_2 > D_1$ and from Eq. (II-5), $c_{zel}(t;K_1) > c_{zel}(t;K_2)$ if $K_2 > K_1$. As we have explained before, for each combination of K and D, the behavior first follows Eq. (II-5) and at long times Eq. (II-4) is reached. The transition between these two regimes takes place at times around the intersection of $c_{zel}(t)$ and $c_{clas}(t)$; see dotted lines in Fig. II-1a. Looking at Fig. II-1a one can realize that for a given dimensionality small crossover times are obtained if the value of K is large and D is small, that corresponds the diffusion-controlled case, because the system tends rapidly to separate A and B due to the high local reactions rate. Contrarily, for a small value of K and large D the system needs a lot of time to segregate due to the high mixing efficiency of the diffusion transport in relation to the local reaction process. This case corresponds to a K-controlled system.

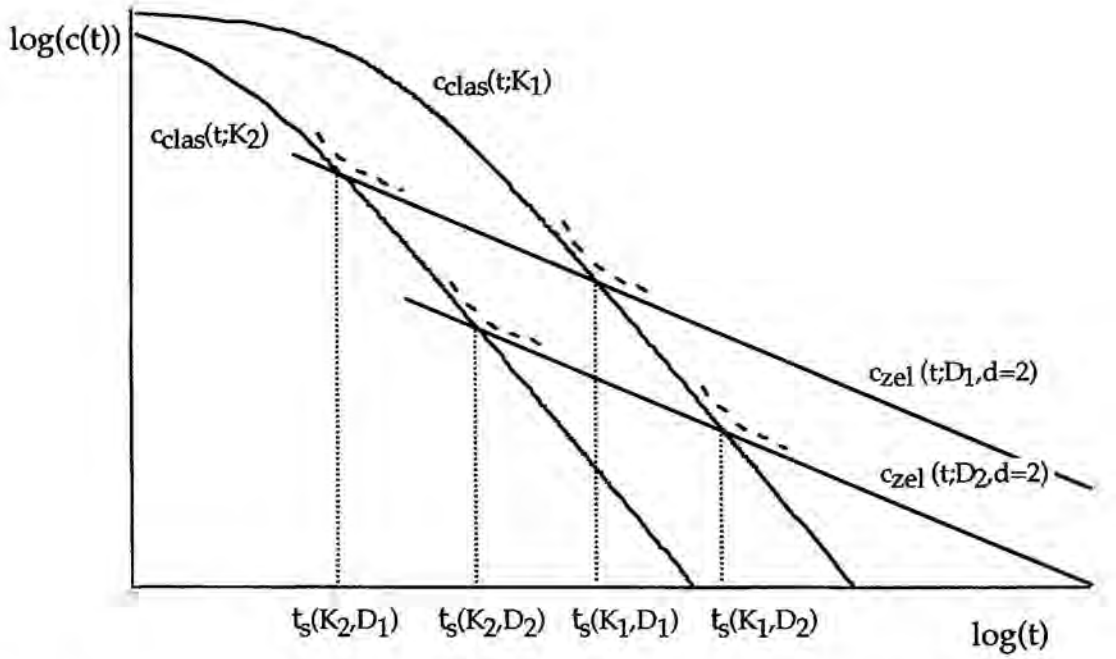

Fig. II-1- a) Generic curves of $c_{clas}(t)$ for two different values of K (with $K_2 > K_1$) and generic curves of $c_{zel}(t)$ in d=2 for two different values of D (with $D_2 > D_1$).

In Figure II-1b we have plotted a generic curve of $c_{clas}(t)$ and three curves of $c_{zel}(t)$ for the same diffusion coefficient but varying the dimensionality. In this case, the asymptotic values of the concentrations in $c_{zel}(t)$ are larger for smaller dimensionalities as one can easily deduce from Eq. (II-4). Notice that for the same values of K and D, $t_{s,1d} < t_{s,2d} < t_{s,3d}$. This means that for the same K smaller D values are required in high spatial dimensions to obtain the fluctuation-dominated kinetics within the same time window than for smaller dimensionalities. Diffusion is less effective in low dimensionalities.

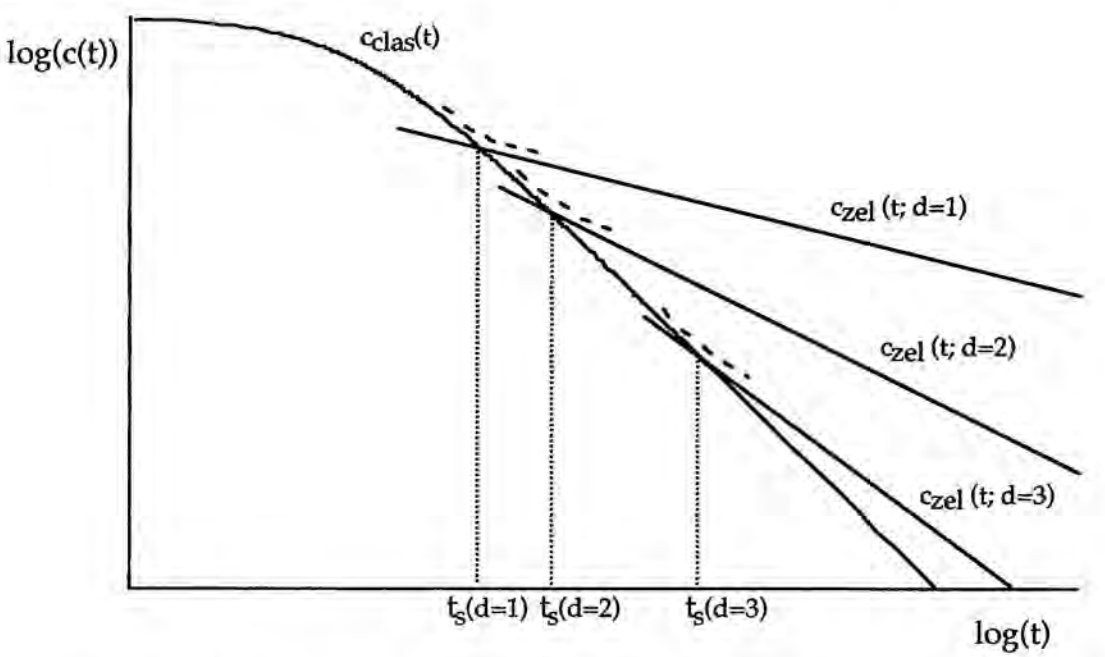

Fig. II-1- b) The same as in Fig. II-1a but now only one curve of $c_{clas}(t)$ and three curves of $c_{zel}(t)$ are depicted with the same diffusion coefficient but for the three different dimensionalities.

These conclusions are very important in order to select the values of K and D chosen to observe anomalous kinetic behaviors in the numerical simulations.

II-1-b Decay laws

We have seen that when $D_A=D_B$ holds, the system described by Eqs. (I-1) and (I-2) can be explored to a large extent analytically. This is due to the fact that the prevailing high symmetry of the problem allows us for introducing the sum and difference functions. For $D_A \neq D_B$ we can not proceed as in Eq. (I-3) since we would obtain a non-closed equation for q. Thus, we can only circumvent these cases by reverting to the numerical procedure. Similarly to what was found with particle-based simulations [Sok91f], the same fluctuation-dominated long-time behavior is found for the cases with equal or unequal diffusion coefficients in our continuum scheme [Rei96a].

For the sake of completeness in Figs. II-2 and II-3 the kinetic behaviors for several (D_A,D_B) values in d=1, 2 and 3 are presented. In Fig. II-2 c(t) is plotted in double-logarithmic scales and in Fig. II-3 the time evolution of the slope α for the log-log decay pattern is represented. According to the discussions about t_s in the last section, $D \equiv (D_A+D_B)/2$ is fixed to 1 in d=1, D=0.1 in d=2 and D=0.01 in d=3. With this choice of the diffusion coefficients values clear evidences of the fluctuation-dominated behavior are observed during a long time window for all three dimensionalities. We fix K=10 and 50 different realizations of poissonian initial distributions are run.

Three different combinations of D_B/D_A (1, 1/3 and 0) are plotted for each dimensionality. In Fig. II-2 one readly recognizes the asymptotic kinetics $c(t) \sim (Dt)^{-d/4}$ (for $d \leq 4$). This regime is obtained, regardless of the specific D_B/D_A ratio, in all three dimensions. The only difference between the equal and unequal diffusion coefficients cases can be observed looking at

Fig. II-3. This figure shows that the asymptotic regime is reached earlier when one of the reactive species becomes less mobile, i.e., when D_A and D_B differ very much. This is not at all surprising, since in the context of diffusion-limited reactions, clusterization and in turn anomalous decay laws are the signature of poor mixing efficiency.

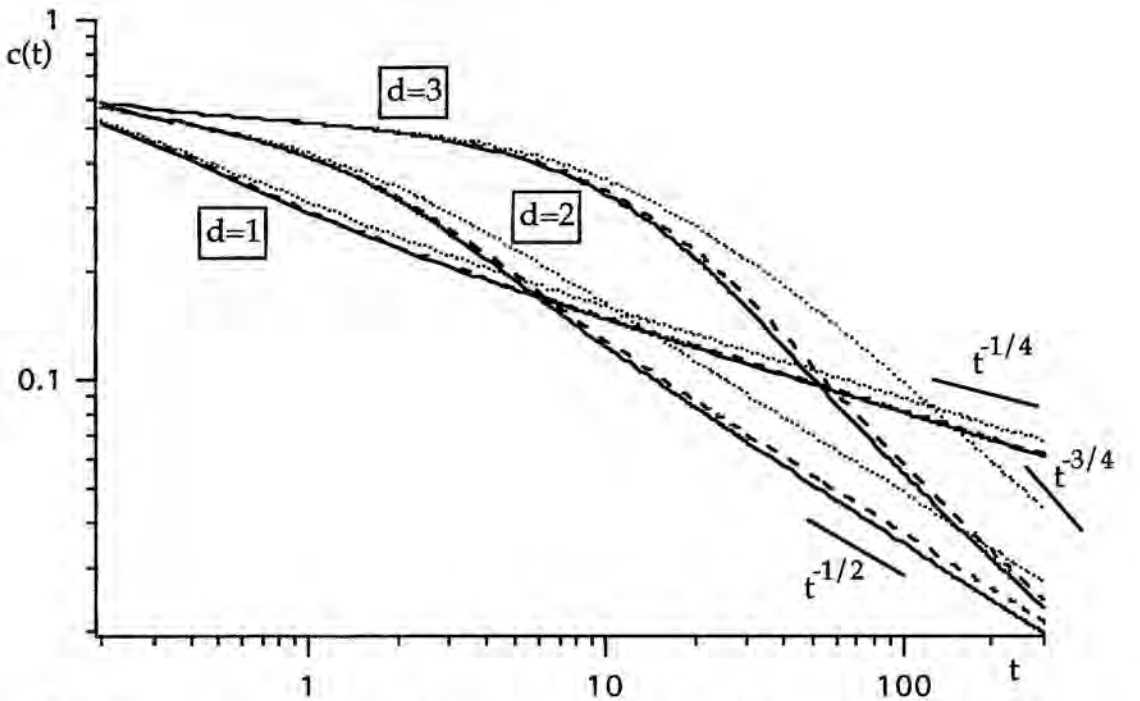

Fig. II-2- Concentrations as a function of time for different dimensionalities and different D_B/D_A ratios: 0 (dotted lines), 1/3 (dashed lines) and 1 (solid lines).

The differences between the predicted Zeldovich exponents and those numerically obtained in Fig. II-2 and II-3 are due to the fact that we are working with a finite reaction rate whereas the diffusion-limited prediction strictly considers $K=\infty$. Therefore, we could improve these exponents by increasing the value of K in our simulations. Notice also that this finite-

reaction-rate effect is more evident in the cases with a higher dimensionality, since in these systems the diffusion transport is more efficient and we need larger values of K to be in the limit of infinitely fast reactions.

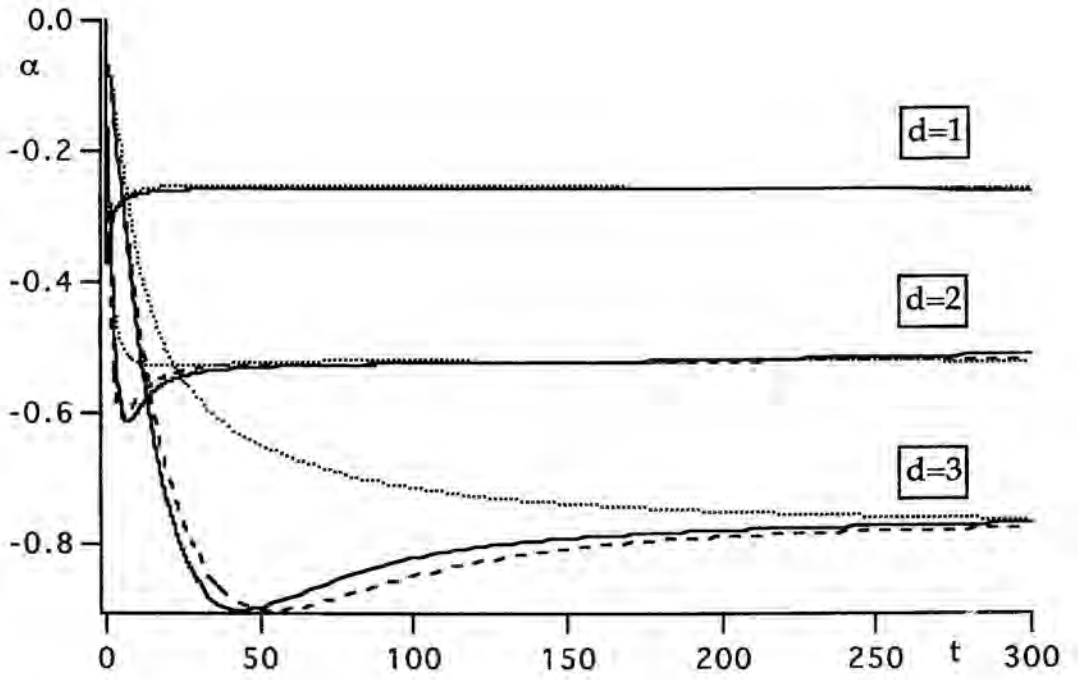

Fig. II-3- Time evolution of the slope (α) of the log-log concentrations decay of Fig. II-2.

It is finally worth noting here that discrete models predict, and their numerical simulations confirm, a transient $c \sim t^{-1/2}$ regime in the d=1 and 2 cases [Arg93]. In a discrete context the reason for this transient can be easily understood. After a short time, when all the nearest unlike particles has reacted, the 'survivers' ones fell a depletion zone at their surroundings. Obviously this depletion-zone transient can not be detected with our continuum model.

II-1-c Short and long time behaviors

In this section the whole sequence of behaviors including those before and after the fluctuation-dominated regime for random and non-correlated initial conditions are reviewed [San96]. In this way the constraints imposed by the reaction-diffusion approach are clearly established in this case.

Short time regimes:

We have argued previously that at extremely early times the kinetics of diffusion-limited systems is classical; that is, with a random distribution of reactants the concentration obeys the classical rate law $c \sim t^{-1}$. It was also noted that this behavior in low dimensions persists only for a time of order t_s, that depends on K, D and d; see Sect. II-1-a. On this time scale the distribution already begins to deviate from random distribution because of the reaction of physically contiguous A and B molecules. At these early times the reaction is in effect reaction-limited, rather than diffusion-limited, because only molecules that are already contiguous and therefore do not need to diffuse are involved. However, because here our analytic results are compared with those obtained numerically according to the discretization scheme described above, we are constrained from consideration of initial concentration inhomogeneities on a spatial scale smaller than Δx. In our discretized reaction-diffusion approach, A and B concentrations that coexist within one cell are consumed on a time scale K^{-1}, and each cell of area $(\Delta x)^2$ is, after a time K^{-1}, occupied essentially only by A or only by B. This implies that in our fast reaction case this classical transient is extremely short.

To illustrate the rapidity of this early behavior, the very early time behavior for two initial conditions is shown in Figure II-4. In both cases an equal amount of A, here set equal to $2c_0$, is randomly placed in half of the N cells of the two- dimensional system (L=150) and an equal amount of B in half of the cells. In the first case both A and B are placed in 25% of the cells ('premixed') and either A or B in 50% of the cells, and 25% of the cells are initially empty. This initial condition in some sense mimics a random initial condition. In the second case each cell contains either A or B ('separated'). The initial global concentration of each species is equal to c_0=1 in both cases. The solid curve in Fig. II-4 is the result of the numerical integration of the (discretized) reaction-diffusion equation with parameters K=1 and D=0.01 for the premixed initial condition. The dotted curve is the result of our numerical integration for the separated initial condition. Clearly, the latter decays more slowly than the former, and the premixed concentration acquires the same slope as the separated one after some time.

We compare the curve for the premixed initial density with an analytic formula to assess the time at which the diffusion first begins to affect the system. Ignoring the diffusion transport, the concentration of the premixed case will obey

$$c(t) = \frac{1}{4} c_{A\&B}(t) + \frac{1}{4} c_{\text{only}A}(t) \qquad \text{(II–6)}$$

where $c_{\text{only}A}(t)$ stands for the concentration inside the cells occupied only by A and $c_{A\&B}(t)$ is the concentration inside the cells occupied by A and B. In fact, $c_{\text{only}A}(t)$ is equal to $2c_0$ if we do not consider diffusion, and $c_{A\&B}(t)$ obeys the classical decay law in Eq. (II-5) replacing c_0 by $2c_0$. Thus,

$$c(t) = \frac{c_0}{4c_0Kt+2} + \frac{c_0}{2} \qquad \text{(II-7)}$$

The dashed line in Fig. II-4 represents this result. One can observe a good agreement between numerical and analytical results of Eq. (II-7) for the premixed case. The results shown in Fig. II-4 have been obtained by averaging over 20 different realizations of the initial conditions.

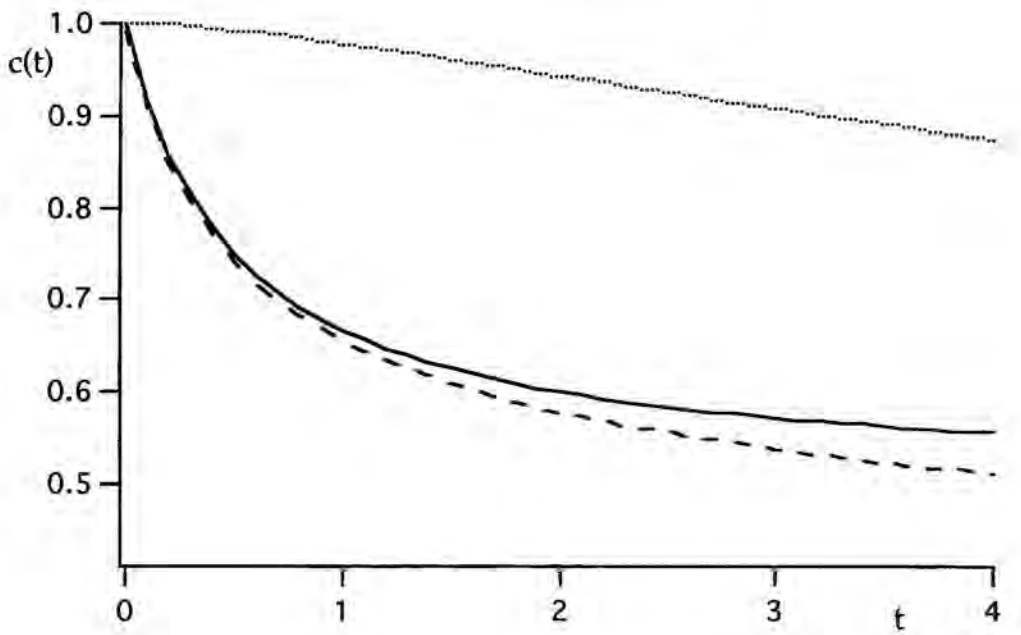

Fig. II-4- Initial kinetic behaviors for the two-dimensional reactant distributions discussed in this section for K=1 and D=0.01. Full line: simulation results for the 'premixed' case. Dotted line: simulation results for the 'separated' case. Dashed line: theoretical prediction in Eq. (II-7).

Long time regimes:

After the very early time behavior, the initially non-correlated system will follow the Zeldovich regime until the finite size effects typical of the numerical approach begin to appear. The segregation of species is obviously limited by the finite size of the system of the numerical scheme. In fact, the periodic boundary conditions will 'mix' the different species, clusters will tend to disappear and therefore the classical decay law $c \sim t^{-1}$ will be restored.

This intuitive conclusion can be analytically checked by considering that at very long times the Green's function has the same value for the whole L^d system. This occurs when its characteristic width $\sqrt{Dt} >> L$; then $G(\vec{r},\vec{r}',t\to\infty) = 1/V$ for all $\vec{r}'$ inside our finite system. Under this assumption Eq. (I-7) reads

$$q(\vec{r},t) = \int d\vec{r}' q(\vec{r}',0) G(\vec{r},\vec{r}',t) \Rightarrow q(\vec{r},t\to\infty) = 0 \qquad \text{(II–8)}$$

This implies that the system has been completely homogenized, since the value of the local difference function is 0. In this regime, the solution of Eq. (I-5) leads to a reaction-limited behavior ($c \sim (Kt)^{-1}$) rather than a diffusion-limited behavior.

In Figure II-5 one observes the progression just presented for several parameter values in a two-dimensional system. The earliest time behavior discussed above is not discernible because it occurs on a too short time scale. Contrarily, one clearly sees the Zeldovich regime $c \sim t^{-1/2}$, followed by a rapid decrease due to finite size effects. Finally, when the system has been homogenized, the classical decay takes over. The slope of this last classical decay is indeed the rate coefficient K. Note also that the finite size effects

appear before and that the asymptotic classical behavior is achieved more rapidly by the systems with the larger diffusion coefficient, as is expected since these systems homogenize more quickly.

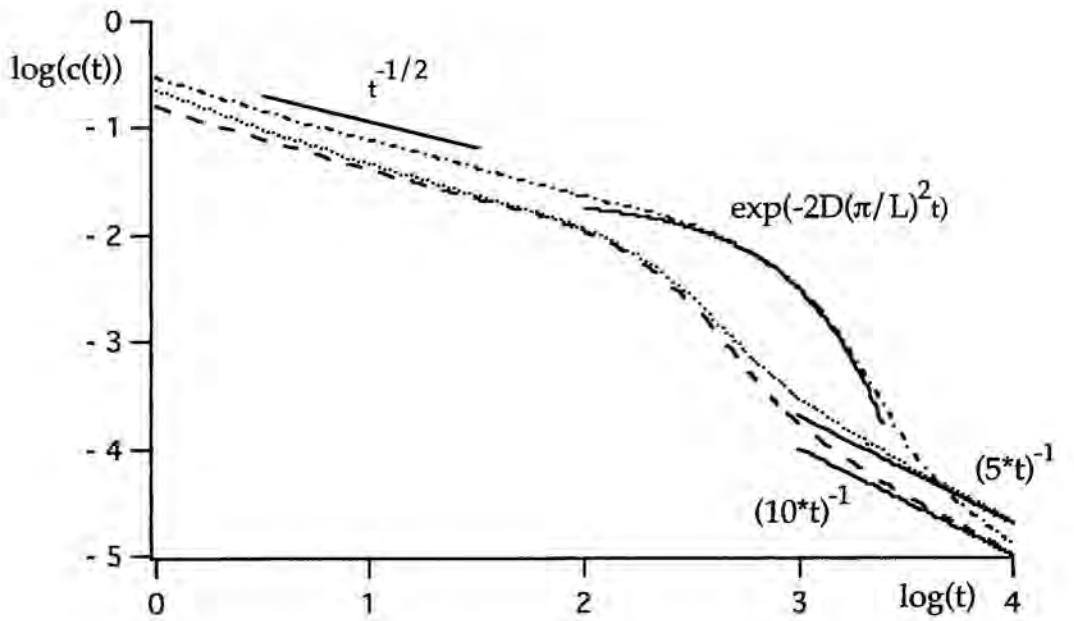

Fig. II-5- Zeldovich, exponential, and classical regimes for two-dimensional system with L=150. Dashed line: D=2 and K=10. Dotted line: D=2 and K=5. Dashed-dotted line: D=0.5 and K=10.

Notice also that the concentration drop caused by finite size effects that connect the fluctuation-dominated and the final classical regimes fits an exponential form as predicted for systems with periodic initial conditions. Actually, due to the periodic boundary conditions the kinetics of the reaction behaves as in the case of a system with an infinite chessboard initial distribution of reactants with squares of size L; see Section II-2-c. This occurs at long but non-asymptotic times when $\sqrt{Dt} \approx L$. The corresponding

exponential law of this kind of periodic systems is plotted with solid line for the case with D=0.5. In Fig. II-5, the full lines are a guide to the eye to be used in relation with the theoretical predictions. The results shown in this figure have been obtained by averaging over 20 different random realizations of initial conditions.

SECTION II-2 -Other Initial Distributions-

II-2-a Theoretical Framework

In this section we are going to push a little bit further the formulation developed in Sect. II-1-a for the estimation of $\langle q^2(t)\rangle$. The purpose is to obtain an expression for this quantity as a function of the initial distribution of reactants. This can be achieved by working with Eq. (I-8) in Fourier space.

First, for systems which are statistically homogeneous, the initial correlation function $g(\vec{r}',\vec{r}'')$ of the q's variables defined through

$$g(\vec{r}',\vec{r}'') = \langle q(\vec{r}',0)q(\vec{r}'',0)\rangle \qquad \text{(II–9)}$$

depends only on the difference of the arguments $\vec{r}'$ and $\vec{r}''$, i.e., $g(\vec{r}',\vec{r}'') = g(\vec{r}'-\vec{r}'')$. Thus, Eq. (I-8) now reads

$$\langle q^2(t)\rangle = \int\int d\vec{r}'d\vec{r}''g(\vec{r}'-\vec{r}'')\cdot G(0,\vec{r}',t)G(0,\vec{r}'',t) \qquad \text{(II–10)}$$

Since $G(0,\vec{r}',t)$ is symmetric in $\vec{r}'$ Eq. (II-10) corresponds to a double convolution with respect to $\vec{r}'$ and $\vec{r}''$. This allows one to express $\langle q^2(t)\rangle$ in terms of the spatial Fourier transforms of the g and G functions. Setting

$$\Gamma(\vec{k}) = \int g(\vec{r})e^{i\vec{k}\vec{r}}d\vec{r} \qquad \text{(II–11)}$$

for the Fourier transform of $g(\vec{r})$, and using the explicit Fourier transform

$e^{-Dt|\vec{k}|^2}$ of $G(0,\vec{r},t)$ in Eq. (I-10), we obtain

$$\langle q^2(t)\rangle = \frac{1}{2\pi}\int \Gamma(\vec{k})e^{-2Dt|\vec{k}|^2}d\vec{k} \qquad \text{(II–12)}$$

Now, the normal procedure will be the following: from the initial distribution of reactants one calculates the difference variable and its corresponding correlation function $g(\vec{r}',\vec{r}'')$. Making the Fourier transformation, Eq. (II-11) of $g(\vec{r}',\vec{r}'')$ one obtains $\Gamma(\vec{k})$ that once integrated according to Eq. (II-12) will provide us directly with the behavior of $\langle q^2(t)\rangle$. Later on, and applying $c(t) \sim \sqrt{\langle q^2(t)\rangle}$ from Eq. (I-13), the decay concentration law according to the corresponding inital distribution is obtained.

According to Eq. (II-12) the asymptotic behavior for $t\to\infty$ will depend on the behavior of $\Gamma(\vec{k})$ for very small values of $|\vec{k}|$. In most of the cases, at least all those considered here, the structure function corresponding to the initial distribution of the difference variable can be expressed as a power law, i.e. $\Gamma(\vec{k}) \sim |\vec{k}|^{\beta}$, at least for the small enough $|\vec{k}|$-values here relevant. Then, the $\langle q^2(t)\rangle$ behavior is given by the asymptotic law

$$\langle q^2(t)\rangle \sim t^{-(d+\beta)/2} \qquad \text{(II–13)}$$

and therefore the concentration decay follows

$$c(t) \sim t^{-(d+\beta)/4} \qquad \text{(II–14)}$$

In the case of random and non-correlated initial distributions of reactants, i.e. the poissonian, the random premixed and the random separated distributions used in the former chapter, the value of $\Gamma(\vec{k})$ is a constant that does not depend on $\vec{k}$. Thus, applying the Eqs. (II-13) and (II-14) the Zeldovich asymptotic regime $c(t) \sim t^{-d/4}$ is recovered.

II-2-b Fractal Initial Conditions

In this section we consider the case in which the initial distribution of reactants is a fractal pattern of fractal dimension $D_f<2$ contained in a two-dimensional system. It is important to differentiate between this kind of initial conditions and the cases where not only the initial distribution but the overall reaction is confined to a fractal support [Ana87, Kop88, Cle90, Lin91, Sok91g, Zum91]. In this section our system will have d=2 although the reactants initial patterns will be fractal.

The initial distribution is generated as follows: the number N of cells in a row is chosen to be a power of 4, $L=4^n$, so the entire system has $\frac{4^{2n}}{(\Delta x)^2}$ cells. We divide L by 4, thereby generating 16 square domains, each of which contains $\frac{4^{2n-2}}{(\Delta x)^2}$ cells. Of these 16, a number m<16 is selected at random. The domains not selected remain empty. Each of the m selected domains is again divided into 16 subdomains, and again m of these are selected for further consideration while those not selected remain empty. We continue this process until the selected domains are as small as possible, that is, the area $(\Delta x)^2$ of an elementary cell. Finally, a constant concentration equal to 1 of one of the reactants is put in all the selected elementary cells. The process is repeated for the second reactant. This leads to a fractal geometry of occupied cells of dimension $D_f = \ln(m)/\ln(4)$ [Vic92]. The initial distribution of the q variable is also characterized by this fractal dimension, and $\Gamma(\vec{k})$ for small $|\vec{k}|$ behaves as a power law with an exponent given by the fractal dimension,

$$\Gamma(\vec{k}) \sim |\vec{k}|^{-D_f} \qquad \text{(II-15)}$$

Note that the exponent is negative; that is the long-wavelength components are enhanced relative to those of a random initial distribution. It should also be noted that the patterns generated in this manner are not ideal fractals because we stop the subdivision at a finite cell size. The largest systems have L=256, so we only go through four generations of subdivisions. Notice that the initial overall concentration value c_0 is equal to $(m/16)^n$, where n is the number of subdivisions that we have done when distributing the reactants. Figure II-6 shows a typical initial pattern with m=10, leading to a fractal dimension D_f=1.66. We notice that in this figure only the initial distribution of one reactant is shown.

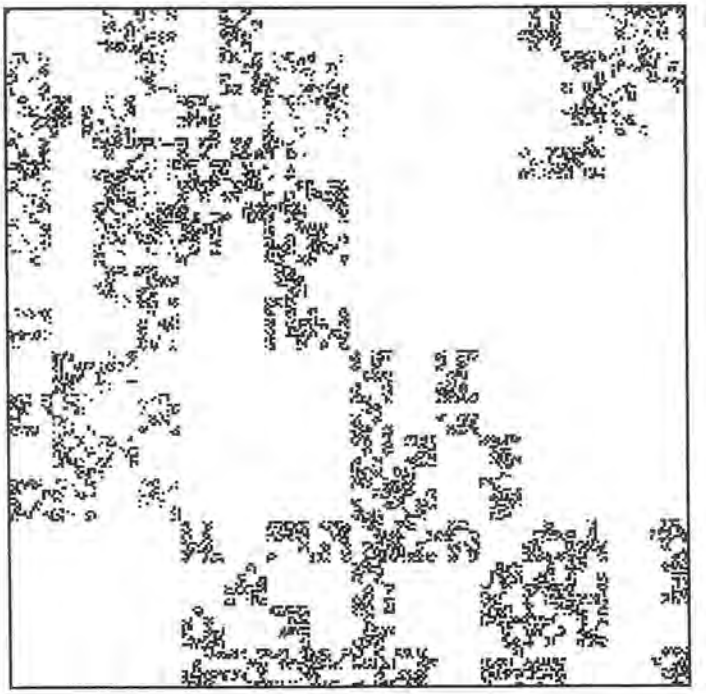

Fig. II-6- Initial pattern of one of the reactants for a two-dimensional system with L=256 and a fractal dimension D_f=1.66.

Consider now the sequence of behaviors that might be expected with this initial condition. Since there may be some premixed cells, there will be a very rapid decay of concentration of these cells as was shown in Section II-1-c. Once this is over, a lull in the activity is expected since aside from the premixed cells, occupied cells are in general quite separate. Indeed, if the fractal dimension is too high, then there are many premixed cells and much of the reactant disappears during the very early time regime. The quiescent period then dominates the time evolution because there is little reactant left and it takes a very long time for reactants to find one another.

During the quiescent period the distribution is rather segregated and the expression of $\langle q^2(t) \rangle$ using Eq. (II-13) and Eq. (II-15) reads

$$\langle q^2(t) \rangle \sim t^{-(d-D_f)/2} \qquad \text{(II–16)}$$

and thus

$$\langle c(t) \rangle \sim t^{-(d-D_f)/4} \qquad \text{(II–17)}$$

Note that this decay is even slower than the Zeldovich behavior. This decay continues until finite size effects and the subsequent classical behavior described earlier takes over.

Figure II-7 shows the results of the numerical integration of the reaction-diffusion equations and the prediction in Eq. (II-17). The very early time behavior discussed above is not visible: indeed, we have chosen parameters so as to shorten those regimes and clearly exhibit the quiescent regime predicted in Eq. (II-17). The 64x64 size system is too small to show any distinctive behavior; finite size effects set in quite before the simulation

finishes. The 256x256 size system clearly shows the slow decay induced by the fractal initial pattern. Actually, the slope of the decay curve follows closely the theoretical line.

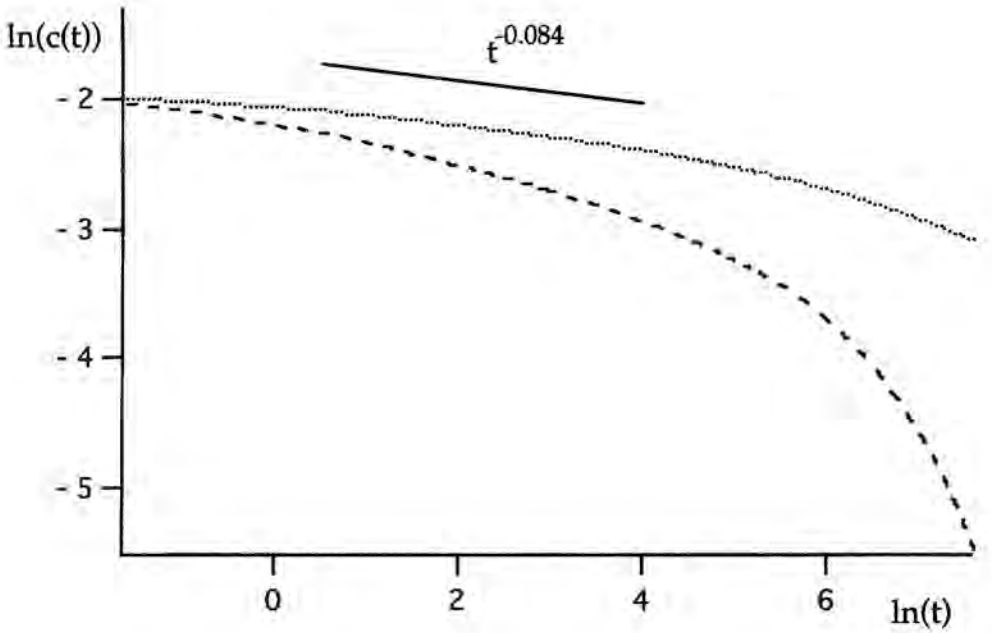

Fig. II-7- Kinetics for the fractal initial pattern shown in Figure II-6. The parameter values are D=0.1, K=10. Solid line: Eq. (II-17). Dashed line: numerical integration with L=64. Dotted line: numerical integration with L=256.

II-2-c Lamellar Initial Conditions

Finally, in this section the kinetic behavior of systems initially distributed in a d-dimensional array of lamellae is studied. The investigation of diffusion-controlled reactions in this kind of systems have received much attention in recent years in relation with different mixing procedures [Sok91d, Sok91e, Muz89a, Muz89b]. More or less complex lamellar structures, consisting of stretched and folded striations, are generated during the mechanically mixing of initially separated A and B reactants [Ott88]. The initial preparation of the system can then be understood in the following way. The system is created by first mixing the nonreacting solutions with A and B initially separated, a procedure which leads to a striation pattern; then the reaction is turned on, for example by a rise in temperature which triggers the thermally activated reactive processes. The kinetic study of this (d+1)-dimensional stirred system is reduced then to the study of a d-dimensional lamellar system in our diffusion-limited context. In this section we work with d=1, from the mixing of two-dimensional initially separated systems, and d=2, from the mixing of three-dimensional initially separated systems.

In d=1 the lamellar system is initially structured according to intervals of A or B with random thicknesses given by the distribution p(l) of striation thicknesses. The same distribution for both reactants is assumed and initial concentrations in the intervals are taken to be equal to c_0. The first and the second moments of p(l) can be simply introduced

$$L_1 = \int_0^\infty l p(l) dl \qquad \text{(II–18)}$$

and

$$L_2 = \int_0^\infty l^2 p(l) dl \qquad \text{(II–19)}$$

An analytical approach for the $\Gamma(k)$ function in this case is fully developed in [Sok91d]. Since we are only interested in the limit of very small k values, the relevant quantity will be the zero-k value of the structure function which reads

$$\Gamma(k=0) = c_0^2 \frac{L_2 - L_1^2}{L_1} \qquad \text{(II–20)}$$

Substituting Eq. (II-20) into Eq. (II-12) one obtains

$$\langle q^2(t) \rangle = \frac{1}{\sqrt{8\pi Dt}} c_0^2 \frac{L_2 - L_1^2}{L_1} \qquad \text{(II–21)}$$

and by replacing this result in Eq. (I-13) the concentration decay leads to

$$c(t) = \frac{1}{\sqrt{2\pi}} \left[\frac{L_2 - L_1^2}{L_1} \right]^{1/2} c_0 (8\pi Dt)^{-1/4} \qquad \text{(II–22)}$$

This result clearly reproduces the Zeldovich behavior.

Notice that Eqs. (I-13) and (II-12) are valid only if the difference function q can be considered Gaussian. This means that Eq. (I-7) has to represent a sum over many independent random variables corresponding to

the initial values of q. In this case, this only occurs when the characteristic width $\sqrt{Dt}$ of the Green's function exceeds a finite correlation radius l_c whose value is estimated as $(L_2-L_1^2)/L_1$ in [Sok91d]. Thus, the Zeldovich regime will appear in these systems $\sqrt{Dt}>>(L_2-L_1^2)/L_1$ and until the finite size effects appear for $\sqrt{Dt}\approx L$. Note that for purely random initial conditions the correlation radius l_c is of the order of the cell size, and therefore the Zeldovich behavior will appear earlier than for lamellar initial distributions.

In d=2, the system is initially distributed on rectangles of A and B with random areas given by the distribution function p(s). In this case, the same analytical calculation can be done and the corresponding Zeldovich regime $c \sim t^{-1/2}$ can be also found.

To summarize all these results, Figure II-8 shows the log-log concentration decay for this kind of lamellar systems in d=1 and d=2. For comparison we also plot the decay patterns corresponding to the poissonian initial distributed cases that we showed in Section II-1-b for d=1 and d=2. Both cases in d=1 are simulated with L=10000, K=10, $D_A=D_B=1$ and $c_0=1$ distributed in a poissonian way or using intervals of random length from 0 to 20. The cases in d=2 are run fixing L=150, K=10, $D_A=D_B=0.1$ and $c_0=1$ distributed in a poissonian way or filling rectangles of random side from 0 to 10. All the calculations have been averaged over 50 different initial distributions.

It is easily observed that the curves of the periodic systems become parallel to the corresponding random ones at longer times. Then, the Zeldovich regime is achieved for these systems as has been demonstrated in Eq. (II-22) but it is also clear that they need more time to reach such an asymptotic regime as it is expected from the condition $\sqrt{Dt}>>l_c$. In Figure II-9

we have drawn the time evolution of a spatial pattern corresponding to one realization of the lamellar system in d=2 for the same simulation parameters of Fig. II-8.

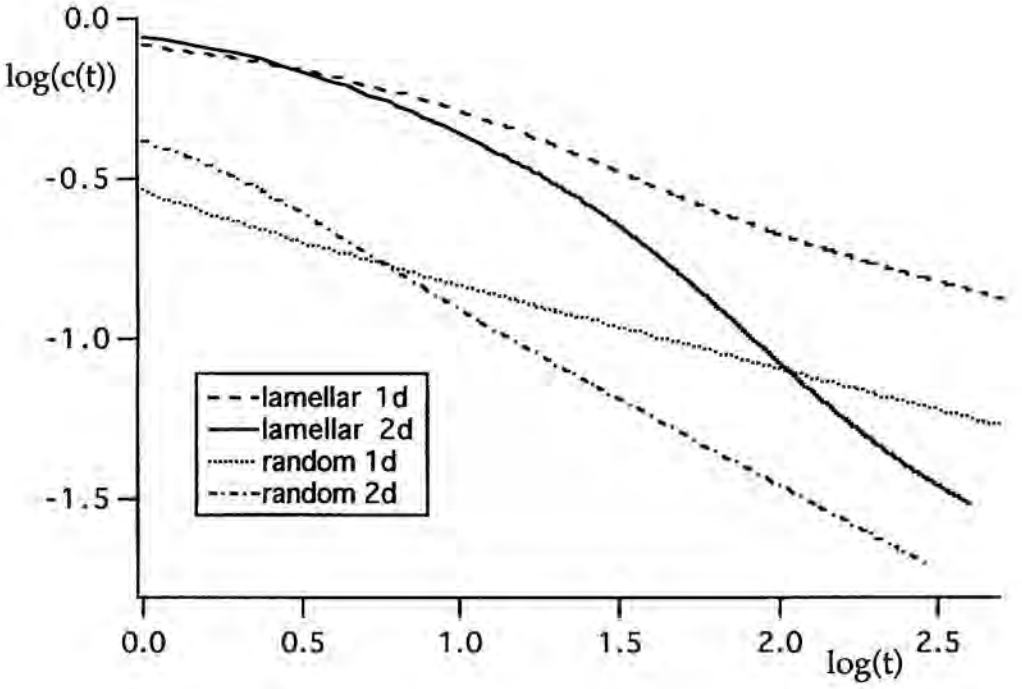

Fig. II-8- Kinetic behavior of the lamellar systems in d=1 (dashed line) and d=2 (solid line). For comparison the decay of concentrations for the poissonian initial distributed systems are also plotted for d=1 (dotted line) and d=2 (dashed-dotted line).

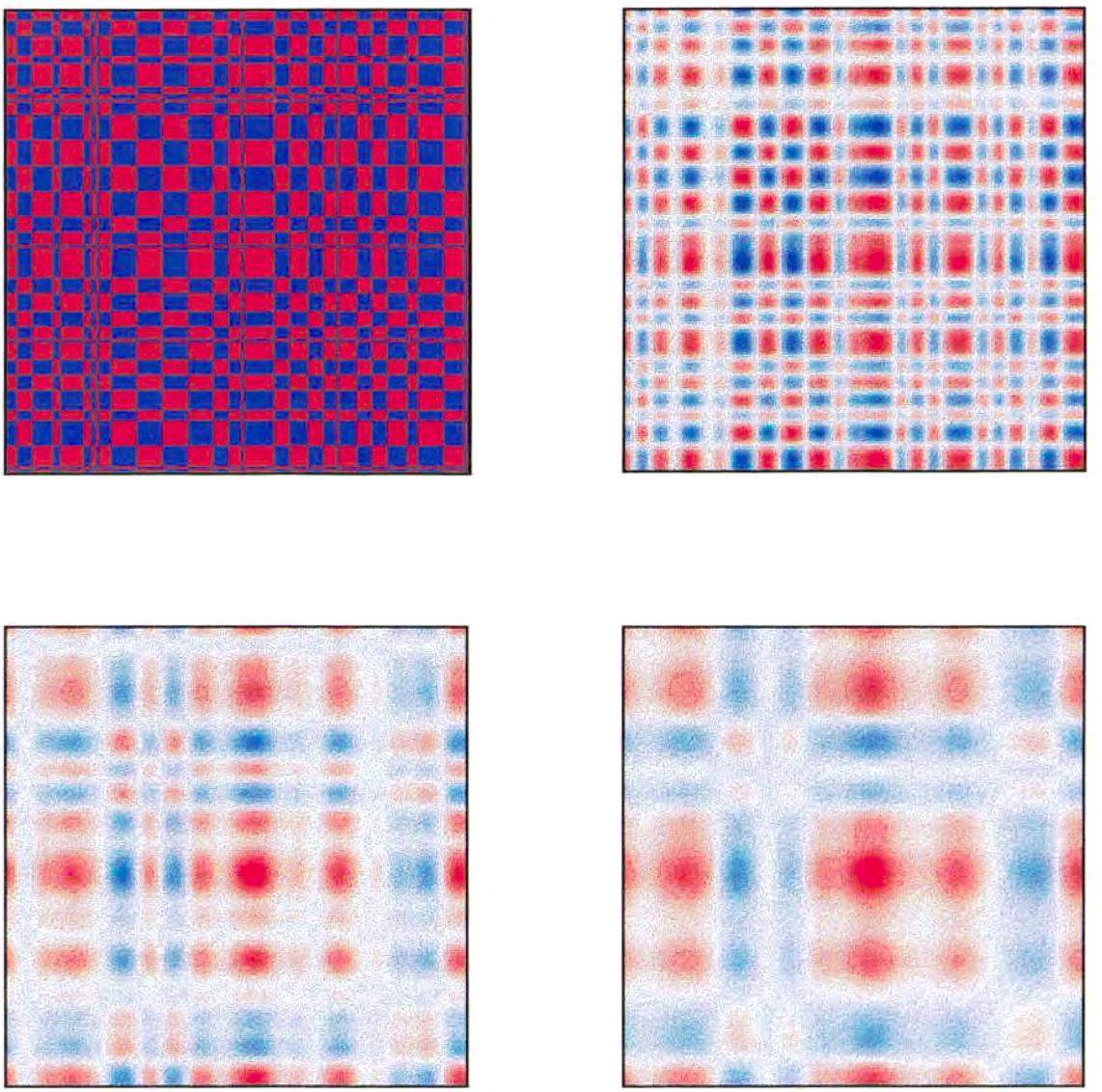

Fig. II-9- Time evolution of a red (A) and blue (B) pattern corresponding to one realization of the lamellar 2D-system of Fig. II-8. The snapshots correspond to t=0, 50, 100 and 200.

A particular case of these previously mentioned behaviors corresponds to the case of strictly periodic systems. In this situation the corresponding $\Gamma(k)$ function is [Sok91d]

$$\Gamma(k) = c_0^2 \sum_{j=0}^{\infty} \frac{4L_1}{(2j+1)^2} \delta(kL_1 - \pi(2j+1)) \qquad \text{(II–23)}$$

for d=1 and

$$\Gamma(k_x,k_y) = c_0^2 \sum_{i=0}^{\infty} \sum_{j=0}^{\infty} \frac{16L_1^2}{(2i+1)^2(2j+1)^2} \delta(k_x L_1 - \pi(2i+1)) \, \delta(k_y L_1 - \pi(2j+1)) \qquad \text{(II–24)}$$

for d=2. Proceeding in the usual way:

$$\langle q^2(t) \rangle \sim c_0^2 \sum_{j=0}^{\infty} \frac{1}{(2j+1)^2} \exp\left(-2\pi^2(2j+1)^2 \frac{Dt}{L_1^2}\right) \Rightarrow c(t) \sim c_0 \exp(-\pi^2 Dt/L_1^2) \qquad \text{(II–25)}$$

for d=1 and

$$\langle q^2(t) \rangle \sim c_0^2 \sum_{i=0}^{\infty} \sum_{j=0}^{\infty} \frac{1}{(2i+1)^2(2j+1)^2} \exp\left(-2\pi^2 \frac{Dt}{L_1^2}\left((2i+1)^2+(2j+1)^2\right)\right)$$

$$\Rightarrow \qquad c(t) \sim c_0 \exp(-2\pi^2 Dt/L_1^2) \qquad \text{(II–26)}$$

for d=2. Let's stress here that the decay of the reactant's concentration follows now an exponential, and not a power law. Note that for periodic systems the boundaries of the lamellas do not move, and the concentration in each lamella decays according to the same law, actually corresponding to the case of an interval or square with absorbing boundaries.

In Figure II-10 one observes the kinetic behavior of the strictly periodic systems in d=1 and d=2. All the simulation parameters are the same as in Fig. II-8 but now the initial distribution of reactants consists on intervals with fixed length or fixed area. For comparison we have also drawn the slopes predicted in Eqs. (II-25) and (II-26). In d=1, D=1 and L_1=10, thus the predicted slope is equal to -0.098. In d=2, D=0.1 and L_1=5, then the predicted slope is equal to -0.078. Good agreement is observed in both cases. In Figure II-11 we have drawn the pattern time evolution of a strictly periodic system in d=2 for the same simulation parameters of Fig. II-10.

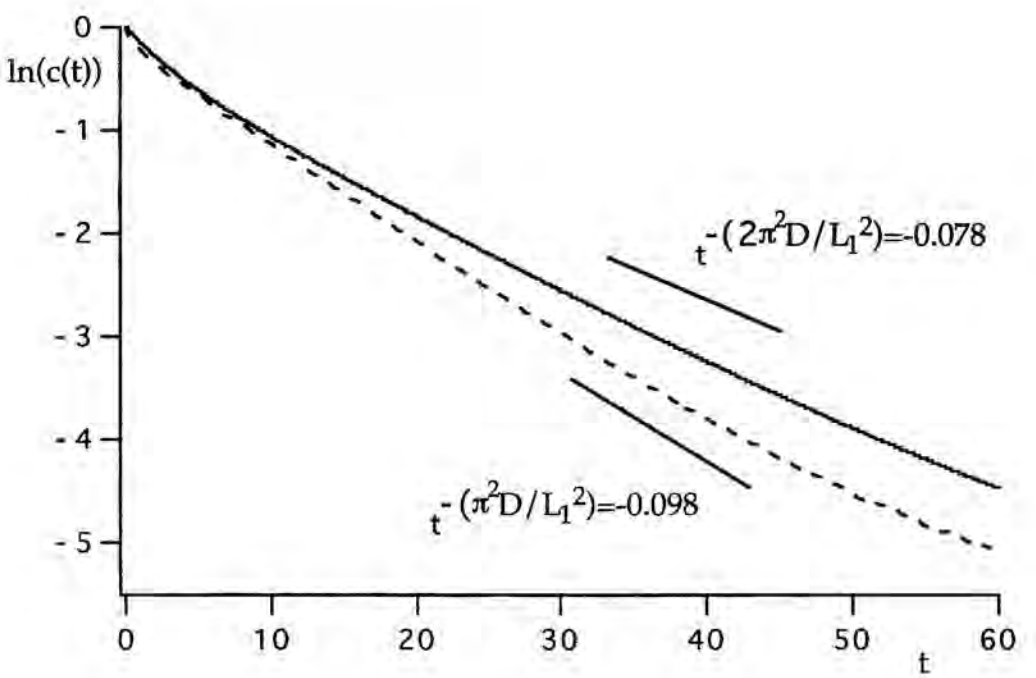

Fig. II-10- Kinetic behavior of the strictly periodic systems in d=1 (dashed line) and d=2 (solid line). For comparison the slope of the theoretical predictions are also plotted.

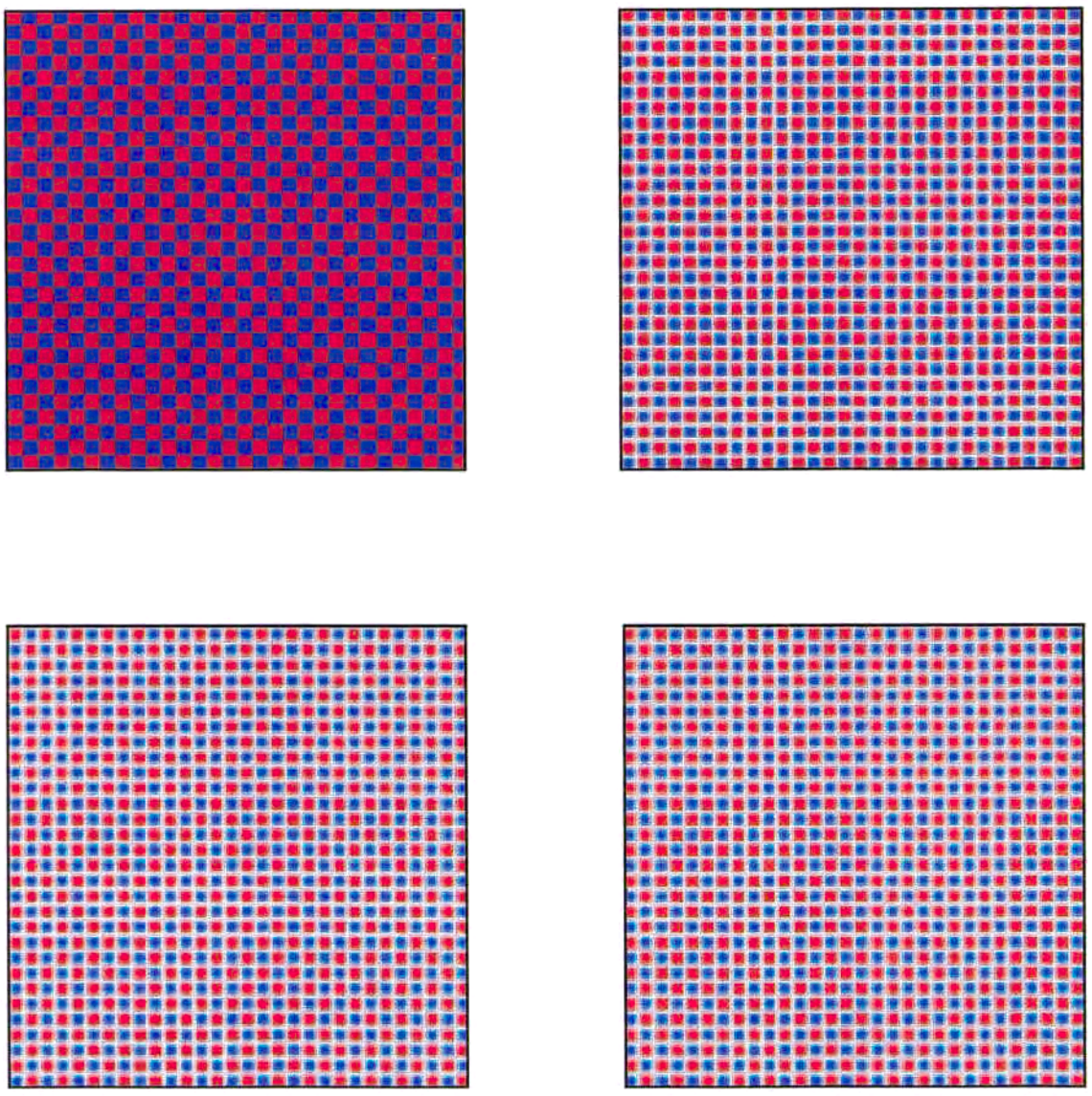

Fig. II-11- Time evolution of a red (A) and blue (B) pattern for the strictly periodic 2d-system of Fig. II-10. The snapshots correspond to t=0, 25, 50 and 100.

CHAPTER III

-Spatial Organization-

In this chapter we will concentrate on the spatial structures that make the decay of the reactants' concentrations slow down. An initially random and non-correlated distribution of reactants is assumed in all this morphological study [Rei96a].

As we mentioned in the introduction of this Part I, the continuum model will allow us to deal in a easier way with morphological variables. In discrete models for one dimension the geometrical arrangement of the system can be well-defined with the statistical treatment of l_{AA}, l_{AB} and L variables showed in this picture [Ley91]

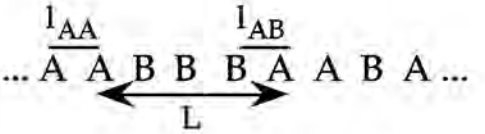

In greater than one dimension, these quantities are less easily defined. In particular, ambiguity arises in the calculation of cluster size L for d>1 [Ley92]. In this chapter we will show that our continuum approach provides a more coherent and handy spatial description of the system.

The clusters emerging during the reaction will be analyzed in terms of correlation functions and cluster cross-section distributions. A standard way is to use density-density correlation functions. For the concentrations of the same species we have

$$C_{AA}(r,t) = \frac{\langle c_A(\vec{r}'+\vec{r},t)c_A(\vec{r}',t)\rangle_{\vec{r}'}}{\langle c_A(\vec{r},t)\rangle_{\vec{r}}^2} \qquad \text{(III–1)}$$

and similarly for $C_{BB}(r)$. For different species one has

$$C_{AB}(r,t) = \frac{\langle c_A(\vec{r}'+\vec{r},t)c_B(\vec{r}',t)\rangle_{\vec{r}'}}{\langle c_A(\vec{r},t)\rangle_{\vec{r}}\langle c_B(\vec{r},t)\rangle_{\vec{r}}} \qquad \text{(III–2)}$$

Note that in both cases spatial averages are indicated even though in our numerical results averages over different initial distributions are also performed. As we explained previously, in the cases studied in this Thesis both averages are identical since the averaged initial distributions do not depend on $\vec{r}$. Moreover, in the case of the correlation functions (Eqs. (III-1) and (III-2)) a radial-average is made for all the values of $\vec{r}$ with the same value of $r = |\vec{r}|$.

The observation of the correlation functions will give us an idea on the degree of segregation in the system. Note that in presence of segregation one has that for small r the correlation functions follow $C_{AB}(r\to 0,t) \approx 0$ as we

can deduce easily from Eq. (III-2) and $C_{AA}(r\to 0,t) \approx \pi$ from Eq. (III-1) and due to the gaussian feature of the problem. Only for large distances r these functions tend to unity. Whereas, completely homogenized systems show $C_{AA}(r,t) \approx C_{AB}(r,t) \approx 1$ for all r. Largely differing correlation functions at the origin will be thus a distinctive signature of strong segregation.

Furthermore, clusters are easily defined in terms of the concentrations. Actually all what we need is to consider the difference function $q(\vec{r},t) \equiv \frac{c_A(\vec{r},t)-c_B(\vec{r},t)}{2}$, which vanishes at the boundaries of the clusters. Hence it is sufficient to determine the zeros of the $q(\vec{r},t)$ in order to have the cluster structure; e.g., for $d\neq 1$ we obtain the distribution of cross sections from the zeros of $q(\vec{r},t)$ along arbitrary straight lines drawn through the system. In d=1, 100 realizations of initial concentrations distributions are taken. In d=2 and 3 we use some 50 realizations and for each realization and at each needed time the zeros of $q(\vec{r},t)$ are determined along 50 random straight lines drawn parallel to the coordinate axis.

For all the simulations in this chapter we take lattices of sidelength L=10000 in d=1, L=150 in d=2 and L=50 in d=3. Time and space are discretized by increments of $\Delta t=0.01$ and $\Delta x=1$ respectively. The initial density distribution is taken to be poissonian (any other random non-correlated distribution would show the same results) with stoichiometrical conditions $c_A(0) = c_B(0) = 1$. We have fixed K=10 and $D_{A,B}=1$ for d=1, $D_{A,B}=0.1$ for d=2 and $D_{A,B}=0.01$ for d=3. The finite-size effects do not appear in any of our results by finishing the simulation before the mean cluster size exceed 0.2L.

We now turn to the presentation of the results, and consider the cases $D_A=D_B$ and $D_A\neq D_B$ separately.

SECTION III-1 -Case $D_A = D_B$-

We start by presenting in Fig. III-1 the correlation functions $C_{AA}(r,t)$ and $C_{AB}(r,t)$ for a bidimensional system with equal diffusion coefficients. Fig. III-1 shows clearly that the system is segregated for the three plotted times since $C_{AA}(r \to 0,t) \approx \pi$ and $C_{AB}(r \to 0,t) \approx 0$. One can also see that the clusters are growing looking at the growth with time of the width of both correlation functions.

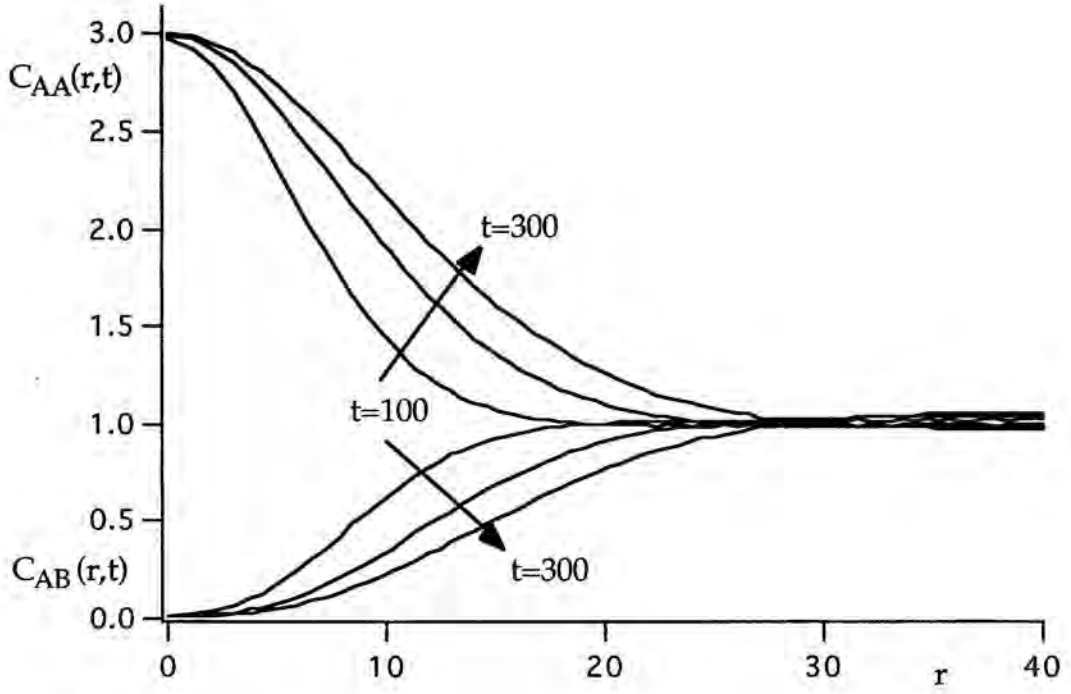

Fig. III-1- Density-density correlation functions $C_{AA}(r,t)$ and $C_{AB}(r,t)$ for d=2. Three times are displayed: t=100, 200 and 300.

Nevertheless, the main point in this Section consists on finding a superuniversal behavior of both correlation and cluster cross section functions. On what respects to the correlation functions, if we plot the results of Fig. III-1 adding the results from other dimensionalities, see Fig. III-2, and from other values of D, we would find that by presenting the curves as functions of the scaled variable $r/(Dt)^2$, all the plots would fall on the same master curve. This is an indication of superuniversal behavior, since the correlation functions behave independently of t, D and d, as a segregation signature of systems under fluctuation-dominated conditions. We interpret that the reason for this behavior arises from the fact that $D_A=D_B$, which renders $q(\vec{r},t)$ Gaussian in space as it was deduced from the solution of Eq. (I-3) in Section I-2.

The two-point correlation of the $q(\vec{r},t)$ function can be defined in this way

$$R(\vec{r}_1,\vec{r}_2,t) \equiv \langle q(\vec{r}_1,t)q(\vec{r}_2,t)\rangle \qquad \text{(III–3)}$$

The expression for $q(\vec{r},t)$ is given by Eq. (I-7). Substituting the Green's function for the diffusion equation given by Eq. (I-10) and taking into account that Eq. (II-1) implies that the initial $q(\vec{r},t)$ values are δ-correlated, Eq. (III-3) now reads

$$R(r,t) = c_0(8\pi Dt)^{-d/2}\exp(\frac{-r^2}{8Dt}) \qquad \text{(III–4)}$$

with $r=|\vec{r}_1-\vec{r}_2|$.

In the diffusion-limited case, for $K\to\infty$, the cluster boundaries are very narrow. Evidently, to a very good approximation Eqs. (I-11) and (I-12) hold

and from these expressions the correlation functions in Eqs. (III-1) and (III-2) follow [Vit88]:

$$\langle c_A(\vec{r},t)c_X(\vec{r}+\vec{r}',t)\rangle = \int_0^\infty \int_{-\infty}^\infty q_1 q_2 \theta(\pm q_2) P(q_1,q_2;\vec{r}')\, dq_1 dq_2 \qquad \text{(III-5)}$$

where the sign is positive for X=A and negative for X=B. Moreover

$$P(q_1,q_2;r) = \frac{1}{2\pi R(0,t)\sqrt{1-g^2}} \exp\left(-\frac{q_1^2+q_2^2-2q_1q_2g}{2R(0,t)(1-g^2)}\right) \qquad \text{(III-6)}$$

is the two-point joint probability density for $q(\vec{r},t)$ averaged over all the values of $\vec{r}$ with the same value of $r=|\vec{r}|$, with

$$g(r,t) = \frac{R(r,t)}{R(0,t)} = \exp\left(\frac{-r^2}{8Dt}\right) \qquad \text{(III-7)}$$

The evaluation of the integrals in Eq. (III-5) now readily gives [Vit88]

$$C_{AA}(r,t) = (1-g^2)^{3/2} + g^2(1-g^2)^{1/2} - g \arctan\left(\frac{(1-g^2)^{1/2}}{g}\right) + \pi g \qquad \text{(III-8)}$$

and

$$C_{AB}(r,t) = (1-g^2)^{3/2} + g^2(1-g^2)^{1/2} - g \arctan\left(\frac{(1-g^2)^{1/2}}{g}\right) \qquad \text{(III-9)}$$

In Fig. III-2 we present the correlation functions $C_{AA}(r,t)$ and $C_{AB}(r,t)$ as functions of the scaling variable $r/(Dt)^2$ at different times and different dimensionalities. The analytical expressions Eqs. (III-8) and (III-9) are also plotted in Fig. III-2.

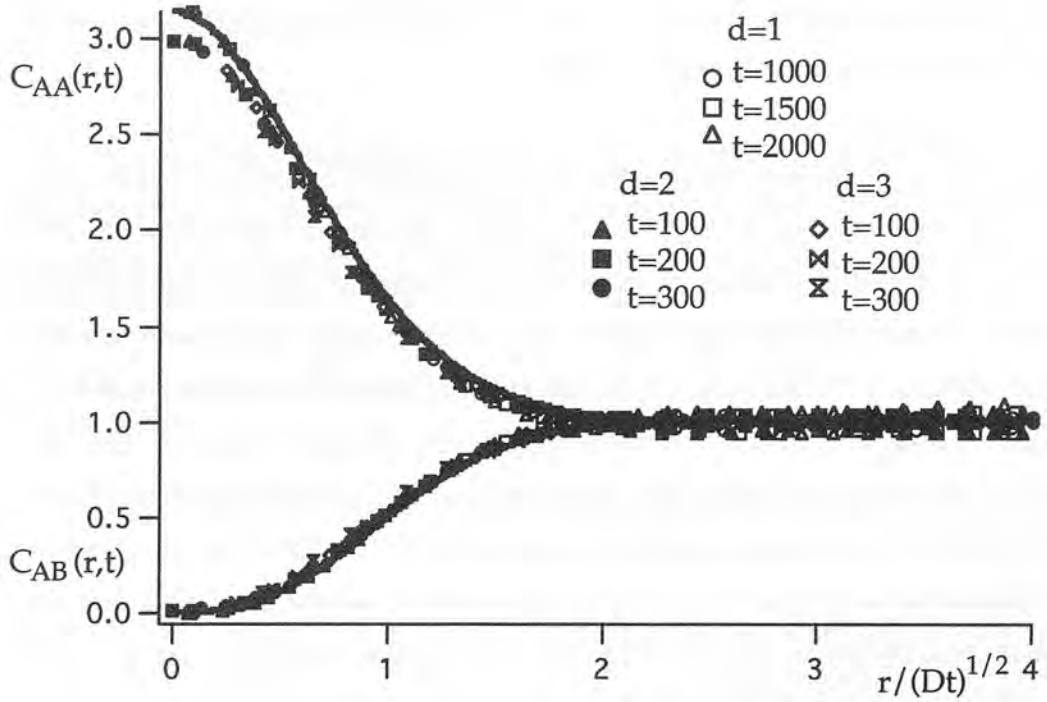

Fig. III-2- Density-density correlation functions $C_{AA}(r,t)$ and $C_{AB}(r,t)$ plotted as a function of $r/(Dt)^2$. The results are computed at different times, for d=1, 2 and d=3. The solid lines are the analytical results in Eqs. (III-8) and (III-9).

This figure demonstrates that the behavior of the correlation functions is really superuniversal, since they do not depend on the time, the value of D and the dimensionality of the problem. Obviously this occurs only during the time regime when the system is diffusion-controlled. One can also observe that the agreement with the theoretical predictions is very good. The small differences with Eqs. (III-8) and (III-9), specially at short values of the scaling variable $r/(Dt)^2$, are due to the fact that the analytical results only hold in the $K\to\infty$ limit, whereas we are using finite values for the constant reaction rate. We have improved these results just by taking a

larger value of K in our simulation. In any case, the results shown here are extremely more consistent with the theoretical predictions than those ones obtained with particle simulations [Vit88].

We turn now to the cross sections of clusters. The cross sections are given by the segments of straight lines inside the cluster boundaries. We denote by p(s,t) the distribution of such cross sections at time t. For d=1 this distribution coincides with the cluster size distribution and some results have been obtained in this case for initial layered systems [Sok91e] and also for random initial distributed systems using the discrete scheme [Ley91]. Moreover, we have previously seen that the simulations with particles have several problems in defining cluster's length in d>1 [Ley92]. Our continuum scheme allows us to define the cluster cross section length and to have an idea about how clusters grow. Thus, all the results obtained for discrete models will be easily extended here to d=2 and d=3, and analogously to what we had for the correlation functions a superuniversal behavior for p(s,t) will be found.

Taking into account that our system is isotropic, for d=2 and 3 lines are drawn parallel to the coordinate axes. Theoretically, the difference variable $q(\vec{r},t)$ considered as a function of the coordinate along this line is a one-dimensional Gaussian random process. The cluster boundaries then correspond to simple zeros of the Gaussian process, whose statistics are well known and can be expressed through the joint probability distribution of $q(\vec{r},t)$ and its spatial derivatives. The calculations are given explicitly in [Sok91e]. Here the results are summarized.

The cluster cross-section distribution p(s,t) can be expressed in terms of the two-point joint probability function in Eq. (III-7) changing the spatial variable r by s. According to the scaling behavior evidenced earlier, g(s,t)

depends on the cross-section length s and time t only through a scaling variable $\xi = s/(8Dt)^{1/2}$.

The scaled distribution density $P(\xi)$, defined as $p(s,t)(Dt)^{1/2}$, can be obtained from the conditional probability $P(\xi|0)$ to find a cluster boundary at ξ, provided there is one at 0. The relation is of Ornstein-Zernike type:

$$P(\xi|0) = p(\xi) + \int_0^{\xi} p(\zeta)P(\zeta-\xi|0)d\zeta \qquad \text{(III–10)}$$

Equation (III-10) can be readily evaluated numerically. $P(\xi|0)$ is given by

$$P(\xi|0) = \frac{(\mu_{33}^2-\mu_{34}^2)^{1/2}}{\pi^2[1-g^2(\xi)]^{3/2}}\left(1+\frac{\mu_{34}}{(\mu_{33}^2-\mu_{34}^2)^{1/2}}\arctan\frac{\mu_{34}}{(\mu_{33}^2-\mu_{34}^2)^{1/2}}\right) \qquad \text{(III–11)}$$

written in terms of the functions

$$\mu_{33} = g''(0)[1-g^2(\xi)] + g'^2(\xi) \qquad \text{(III–12)}$$

and

$$\mu_{34} = g''(\xi)[1-g^2(\xi)] + g'^2(\xi)g(\xi) \qquad \text{(III–13)}$$

with $g(\xi) = \exp(-\xi^2)$, Eq. (III-7).

As we observed for the correlation functions, the distribution $P(\xi|0)$ in Eq. (III-11) at large times also turns out to be universal. According to Eq. (III-11), clusters grow with $(Dt)^{1/2}$ and the mean cluster size can be evaluated giving $\langle s\rangle = 2\pi\sqrt{Dt}$.

In Fig. III-3 we show the cluster cross-section length distributions p(s,t) calculated in our simulations. These results correspond to a bidimensional system with equal diffusion coefficients and they are plotted for different times. Obviously, for the case $D_A=D_B$, both distributions $p_A(s,t)$ and $p_B(s,t)$ behaves identically. From Fig. III-3 one can clearly observe how the cluster grow with time.

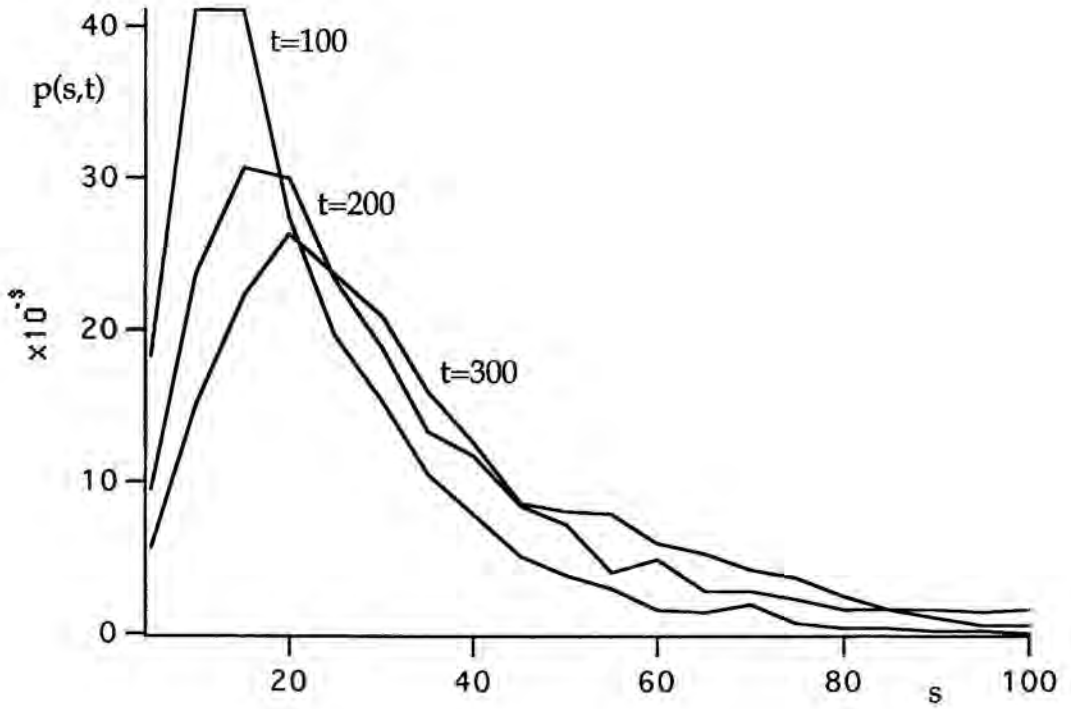

Fig. III-3- Cluster cross-section length distributions as a function of s for d=2. Three different times are displayed: t=100, 200 and 300.

The corresponding scaled curves for different times and also for different dimensionalities together with the analytical scaling curve are plotted in Figure III-4. Note that the cross-section distributions obtained here

for d=2 and d=3 mimic the behavior found in d=1 (see also simulations in [Ley92] using a discrete scheme): P(ξ) increases linearly for small ξ and decays exponentially for large ξ.

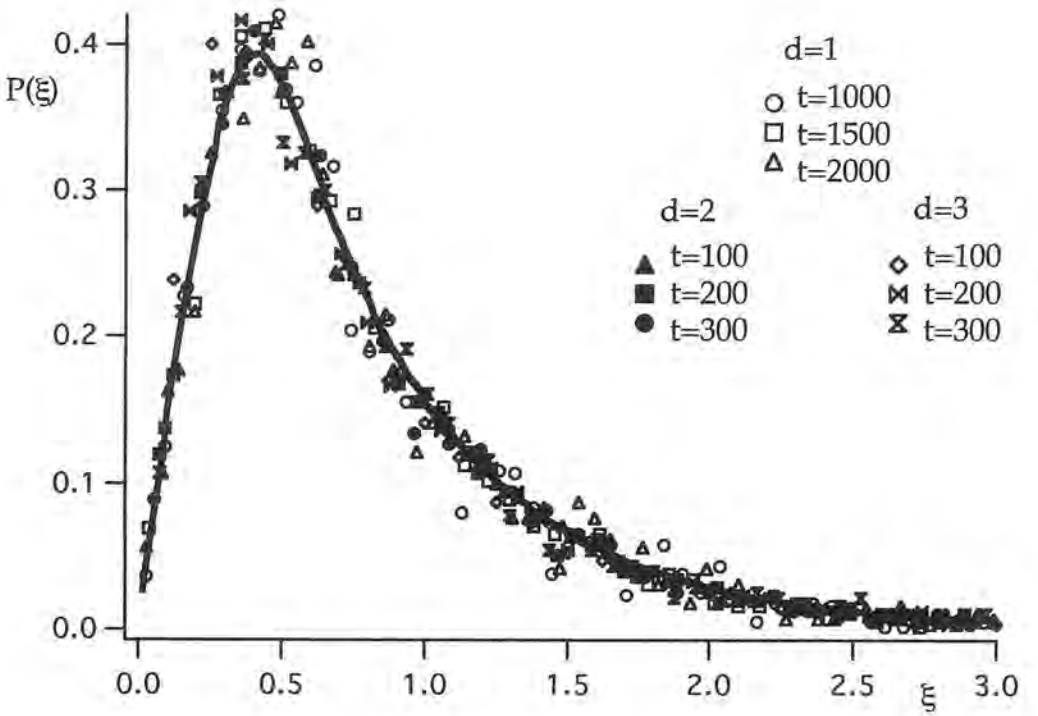

Fig. III-4- Cluster cross-section length distributions as a function of $\xi = s/(8Dt)^{1/2}$. The results are computed at different times, for d=1, 2 and d=3. The solid line corresponds to the analytical result in Eqs. (III-10)-(III-13).

The reaction kinetics changes from t^{-1} to $t^{-d/4}$ because of the formation of domains and because the reaction proceeds intensively only along the domain walls, i.e., along the points, lines or surfaces with q=0. The large-scale structure formed as a result of the reaction is determined by the structure of these domains, characterized by its linear size Λ, and the reaction

zones, characterized by its width w. In our problem $\Lambda \sim \langle s \rangle \sim t^{-1/2}$ for any dimension and $w \sim t^{(d+2)/12}$, see [Sok86]. Since $d<4$, the width of the domain wall (w) increases slower than the domain itself (Λ), and then the domain structure becomes more clearly defined with the passage of time. For $d \geq 4$, this relationship do not apply, the reaction zones grows at least as fast as the domains and then total homogenization sets in over time.

SECTION III-2 -Case $D_A \neq D_B$-

For different diffusivities $D_A \neq D_B$, the analytical procedures developed in the later section can not be used [Sok91f]. Therefore, in this section only numerical results and qualitative conclusions will be presented [Rei96a]. Without loss of generality for all the results of this section we take $D_A > D_B$, and we define $D = \frac{D_A + D_B}{2}$. For d=1 we keep D=1, for d=2 D=0.1 and for d=3 D=0.01.

In Figures III-5 the density-density correlation functions for a bidimensional system with different diffusivities are plotted at three different times. In comparison with Fig. III-1, note that the like-particle correlation functions are now separated for the two species. The curve corresponding to the less diffusive species (B) has a larger peak at r->0 whereas the value at intermediate distances is smaller than the corresponding for the more diffusive species (A). This means that the clusters of B are denser but narrower than the A-ones. The case with $D_B=0$ in Fig. III-5b shows, but amplified, all these last features. We have not plotted the results for d=1 and d=3 because they show the same characteristics as in d=2.

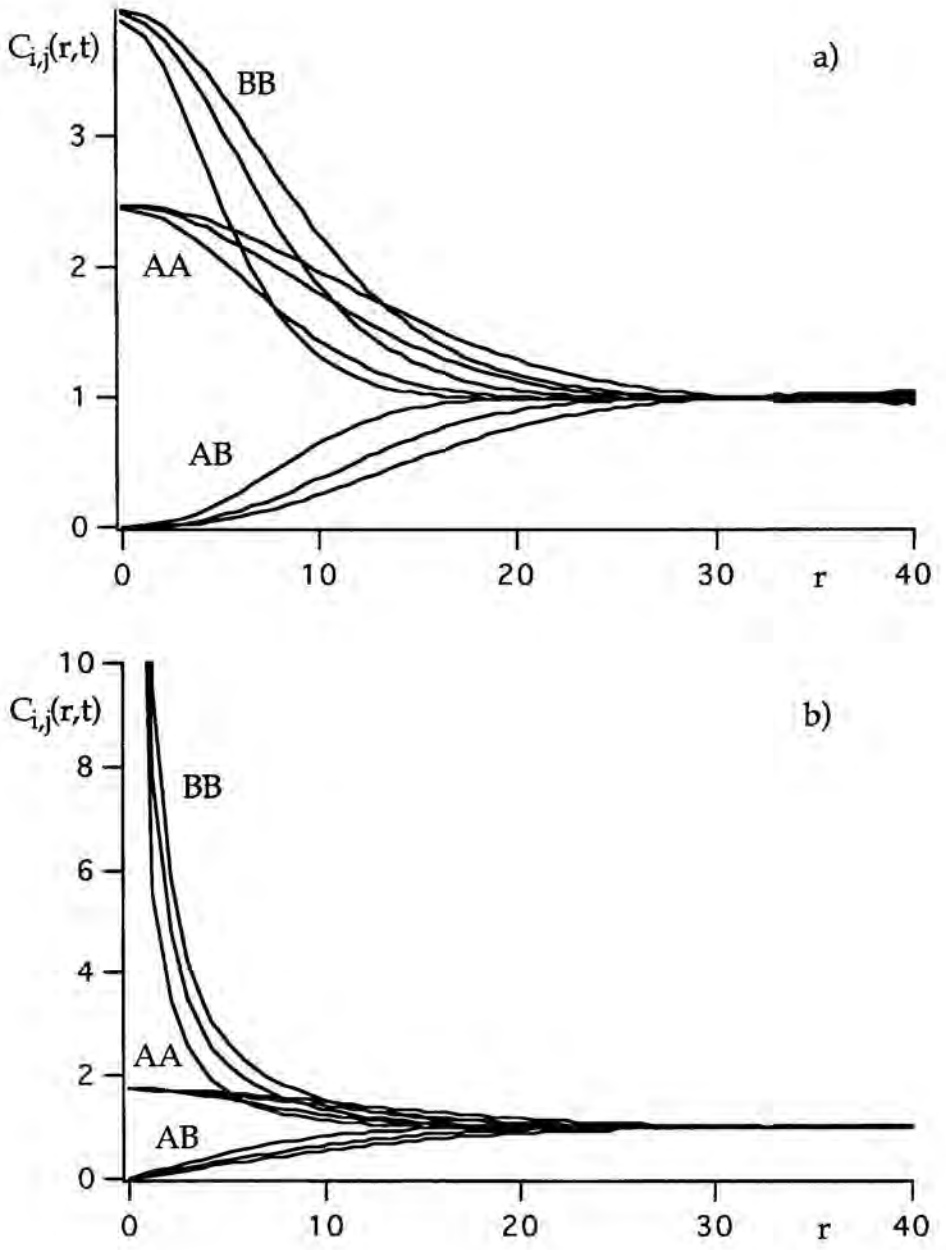

Fig. III-5 a)- Density-density correlation functions as a function of r for the case with D_A=0.15 and D_B=0.05 in d=2. b) The same as in a) but now the case with D_A=0.2 and D_B=0. Three different times are plotted: t=100, 200 and 300 from bottom to top for $C_{i\,i}$ and from top to bottom for C_{AB}.

In Figures III-6 the scaling form for the correlation functions in Figs. III-5 are shown. We have chosen the mean diffusion coefficient for the scaling variable $r/(Dt)^{1/2}$. For $0<D_B<D_A$, in Fig. III-6a, the results are qualitatively similar to those for $D_B=0$ shown in Fig. III-6b, apart from the fact that C_{BB} stays finite at r=0. Our findings in Figs. III-5 and III-6 are summarized as follows:

i) All correlations functions scale with $t^{1/2}$.

ii) C_{AA} and C_{BB} depend strongly on D_A and D_B. For $D_B=0$, C_{BB} is very large for small r; furthermore, for small r, C_{AA} is smaller than C_{BB}. This is a reflection of the fact that now large and sparsely populated A domains are randomly 'drilled' by small but densely populated B domains; the later retain their initial Poisson distribution.

iii) We were not able to find any universal scaling for the correlation functions. Their form depends on details, such as the particular D_A, D_B values and on the spatial dimension.

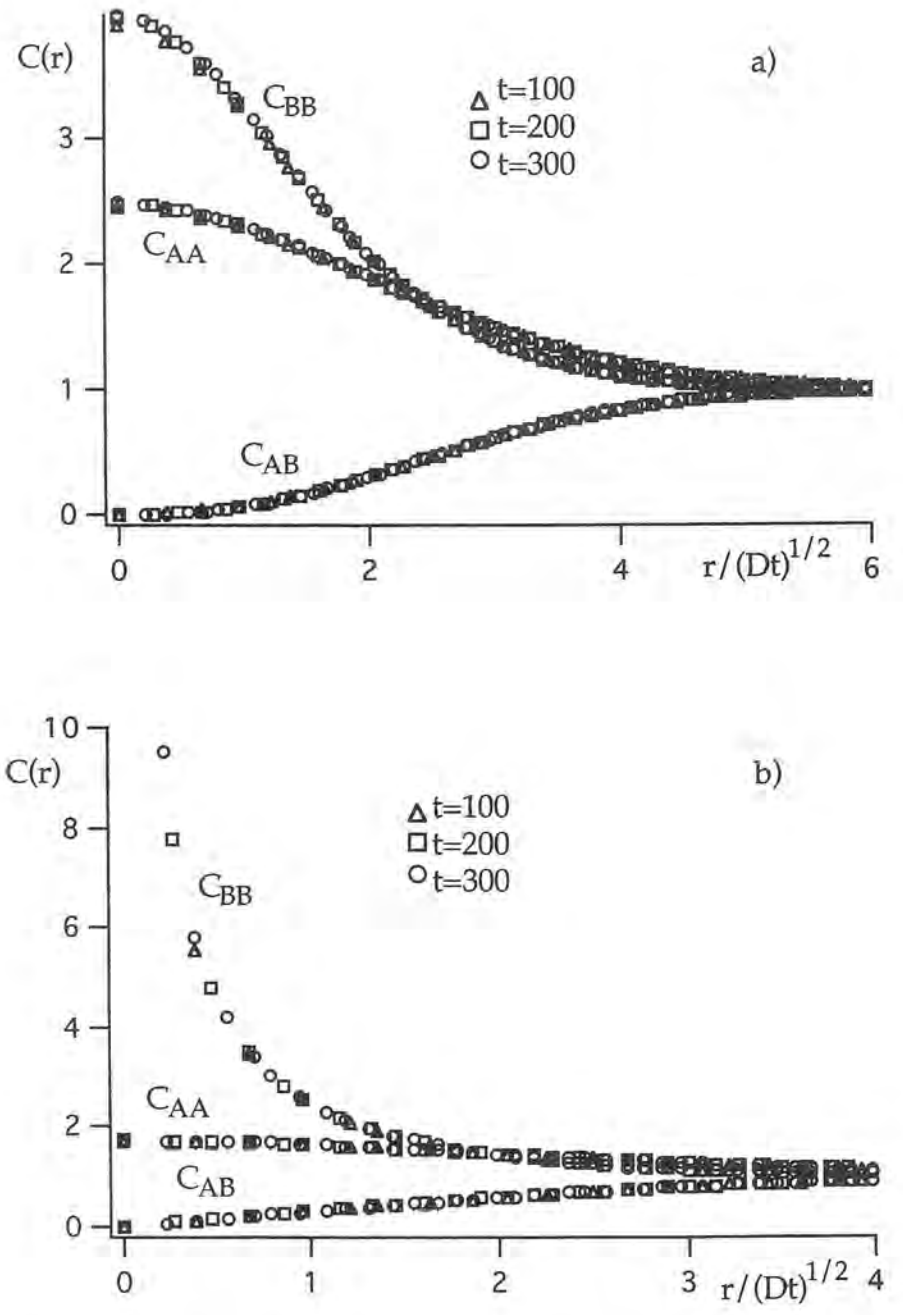

Fig. III-6 a), b)- Density-density correlation functions of Figs. III-5a and III-5b but now as a function of $r/(Dt)^{1/2}$.

Now we turn to the distribution of cluster cross section lengths for $D_A > D_B$. The results for $D_B \neq 0$ are qualitatively similar to those for $D_A = D_B$: both $p_A(s,t)$ and $p_B(s,t)$ scale with $\xi = s/(8Dt)^{1/2}$, but now show different forms, which depend on D_A and D_B. In Figure III-7a both $p_A(s,t)$ and $p_B(s,t)$ are plotted for d=2 as a function of s for three different times. It is clearly observed that the A-clusters grow faster than the B ones due to its high diffusion coefficient. In Figure III-7b the scaled functions $P(\xi)$ corresponding to the case of Fig. III-7a are plotted as a function of $\xi = s/(8Dt)^{1/2}$. Note that the curves of each species collapse differently.

On the other hand, the results for $D_B = 0$ are very special and will specifically analyzed on what follows. In Figure III-8a the A-cluster cross-section length distributions at different times for $D_B = 0$ are presented in d=2, and in Figure III-8b the same in d=1. To facilitate the comparison with Fig. III-4 we have rescaled the results as a function of ξ. The situation in d=3 is qualitatively similar to the d=2 case, and we refrain from presenting any figure of this case here. Note that for one immobile species the scaled curve have lost their initial peak for small values of ξ.

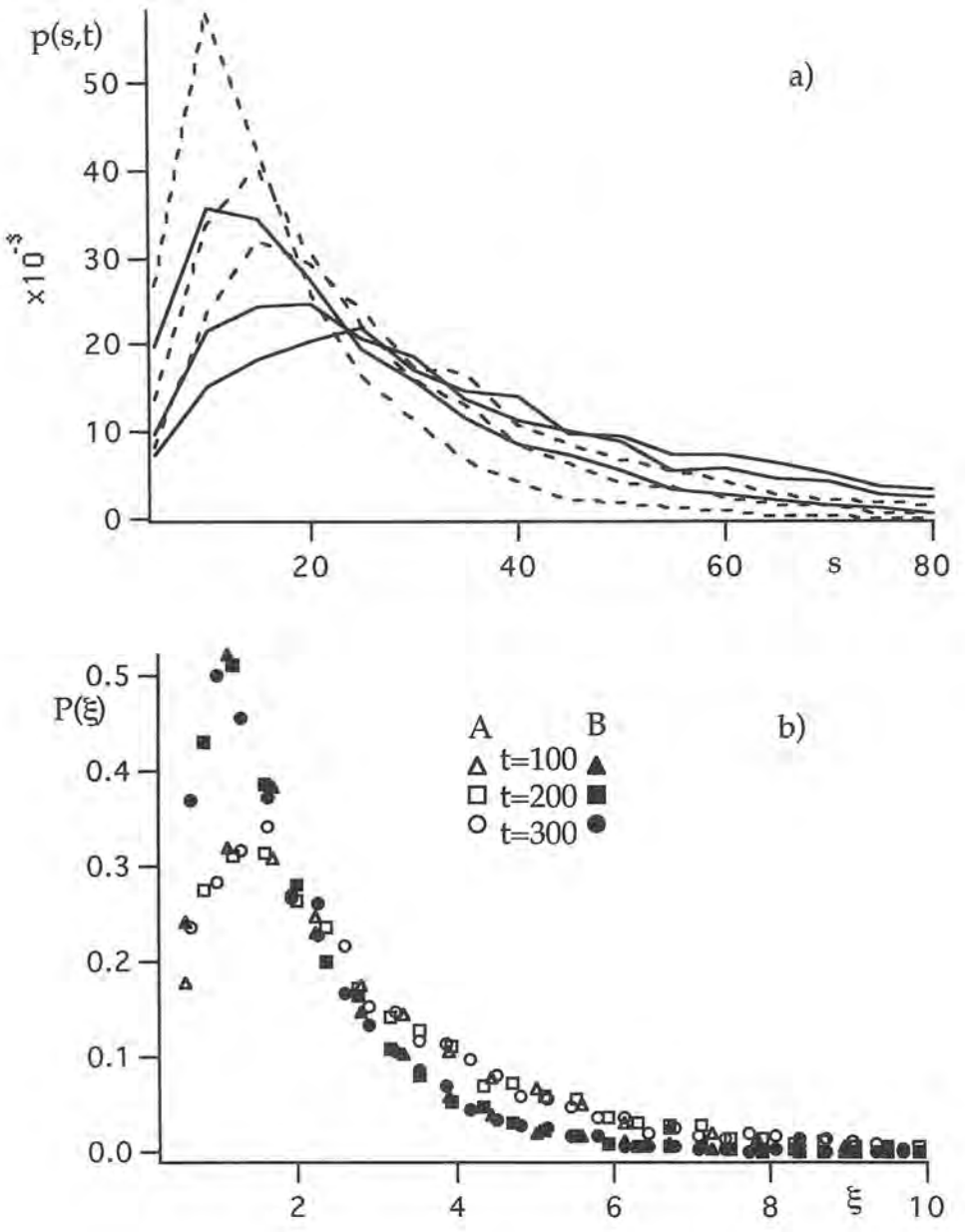

Fig. III-7- a) Cluster cross-section length distributions for the A (solid lines) and the B (dashed lines) clusters in d=2 for D_A=0.15 and D_B=0.05. As in Fig. III-3, three times are displayed: t=100, 200 and 300. b) The same as in a) but now the scaled functions P(ξ) represented as a function of $\xi = s/(8Dt)^{1/2}$.

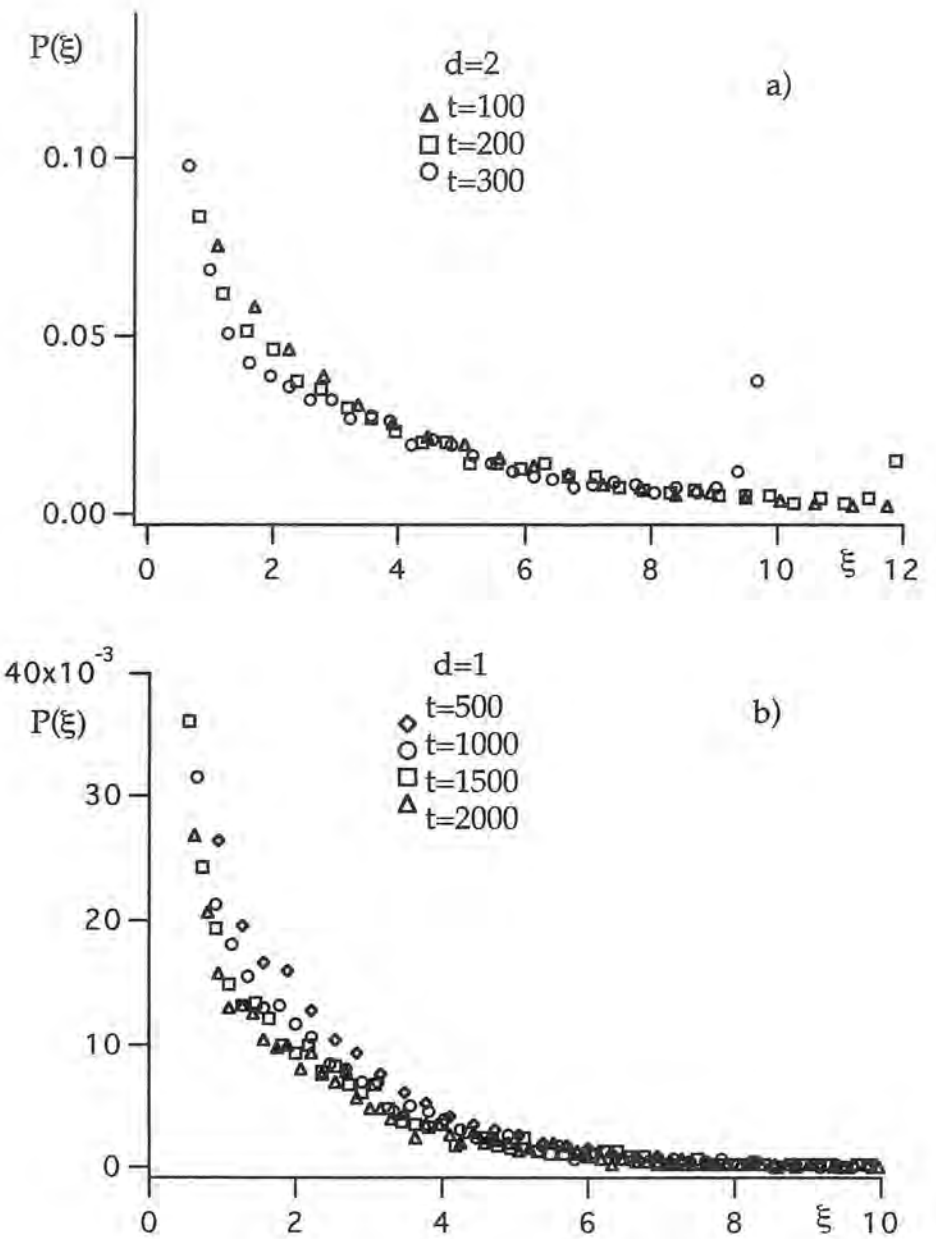

Fig. III-8- a) Cluster cross-section length distributions for the A clusters in d=2 for D_B=0. We also fix D_A=0.2. b) The same as in a), now in d=1 (D_A=2).

In view of the results of Figs. III-8 for $D_B=0$, scaling is less conclusive than for $D_A=D_B$. The distribution $p_A(s,t)$ seems to scale for large, but not for small, ξ. To gain a better understanding of the scaling properties of the cross-section distributions, we now focus on the reduced moments $\langle s_A{}^n(t)\rangle^{1/n}$. If all the moments obey the usual diffusive pattern, one would find $\langle s_A{}^n(t)\rangle^{1/n} \sim t^{1/2}$ for all n. In Fig. III-9 we present the first three moments (n=1,2 and 3) for d=2 and in Fig. III-10 those for d=1.

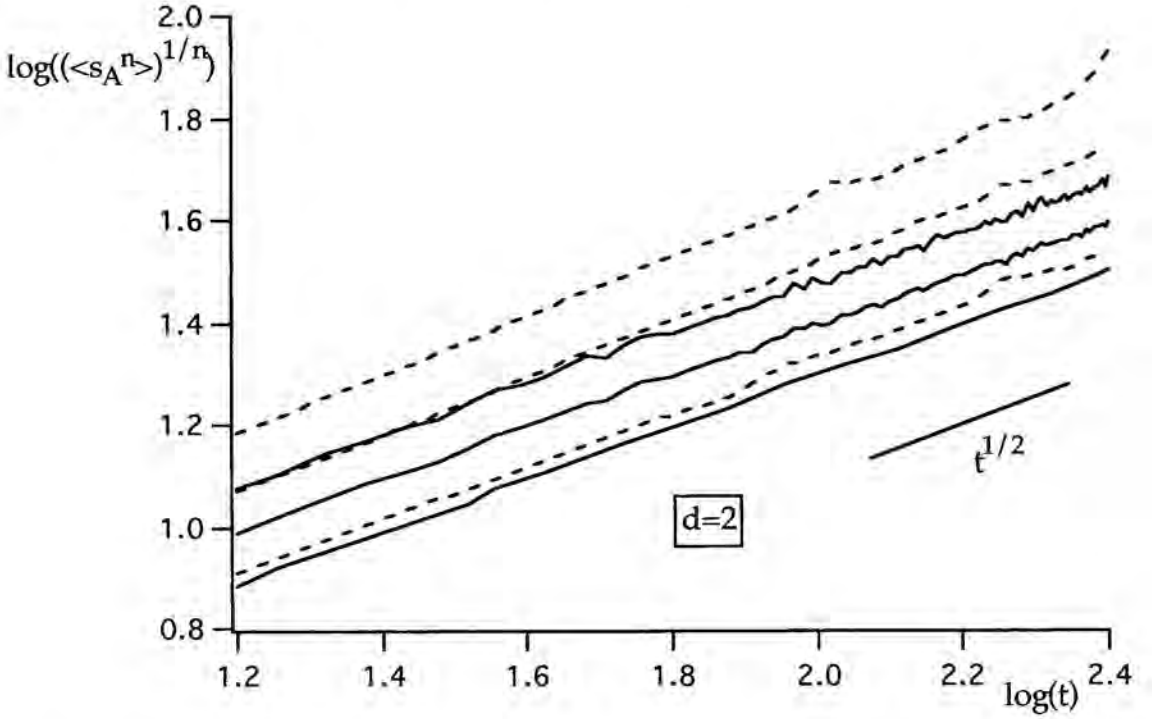

Fig. III-9- The first three reduced moments $\langle s_A{}^n(t)\rangle^{1/n}$ of the A-cluster cross-section length distribution (n=1, 2 and 3 from bottom to top) in d=2. The solid lines correspond to $D_A=D_B=0.1$, the dashed ones to the case $D_B=0$ ($D_A=0.2$).

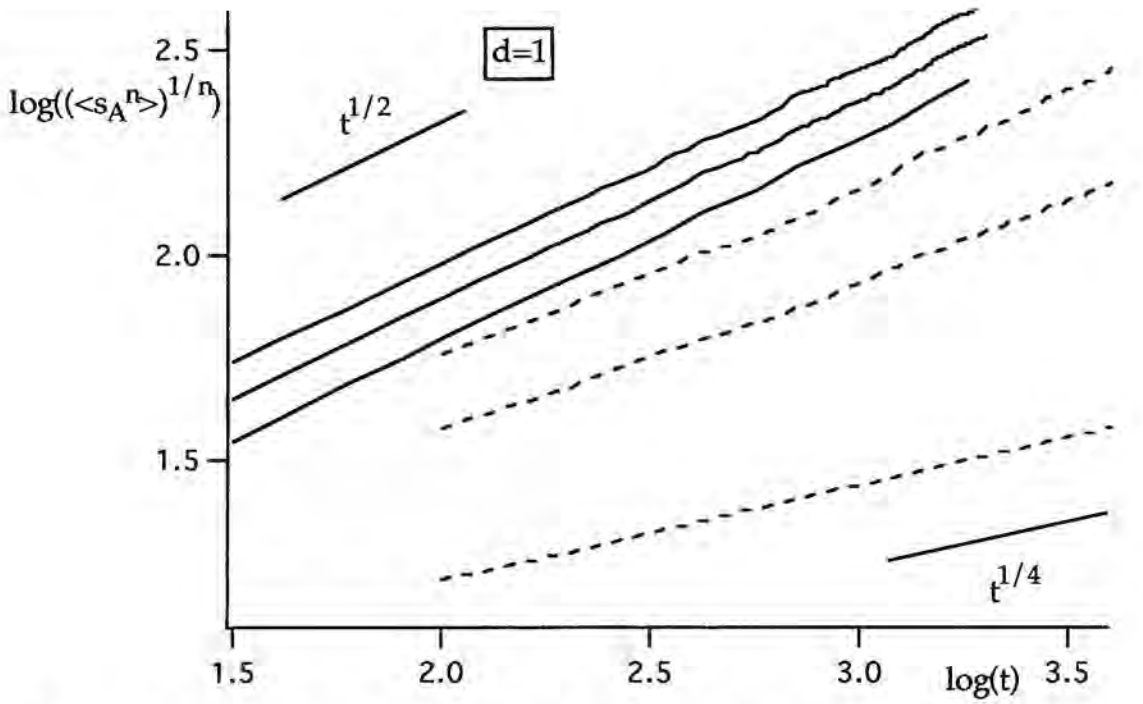

Fig. III-10- Same as in Fig. III-9, now in d=1 ($(D_A+D_B)/2=1$).

For $D_A=D_B$ all three moments scale with $t^{1/2}$ both in d=1 and in d=2. For $D_B=0$ our conclusions are as follows:

i) For d=2 scaling practically obeys t^{α}, with α being the same for n=1, 2 and 3, and being only slightly different from 1/2. The difference may even be due to finite-size effects or to higher-order corrections to scaling. The same holds in d=3.

ii) In d=1 the situation is singular. We now have $\langle s_A^n(t)\rangle^{1/n} \sim t^{\alpha_n}$, where the exponents α_n increase with n, possibly tending to 1/2; this may indicate that only the largest clusters grow diffusively. This finding, and the fact that C_{BB} seems to depend little on time, contrasts with the result of the discrete models [Ley92], which reports scaling with $(Dt)^{1/2}$.

A careful analysis of the domain morphology enables us to interpret the peculiar aforementioned behavior in d=1 and D_B=0. In a continuous picture an A cluster can either coalesce with a neighboring one if the B wall between them is thin enough to be consumed away or it persists indefinitely, if its neighboring B walls are very thick. In the last case the particle concentration inside the A cluster decreases with time but does not reach zero at a finite time. Consequently, these small clusters do not grow diffusively and form the nonscaling small-size background seen in Fig. III-8b. Conversely, in a discrete particle picture, small A clusters disappear: when all the A particles between two B walls have reacted, the A cluster ceases to exist. The neighboring B clusters coalesce, a mechanism which gives rise to B-cluster growth and to scaling behavior for both $p_A(s,t)$ and $p_B(s,t)$, as found in [Ley92].

Note that small A clusters with exponentially low concentrations can influence neither the kinetic behavior nor the density-density correlation functions; they show up, however, in considerations of the cluster-size distributions, where they significantly change the normalization constant.

A qualitative way to understand all these behaviors consists on looking directly at how the reactant profiles evolve. In Figs. III-11 and III-12 the time evolution of the q-profiles are plotted for d=1 and d=2 respectively. For each dimension we show three different cases; figures a stands for the systems with equal diffusion coefficients, in figures b the reactant B has lost a lot of mobility and finally in figures c, B has been completely immobilized. Comparing the figures III-11c and III-12c (D_B=0) we realize the previously mentioned effect for the monodimensional case. Even though for high dimensionality the A domains grow indefinitely at the expense of the B

ones, which stay immobile, for d=1 some B clusters form 'walls' which obstruct the growth of some A domains that remain 'frozen'. This effect is due to the low efficiency of the diffusion for the monodimensional systems, whereas in bigger dimensionalities the diffusion of the A reactant is able to destroy the islands of B and it allows the growth of the mobile component. For two and three dimensions the A domains can 'cooperate' better among themselves and grow, meanwhile in one dimension they can remain 'captured' with facility.

This finding shows that the geometrical properties of clusters may depend sensitively on the underlying microscopic model; thus continuum models in d=1 give rise to nonuniversal behavior. This nonuniversality may be either an artifact, if it is only a mesoscopic approximation for a discrete system, or a physical effect, say in a system with initial macroscopic inhomogeneities, e.g. a layered system; see Section 4 of [Sok91a].

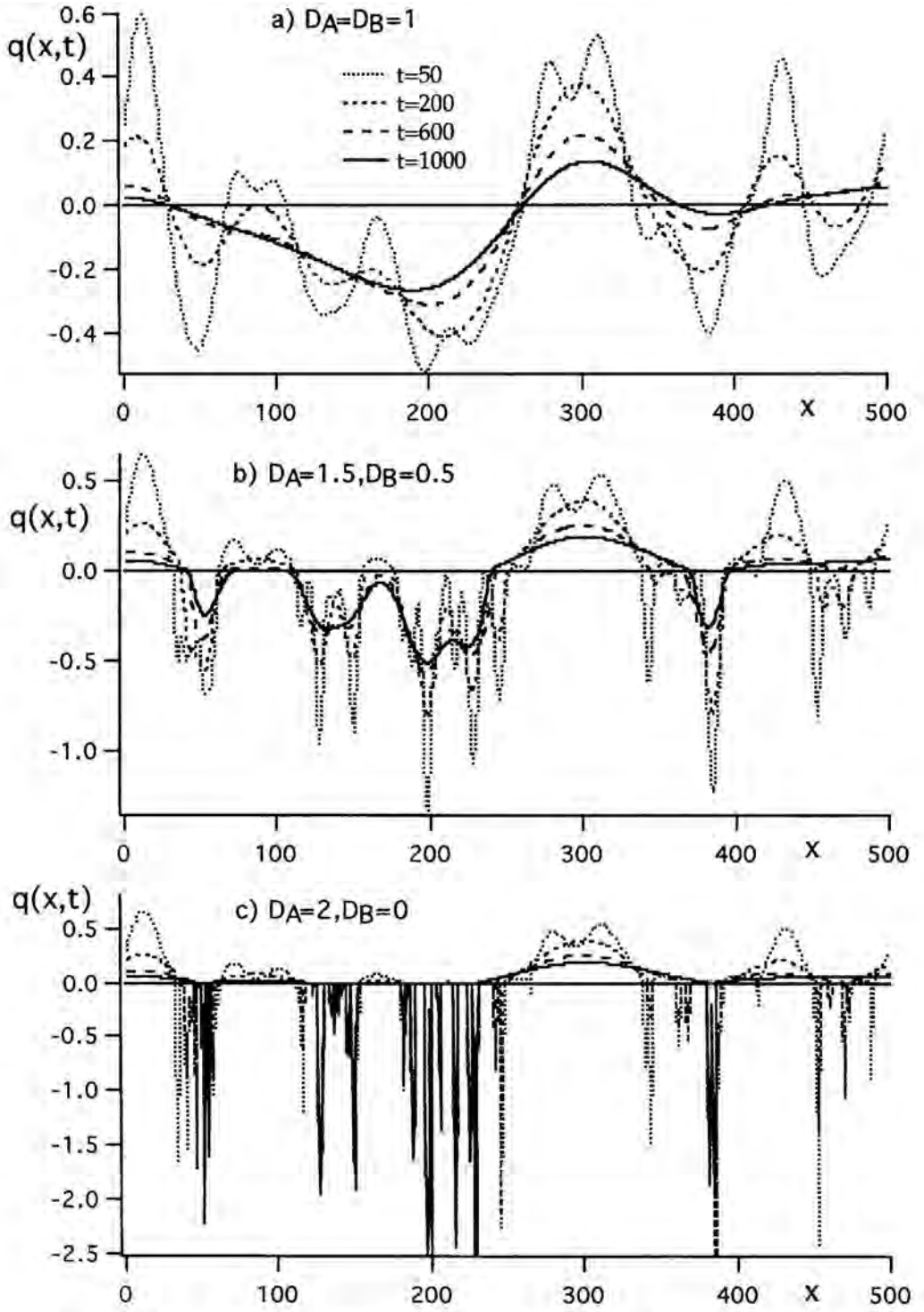

Fig. III-11- q-profiles at t=50, 200, 600 and 1000 in the case d=1.

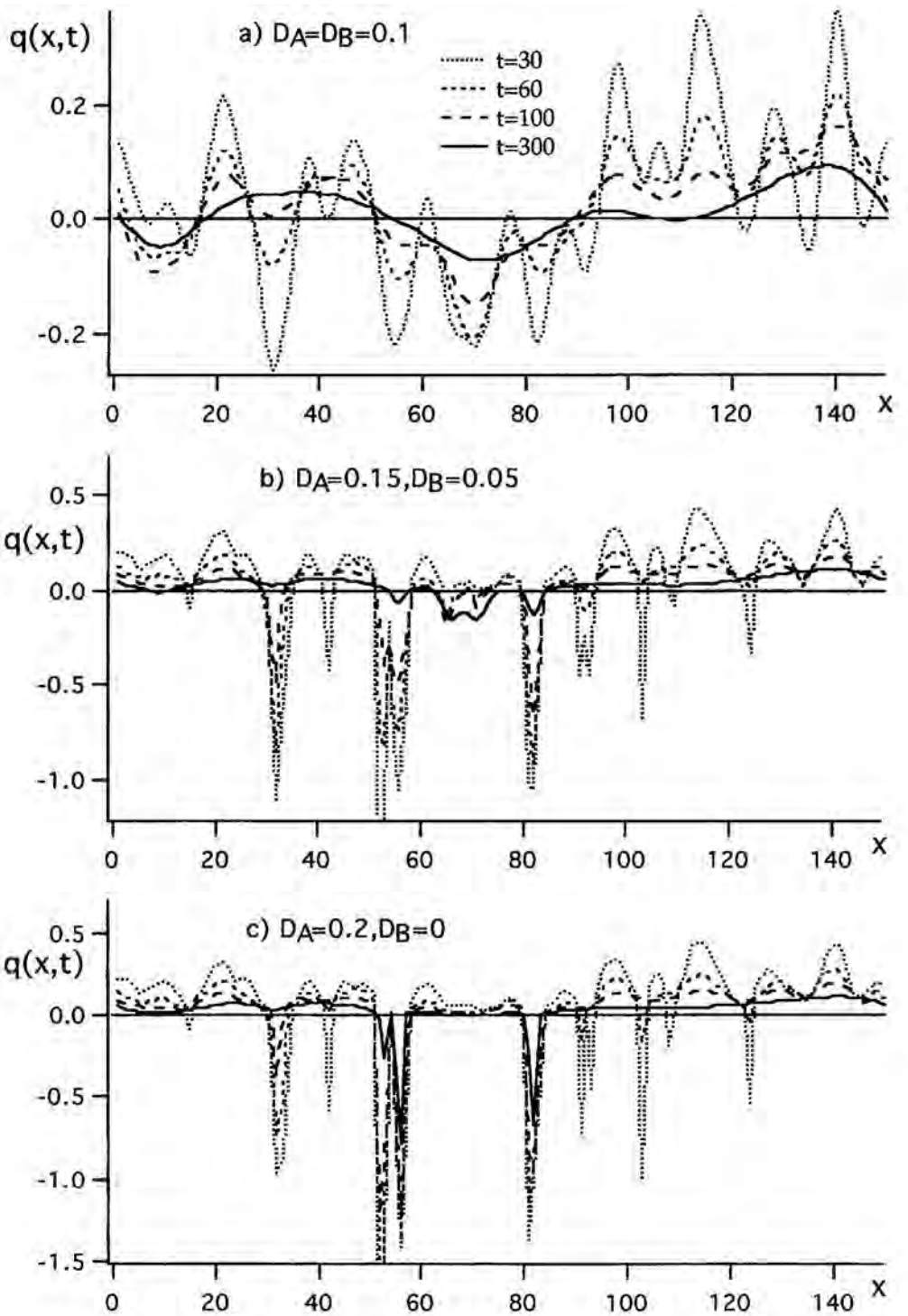

Fig. III-12- q-profiles at t=30, 60, 100 and 300 in the case d=2.

CHAPTER IV

-Conclusions-

In this Part I we have presented an extensive study of the anomalous behavior showed by the irreversible (and therefore nonequilibrium) reaction A+B->0 in a d-dimensional system under stoichiometric conditions. After introducing our numerical tools in Chapter I we have separated in Chapter II and Chapter III the two main areas that can be treated in this topic: kinetics and spatial organization respectively.

On what respects to the kinetic aspects, the Zeldovich regime for initial randomly distributed conditions have been deduced by analytical procedures and also proved with numerical results in d=1, 2 and 3. We have also focussed on the effects of the initial pattern of the difference function and have stressed that this pattern will determine the future evolution of the system. In particular, the long-wavelength components of the initial difference distribution in Fourier space determine the asymptotic decay of the reactant concentrations. Apart from the random case, two more initial patterns have been studied: the periodic case with its exponential decay and the fractal one that leads to the very slow decay $c \sim t^{-(d-D_f)/4}$.

We have emphasized the fact, also well-known, that no single exponent characterizes the density decay for all time. Instead, we have indicated that it is often possible to characterize the decay by a single exponent for a considerable length of time compared to the other time scales in the problem, as determined by the reaction rate coefficient and the diffusion coefficient, followed by a crossover of relatively short duration that leads to another exponent for a considerable time span, etc. The sort of analysis presented here is only appropiate when these time scale separations are possible. We have easily carried out this problem by fixing the correct values for K and D according to c_0, L, d, t_{max}, and all the other simulation parameters.

On the other hand, our numerical work is based on a direct integration of the reaction-diffusion equations and introduces, in all cases, the long-wavelength constraints imposed by a finite system size. Thus, although the decays indicated above would be expected to persist forever in infinite systems, in the work presented here they persist only up to a time t_f, at which finite system size efects become apparent and the behavior reverts to the classical; see Sect. II-1-c. Finite size effects limit the certainty of some of our conclusions by limiting the time scales over which some of the single-exponent decays persist.

This kind of limitations can only be overcomed by simulating at longer times and with large enough systems. In fact, all these problems concerning to the exponent consistency and to the finite size effects will appear in a more pronounced way in the stirred systems studied in the following chapters.

In Chapter III the spatial organization of the initial randomly distributed systems have been analyzed. We have studied the statistical properties of clusters formed during the A+B->0 reaction. The clusters are characterized by the density-density correlation functions and by their cross-section distributions. We have found that, for equal diffusion coefficients $D_A=D_B$, the behavior of both quantities is superuniversal. This implies that the morphological behavior of these systems is governed only by the diffusion length $\Lambda \sim (Dt)^{1/2}$, independently of the dimensionality of the system. When $D_A \neq D_B$ the correlation functions scale, but their explicit forms depends on d and on D_A and D_B. For $D_B=0$ and d=1 no scaling is evident in the cross-section distribution due to the fact that we are using a continuum model that allows the matter interpenetration contrarily to the discrete models.

PART 2

-MIXING FLOW EFFECTS-

Introduction

Mixing is a widespread process both in chemical technology and also in our everyday life. The industrial relevance of mixing can hardly be exaggerated. Chemical, petrochemical, and pharmaceutical processes usually need bringing reactants into close contact by imposing a mixing flow. Unfortunately, mixing is often inefficient and several important effects may result: desired reactions are slowed and even stopped before finishing, undesired reactions are enhanced, and thus, product selectivity is decreased. Then, the study of mixing procedures will allow engineers to adapt and modify the already available stirring mechanisms or even to develope new ideas in order to improve production rates in the chemical industry. The knowledge of how flows mix can also provide a better understanding of some chemical, physical and biological processes that take place under the influence of velocity fields.

In our case, we are interested in the effect of mixing flows in our A+B->0 fluctuation-dominated system. The idea consists on the implementation of an advection flow in our problem in order to supplement the diffusion transport trying to mix the initial inhomogeneities. It might be conceived that hidrodynamic mixing would destroy the clusters and restore classical kinetics, but actually this is more difficult than one could expect. Firstly, we want to study the different kinetic laws and the spatial structuration that emerges with the new situation. Secondly, we use our system as an efficiency test for some mixing procedures. In this sense, diffusion-limited problems are maybe the strongest test for a flow to measure its mixing efficiency, since this kind of systems continuosly tries to become segregated in spite of the transport processes.

Some attempts to enhance the transport processes in the A+B->0 diffusion-limited system have been developed by including a drift in the diffusive motion of particles [Ara92, Jan95a, Jan95b, Isp95]. Nevertheless these models are too simple to really reproduce the behavior of these systems under mixing flows. More detailed analysis is needed in the study of mixing processes.

It is known that fluids have two limiting behaviors. On one hand we have laminar fluids and on the other turbulent fluids. Laminar fluids flow smooth and regularly [Sok91a], meanwhile in turbulent fluids the magnitudes of the flow (like velocity, pressure, etc...) quickly vary in space and time in a chaotic way [Bat70, Mon75m Cho94].

The transition between laminar and turbulent flow was extensively studied by Reynolds in his pioneering work of 1894 [Rey1894]. He established

the importance of the so-called Reynolds number, Re=UL/ν, where L and U are the characteristic length and the velocity of the flow respectively, and ν is the kinematic viscosity. This parameter stands for a dynamical interpretation as the ratio between inertial forces, that transfer energy from large to small scales forming the inhomogeneities of the turbulence, and viscous forces, that favor the homogeneity of the system through energy dissipation. We shall expect, then, that for high Re the system behaves in a turbulent way, while for low Re it does in a laminar way.

In general, fluid mixing is poorly understood. However, some easy models can be developed and explored in order to capture some main features. The study of mixing of fluids in two-dimensional time-periodic flows is important because it serves as a useful model for the understanding of a variety of mixing processes. Some important concepts can be captured by computational, theoretical or experimental studies of these flows. The main motivation of all these works consists on obtaining efficient mixing procedures. Moreover, the idea of efficient mixing flow is closely related to the capacity of this flow to extend chaos in the system.

Fluid efficient mixing consists on an appropriate distribution of fluid elements throughout space. It can be viewed as the creation of interfacial area and reduction of length scales between initially segregated fluids. Therefore, mixing is intimately related to the stretching and folding mechanism of fluid elements that, on the other hand, constitute a signature of chaos. Repeated stretching and folding is schematically shown in the next figure.

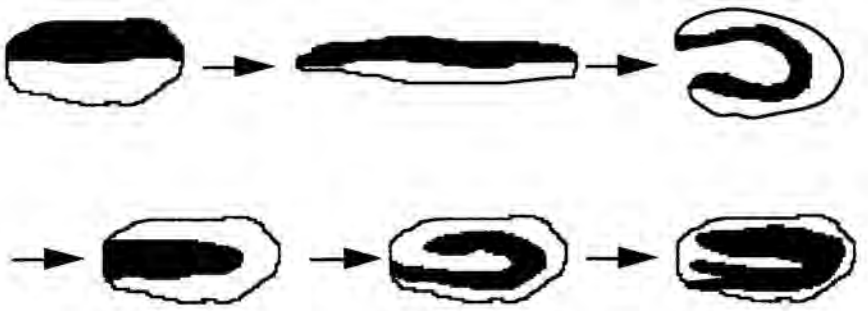

-Stretching and folding as an effective way of mixing-
Figure extracted from [Sok91a]

Simple theoretical models can reproduce a large variety of stretching and folding mechanisms. The simplest model corresponds to the so-called baker's transformation that can be viewed as taking place in three stages: squeezing, cutting and then pasting together the cut parts of the system. These three stages are shown in the next picture:

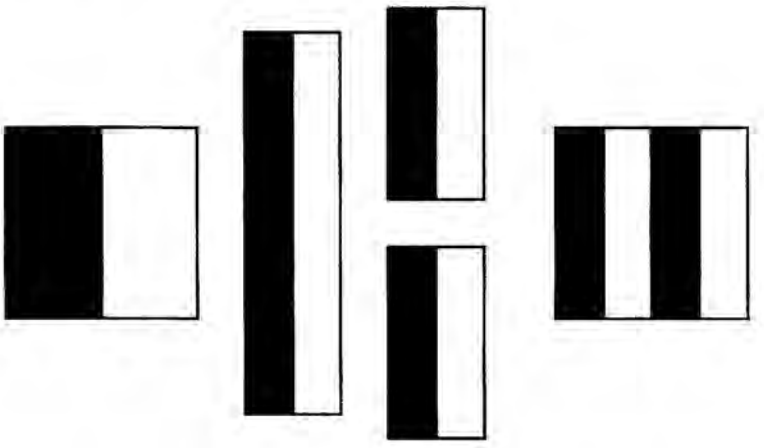

a) b) c)

-The baker's transformation: a) squeezing, b) cutting and c) pasting-
Figure extracted from [Sok91a]

A lot of models of such type have been introduced as prototypes for efficient laminar mixing. We can mention two more examples of these effective models of mixing: the shear-flow mixing [Sok92b] and the tossing mixing [Arg87, Arg89]. We need to remark that all these theoretical mechanisms require for their modelling in finite vessels a discontinuous cutting and pasting stages. Some attempts have been done by Sokolov [Sok91b, Sok91c, Sok92b, Sok93b] in order to implement a continuous scheme of these models in the deterministic equations of the A+B->0 system. From all these theoretical models, laminar mixing of two initially separated reactants produces a lamellar structure of alternating striations. That is the reason why the study of A+B->0 diffusion-limited systems under initial one-dimensional lamellar distribution is important when analyzing the kinetic behavior of binary systems that have been under the influence of two-dimensional laminar mixing [Muz89a, Muz89b, Sok91d].

In the other hand, the majority of real mixing procedures involving flows in two dimensions in finite vessels are less effectives [Ott89]. For example chaos is impossible in steady and bounded two-dimensional flows. In these cases the flow is totally characterized by time-invariant closed lines that do not mix at all; however, in three dimensions some classes of steady flows can provide chaos in some parts of the system [Cri91]. A necessary condition for chaos is the 'flow line crossing' at arbitrary times. This crossing can create some sort of folding called horseshoe map, that like the stretching and folding mechanism is also a signature of chaos. Stretching combined with this folding provides effective mixing within chaotic regions. This can be performed by suitably designed time-periodic flows in two dimensions.

Numerous computational examples of this time-periodic flows can be modeled and resulting in chaotic mixing. For example, the egg-beater flow model [Muz92] which can be described as the composition of two shear flows acting on a square. The first flow acts horizontally for a time T and the second flow acts vertically also for a time T. Both flows are combined periodically and different efficiency levels are shown in function of the period time. Depending on T, the flow can be completely regular or almost chaotic.

However, for this kind of two-dimensional flows, mixing is not totally widespread. In general, poorly mixed regions, also called island or coherent regions, coexist with chaotic (well-mixed) regions. Fluid inside an island can never escape and fluid outside an island can never enter. In this situation only the diffusion transport, that we know that is extremely inefficient, can mix the system. The formation of coherent structures in this flows has been intensively reported in the works of Muzzio and Ottino [Ott88, Ott89, Muz91, Ott92, Muz92].

Laboratory experiments of time-periodic and two-dimensional systems are performed in order to test the mixing efficiency and the formation of segregated poor-mixed regions. The most famous experimental mixing device is the cavity flow [Chi86, Ott88, Leo89]. It consists on a rectangular container where one or two walls are allowed to move tangentially, according to some prescribed patterns of motion. Another class of experimental mixing scheme is known as the journal-bearing flow [Ott88, Swa90, Muzz91, Muzz92] where the fluid moves between two co-rotating or counter-rotating eccentric cylinders. Finally we want to mention the capillary-waves flows [Ram90, Ram91] which consists on a thin layer of liquid in a tray that is vibrated vertically. By averaging over the vertical coordinate the system can be viewed as two-dimensional. In all the cases coherent structures of the flow are observed and studied.

The conclusion of all these studies could be that what is really important in order to obtain an efficient mixing mechanism is not the intensity of the flow but how it mixes. A clear example of this idea is reported in [Lam96]. In this work by Lamberto et. al. an acid-base neutralization reaction and a pH indicator are used to reveal the existence of segregation regions in a tank stirred by radial flow impellers. Both reactants, acid and base, are initially separated and then the impeller starts rotating with a fixed angular velocity. After few minutes the system is mixed only in part: two torus-like structures appear above and below the impeller according to the closed flow lines. These islands would remain permamently, only mixed by diffusion, avoiding the possibility of total neutralization in a reasonable time. Mixing with a large angular velocity would not be the solution of the problem since other closed flow lines would appear. Paradoxically, they solve the problem by decreasing the velocity of the impeller: the closed flow lines are changed and, therefore, some of the acidic fluid in the well-mixed region becomes part of the newly formed segregated region, and a significant fraction of basic fluid escapes into the chaotic region. If we repeat this process periodically several times we will mix the system in few minutes. As it is demonstrated with this experimental example, a factor leading to mixing enhancements is to perturb the flow continuously, preventing the formation of coherent segregated regions. For example, the role of periodic contractions of mixing in the duodenum [Mac80] can be considered as an application of this idea in nature.

The concept of coherent islands in mixing flows can also serve as useful example for various problems in nature and technology spanning several orders of magnitude in length and timescales. For example, this kind of idealization can help in understanding the complex structures which

appear during mixing, mostly in low Reynolds number flows, such as in structure organization in the earth's mantle [McK83, Hof85] (mineral formation), the persistence of structures in oceans [Tak70, Rhi83] and two-dimensional mixing in planetary atmospheres [Ear93].

Finally, in recent years, Levy flights have been implemented as a mixing process in diffusion-limited models. The basic idea of Brownian motion, as a model for normal diffusion transport, is that of a random walk associated to a Gaussian probability distribution for the position of the random walker. However, the Levy model allows the particles to make jumps according to some Levy distribution [Shl87, Zum93, Kla96] whose second moment is infinite. This means that there is no characteristic size for the random walk jumps contrarily to the non-enhanced diffusion case. Therefore, Levy flights provide a method to enhance diffusion and hence, an alternative way to simulate chaotic mixing. Deterministic model of this enhanced diffusion has been implemented in A+B->0 systems showing that it can accelerate the assymptotic fluctuation-dominated kinetics and even recover the classical behavior in some three-dimensional cases [Zum94, Zum96a, Zum96b].

In this Thesis we shall consider two different mixing mechanisms applied to our A+B->0 diffusion-limited system. First, we will implement a regular steady flow corresponding to a two-dimensional lattice of eddies. There are a lot of works where similar spatially periodic flows have been considered but in different contexts. For example in two-dimensional turbulence [Tab91, Car96], in diffusive transport in Rayleigh-Benard cells [Shr87], in fast dynamo [Sow87], in astrophysical problems [Mof83] and also in percolation phenomena [Isi92]. We anticipate that this steady and deterministic two-dimensional flow will be not capable to mix our

fluctuation-dominated system. In any case we are interested in studying the relation between the closed lines of such a flow and some kinetic behaviors there found.

Secondly, we shall work with a statistical model for a stationary, homogeneous and isotropic two-dimensional turbulent flow. This kind of flow could be modeled in principle by going to the Navier-Stokes equation, but in practice there are many theoretical and practical difficulties in following such a procedure. The alternative consists on the synthetic generation of a velocity field with some well prescribed statistical properties without invoking the Navier-Stokes scheme. These properties are the energy spectrum, the intensity, and the space and time correlations of the flow. The energy spectrum stands for the way that energy is injected in the different spatial scales of the flow and can be arbitrarily chosen in this scheme. In all the work that follows the so-called Kraichnan spectrum [Kra70] will be considered.

This pragmatic point of view offers much simplicity in the implementation of realistic properties of turbulent flows, together with the possibility to control their parameters. This kind of flows viewed as a sort of 'synthetic' or 'kinematic' turbulence has received a lot of attention during these last years [Car93b, Mar97].

It is well known that a passive scalar evolving under the influence of a turbulent velocity field spreads out diffusively with an enhanced turbulent diffusion [Car93a, Car94]. We are also interested on calculating the effective diffusion coefficient in turbulent conditions because this value will be closely related to some kinetic behavior that we shall find in the application of turbulent mixing in our binary diffusion-limited system. We shall

simulate passive scalars convected by turbulence in order to numerically calculate the effective (turbulent) diffusion coefficient.

Both mixing flows, the eddy-lattice flow and the turbulent one, are implemented in our continuum model by adding a drift term, $\vec{v}\vec{\nabla}c$, that describes the transport of the reactants by an incompressible flow whose velocity field is $\vec{v}$. All the procedure for the analytical and numerical implementation of both mixing flows is reported in Chapter V.

In Chapter VI, numerical results are shown for the eddy-lattice flows (Sect. VI-1) and for the turbulent flow (Sect. VI-2). Both cases show a diversity of transient kinetic regimes closely related to the spatial organization of the system at each time. Nevertheless, for long times we always recover the asymptotic Zeldovich behavior in both flows. It is really interesting to observe that, even the more chaotic two dimensional flow, our turbulent case, can only support the classical kinetic law transiently before the system completely segregates. When this occurs the system behaves in a fluctuation-dominated way but with the corresponding effective diffusion coefficient. In the last section (Sect. VI-3) of this chapter an analytically tractable model, namely, shear flow mixing on a cylinder surface is presented. This model allows us to reproduce many of the findings of the eddy-lattice flow [Sok96, Rei96b, Rei97a].

In Chapter VII we concentrate on the spatial organization for the systems under turbulent flow. We discuss the properties of the clusters and of the reaction zones and study the interplay between the kinetic patterns and the spatial organization of reactants. Special attention is payed to the occurence of rather fast reactions even when the reactants are strongly segregated [Rei97b]. Finally, the conclusions of all this work have been summarized in Chapter VIII.

In all the analytical and numerical calculations presented in this part of our work dealing with mixing, the standard case of A+B->0 diffusion-limited system is considered: two dimensions, poissonian and stoichiometrical initial conditions and equal diffusion coefficients (D) for both reactants.

CHAPTER V

-Model Equations and Numerical Procedure-

The kinetics of the A+B->0 reaction is modeled in terms of the usual reaction-diffusion equations under a superimposed advective drift [Rei96b]

$$\frac{\partial c_A(\vec{r},t)}{\partial t} + \vec{v}\cdot\vec{\nabla}c_A(\vec{r},t) = D\nabla^2 c_A(\vec{r},t) - Kc_A(\vec{r},t)c_B(\vec{r},t) \qquad (V\text{–}1)$$

and

$$\frac{\partial c_B(\vec{r},t)}{\partial t} + \vec{v}\cdot\vec{\nabla}c_B(\vec{r},t) = D\nabla^2 c_B(\vec{r},t) - Kc_A(\vec{r},t)c_B(\vec{r},t) \qquad (V\text{–}2)$$

The drift term $\vec{v}\cdot\vec{\nabla}c$ describes the transport of the reactants by an incompressible fluid whose velocity field is $\vec{v}$. The numerical implementation of the reaction-diffusion-advection equations follows the standard procedure explained in Chapter I. Periodic boundary conditions are also used for the flow.

Two examples of two-dimensional incompressible flows are examined. The first one corresponds to a completely integrable and time-independent velocity field, whereas the second one is a space- and time-dependent random flow. The velocity field $\vec{v}$ is generated in both cases from the stream function $\eta(x,y)$ through the prescription

$$\vec{v}(\vec{r},t) = \left(-\frac{\partial \eta}{\partial y}, \frac{\partial \eta}{\partial x}\right) \qquad \text{(V–3)}$$

Eddy-lattice Flow:

Here, we start with a time-independent, spatially periodic stream function given by

$$\eta(x,y) = \frac{2Lu_0}{n\pi}\cos\left(\frac{n\pi x}{L}\right)\cos\left(\frac{n\pi y}{L}\right) \qquad \text{(V–4)}$$

where u_0 is the intensity of the velocity field and n stands for the number of eddies along the side of the lattice whose linear dimension is given by L. The velocity field given by Eq. (V-4) is then expressed as

$$v_x(x,y) = 2u_0\cos\left(\frac{n\pi x}{L}\right)\sin\left(\frac{n\pi y}{L}\right) \qquad \text{(V–5)}$$

and

$$v_y(x,y) = -2u_0 \sin(\frac{n\pi x}{L})\cos(\frac{n\pi y}{L}) \qquad (V-6)$$

Such a flow was experimentally considered by Tabeling et al. [Tab91, Car96]. To be consistent with the periodic boundary conditions for the flow, n is taken to be an even integer.

In Figure V-1 a pattern for the eddy-lattice velocity flow corresponding to the particular case of n=2 are shown.

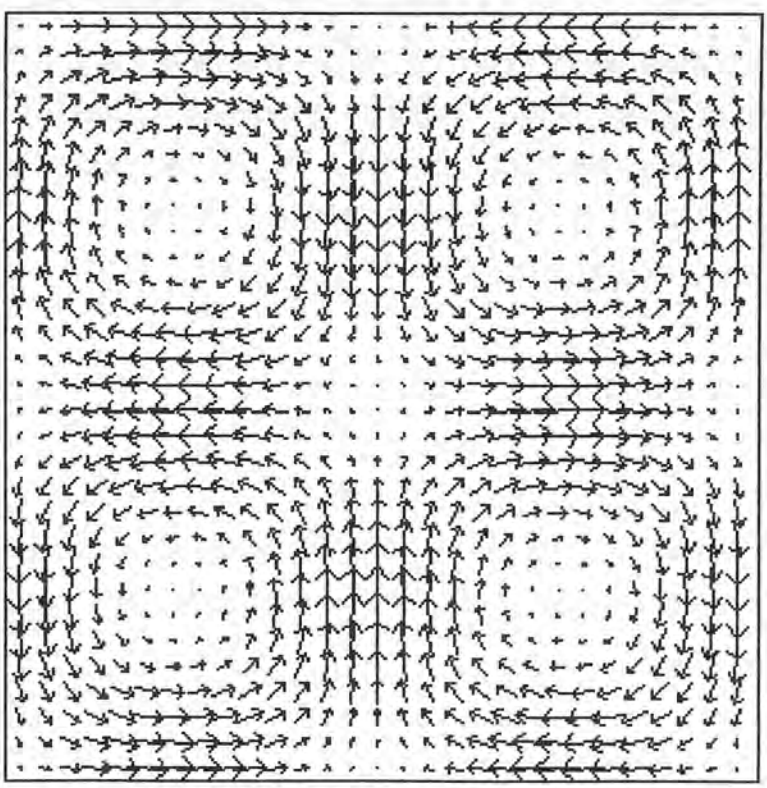

Fig. V-1- Flow pattern for the eddy-lattice configuration.

Turbulent Flow:

Based on a versatile algorithm to simulate (synthetic) turbulence [Car93b, Mar97] we create space- and time-dependent velocity fields, which mimic statistically isotropic, homogeneous and stationary turbulent flows. This pragmatic point of view allows us to display the role of generic effects of turbulence on chemical reactions. This strategy offers much simplicity in the implementation of realistic properties of turbulent flows, together with the possibility to control closely their parameters, such as spectra, intensities and spatial and temporal scales.

To generate the synthetic turbulent flow the stream function $\eta(x,y)$ is assumed to be a Gaussian random process (colored noise in space and time) with well-prescribed statistical properties; see [Gar92]. Detailed versions of the method are given elsewhere [Car93b, Mar97] but we will summarize here the main ideas in a short, self-contained presentation. The starting point is the Langevin equation for the stream function $\eta(x,y)$

$$\frac{\partial \eta(\vec{r},t)}{\partial t} = \nu\nabla^2\eta(\vec{r},t) + Q(\lambda^2\nabla^2)\vec{\nabla}\cdot\vec{\xi}(\vec{r},t) \qquad \text{(V–7)}$$

where ν stands for the kinematic viscosity and $Q(\lambda^2\nabla^2)$ is a differential operator, with λ being the typical length scale of the flow; furthermore $\vec{\xi}(\vec{r},t)$ is a two-component random Gaussian process with zero mean value and correlation function

$$\left\langle \xi_i(\vec{r_1},t_1)\xi_j(\vec{r_2},t_2)\right\rangle = 2\varepsilon\nu\delta(t_1-t_2)\delta(\vec{r_1}-\vec{r_2})\delta_{ij} \qquad \text{(V–8)}$$

The parameter ε in Eq. (V-8) fixes the intensity of the random flow. On the other hand, the operator Q will be directly related to the energy espectrum of

the turbulent flow.

In steady state the statistical properties of $\vec{v}$ can be expressed in terms of the autocorrelation tensor

$$R_{ij}(\vec{r_1}-\vec{r_2},t_1-t_2) = \langle v_i(\vec{r_1},t_1)v_j(\vec{r_2},t_2)\rangle \qquad (V-9)$$

For flows which are statistically isotropic and homogeneous in space and time the radial correlation function is defined as

$$R(r,s) = \frac{1}{2}\left[R_{xx}(r,s) + R_{yy}(r,s)\right] \qquad (V-10)$$

where $r = |\vec{r_1}-\vec{r_2}|$ and $s = |t_1-t_2|$. The parameters which characterize the flow, the intensity and the characteristic integral time and length scales are determined through R(r,s)

$$u_0^2 = R(0,0) = \int_0^\infty E(k)\, dk \qquad (V-11)$$

$$t_0 = \frac{1}{u_0^2}\int_0^\infty ds\, R(0,s) \qquad (V-12)$$

and

$$l_0 = \frac{1}{u_0^2}\int_0^\infty dr\, R(r,0) \qquad (V-13)$$

Another relevant quantity introduced above is the energy spectrum E(k), which is the Fourier transform of R(r,0), and contains information on the way the energy is distributed between the different spatial modes.

The statistical quantities of the random velocity field are easily obtained from those of the scalar stream function η. In particular, the most important quantity, i.e. the correlation function R(r,s), is directly related to the correlation function of η,

$$C(r,s) = \langle \eta(\vec{r_1},t_1)\eta(\vec{r_2},t_2) \rangle \qquad (V-14)$$

where $r=|\vec{r_1}-\vec{r_2}|$ and $s=t_1-t_2$.

Actually, it turns out that invoking the statistical properties of isotropic, stationary and homogeneous flow

$$R(r,s) = \frac{1}{4\pi}\int_0^\infty J_0(kr)\, k^3 C(k,s)dk \qquad (V-15)$$

where $J_0(kr)$ is the Bessel function of zero-th order and C(k,s) is the Fourier transform of C(r,s).

In order to obtain an explicit expression for C(k,s) we can Fourier transform Eq. (V-7)

$$\frac{\partial \eta(\vec{k},t)}{\partial t} = -\nu k^2 \eta(\vec{k},t) - iQ(-\lambda^2 k^2)\sum_j \xi_j(\vec{k},t)k_j \qquad (V-16)$$

where now the operator Q is just a function of k. The correlation properties of the Fourier components of the noise $\xi_j(\vec{k},t)$ follow from Eq. (V-8). In the steady state the formal solution of Eq. (V-16) leads to the following expression:

$$C(k,s) = \varepsilon Q^2(-\lambda^2 k^2)e^{-\nu k^2 s} \qquad \text{(V–17)}$$

The energy spectrum is then given by

$$E(k) = \frac{\varepsilon}{4\pi} k^3 Q^2(-\lambda^2 k^2) \qquad \text{(V–18)}$$

By a judicious choice of the differential operator $Q^2(\lambda^2 k^2)$ in Eq. (V-12) and of the noise parameters ε, λ and ν, we may easily reproduce standard turbulent spectra, with precisely specified characteristics. In what follows we choose the so-called Kraichnan's flows as a model for the velocity field; for this flow the energy spectrum E(k) in two dimensions is given by [Kra70]:

$$E(k) \propto k^3 \exp(-k^2/k_0^2) \qquad \text{(V–19)}$$

where k_0 is a characteristic wave number corresponding to the peak of the spectrum. In this case the operator Q has the form [Mar97]

$$Q(\lambda^2 \nabla^2) = \exp\left(\frac{\lambda^2 \nabla^2}{2}\right) \qquad \text{(V–20)}$$

with $\lambda = k_0^{-1}$. The corresponding velocity autocorrelation function obtained from Eqs. (V-15), (V-17) and (V-20) is then

$$R(r,s) = \frac{\varepsilon}{8\pi(\lambda^2+\nu s)^2}\left[1 - \frac{r^2}{4(\lambda^2+\nu s)}\right]\exp\left(-\frac{r^2}{4(\lambda^2+\nu s)}\right) \qquad \text{(V–21)}$$

Using Eqs. (V-11) to (V-13) we can relate the flow parameters to the model parameters ε, λ and ν, obtaining

$$u_0^2 = \frac{\varepsilon}{8\pi\lambda^4} \qquad \text{(V–22a)}$$

$$t_0 = \frac{\lambda^2}{\nu} \quad \text{(V–22b)}$$

and

$$l_0 = \frac{\lambda\sqrt{\pi}}{2} \quad \text{(V–22c)}$$

The whole numerical procedure of flow generation is conveniently handled in Fourier space. It is worth remarking here that Eq. (V-16) describes a set of noncoupled, ordinary differential linear equations, which can be solved exactly for a finite set of values of $\vec{k}$ prescribed by the discretization scheme, and used for constructing the Fourier transform of the stream function. Any each time step the velocity field is obtained by backtransforming $\eta(\vec{k},t)$ and using Eq. (V-3). Independently of the initial conditions the flow will converge to a steady state in which the energy spectrum is given by Eq. (V-19). In order to skip this initial, relaxational stage and to start directly from a steady state situation we chose the initial values $\eta(\vec{k},0)$ in such a way that the energy spectrum of the flow is stationary from the very beginning [Car93b, Mar97].

Before going to the numerical results we briefly show in Figs. V-2 and V-3 turbulent flow patterns obtained for individual realizations of the random velocity field. Figure V-2 displays the presence of flow lines and eddies of different size and shape subjected to the prescribed periodic boundary conditions. The basic difference between Figs. V-2a and V-2b is the mean eddy size. Actually this size is directly related to l_0. Shown in Figs. V-3 are two snapshots of a particular realization of the stochastic turbulence taken at different times. They give us an idea on how fluid moves subject to the incompressibility condition.

In the following chapters we shall work with d=2, $\Delta x=1$ and $D_A=D_B=D=0.1$. Almost the majority of the simulations are run with K=10. Sometimes, when the value of u_0^2 is very large, the discretization in time will be fixed to smaller values than 0.01 with the purpose of maintaining the numerical convergence.

The code was also programmed in FORTRAN-77 using a fast Fourier transform subrutine. The calculations have been performed on the CRAY Y-MP/232 of Centre de Supercomputació de Catalunya (CESCA) and on a Power Indigo-2 SiliconGraphics workstation. The numerical simulations with stochastic the flow needs ten times more CPU time than the runs without flow or with a deterministic flow because of the Fourier transformation procedure. Graphic outputs of these simulations were displayed using some C-software rutines originally developed in the SiliconGraphics computer.

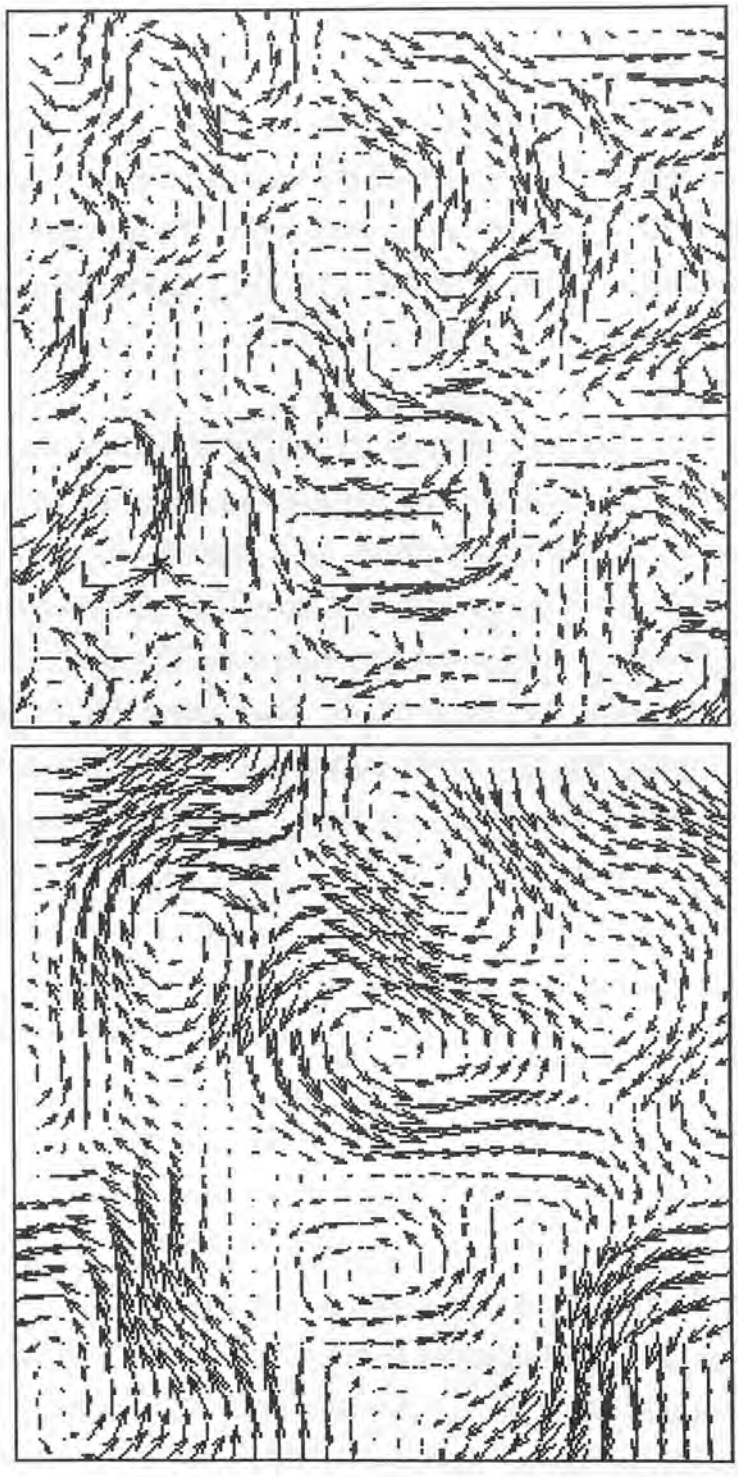

Fig. V-2- Flow patterns for particular realizations of the turbulent velocity field corresponding to $u_0^2=2.10^{-2}$, $l_0=8.86$ and $t_0=1$ in a) and $u_0^2=1.2.10^{-3}$, $l_0=17.7$ and $t_0=4$ in b). L=200 in both cases.

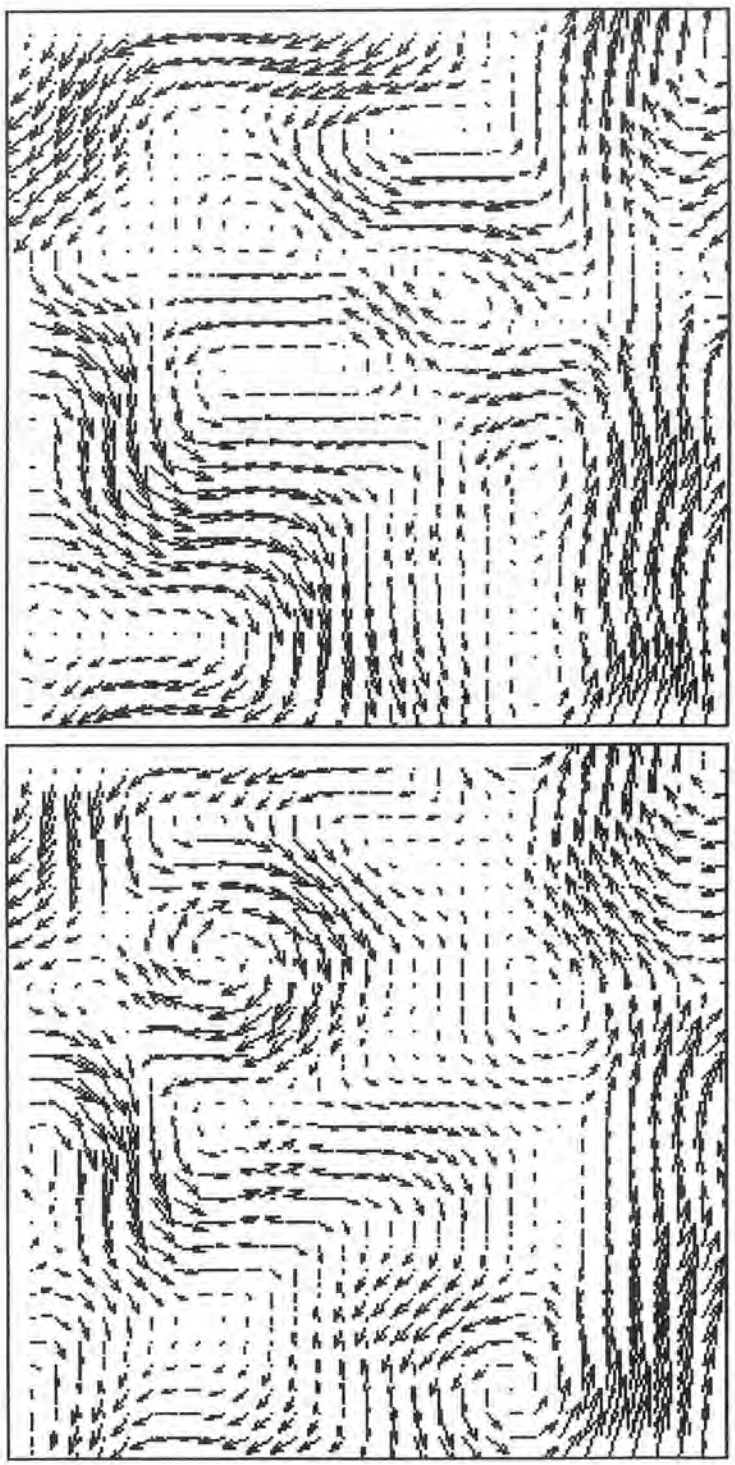

Fig. V-3- Two snapshots of turbulent flow patterns similar to those of Fig. V-2b taken at different times. a) t=2 and b) t=4.

CHAPTER VI

-Kinetic Laws: Analytic and Numerical Results-

In this chapter we are going to summarize all the analytic and numerical results on what respects to the kinetic aspects of the A+B->0 fluctuation-dominated system under different flows.

In the first section the eddy-lattice flow is studied, and a diversity of transient regimes are shown. In the second section we concentrate on the turbulent flow and its long-time Zeldovich regime is stressed. Both sections show that these two-dimensional stirring procedures are not totally effective since they are not capable of mixing indefinitely the reactants. Rather, the standard fluctuation dominated behavior in two dimensions is observed for both flows at sufficiently long times. In any case what is interesting is to correlate qualitatively the different kinetic behaviors observed during the course of the reaction with the spatial organization which emerge from these flows. Later on, in Chapter VII, such a relation between kinetic behavior and reactants spatial organization will be re-examined from a more quantitative point of view.

Finally, in the third section an analytical shear flow model on the surface of a cylinder is introduced with the aim of better understanding some of the kinetic regimes that appear in the eddy-lattice case.

SECTION VI-1 -Eddy-lattice Flow-

When analyzing the class of fluctuation-dominated reactions here considered under time-independent spatially periodic flows a very rich behavior is found [Rei96b, Rei97a, Sok96]. The observed power-law decay patterns $c(t) \sim t^{-\alpha}$ determine different regimes, each one described by its own exponent α, and separated by crossover zones.

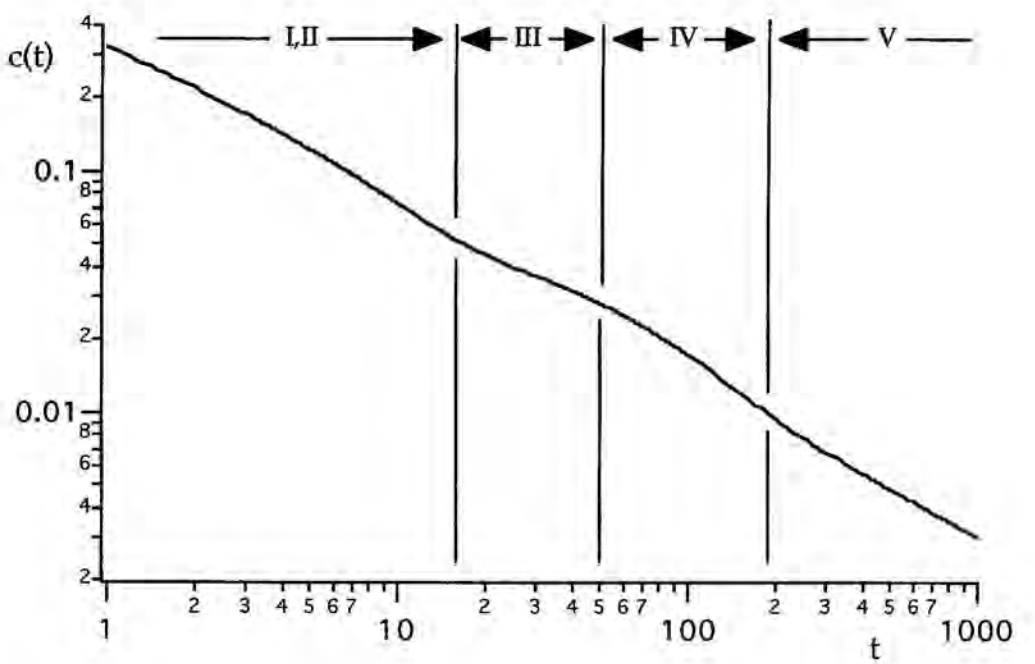

Fig. VI-1- Double-logarithmic plot of c(t) vs. t for the eddy-lattice flow. The parameters of the flow are u_0=2, n=30 and L=300. The roman figures denote different decay regimes.

Figure VI-1, in which the c vs. t dependence is shown in double-logarithmic scales, captures the whole set of dynamic scenarios to which we will refer in what follows. To supplement and better understand this kinetic behavior we display in Fig. VI-2 a comprehensive mosaic of patterns for the reaction zones, patterns which correspond in Fig. VI-1 to different kinetic regimes.

First, the Zeldovich ($\alpha \approx 1/2$) regime (I) appears at very early times when the kinetics are still unaffected by the flow [How96]. Following this slow transient regime the reaction strongly speeds up while entering a regime (II) of mixing along the closed flow lines. In Fig. VI-1 this regime is not well developed. Using another set of parameters, see Fig. VI-3 below, one can infer that in regime II the classical $c(t) \sim t^{-1}$-law tends to hold.

After this fast regime, the dynamic behavior experiences a clear crossover towards a much slower kinetics (III); numerically we find for III that $\alpha \approx 1/4$. This corresponds to the anomalous, Zeldovich-like, kinetic behavior for d=1, i.e., to a one-dimensional diffusive motion. The explanation for this behavior is the following. During the previous mixing stage the flow has been mixing along the direction of the flow lines until the concentric zones connected by the closed flow lines are completely homogenized. In this situation the flow does not mix at all and only the diffusion process perpendicular to the flow lines can mix both A and B reactants. Thus, we associate this finding with a Zeldovich kinetics picture for the transversal diffusion across the closed flow lines. In fact, we can expect this effect in all the simulated two-dimensional and stationary flows with closed flow lines, because we are not capable of avoiding the formation of one-dimensional clusters without changing the flow's topology. In our eddy-lattice case the formation of one-dimensional concentric structures

(rings) is shown in Fig. VI-2b. We will support all this interpretation by analytical arguments which are going to be presented in Section VI-3.

After this stage, the reaction inside each individual eddy has practically finished and what is left is just the initial excess of the majority component (A or B) within each eddy. As a consequence, the reaction zones concentrate more and more at the boundaries between eddies, where a large recirculation allows the whole reaction to go on to form a quasiperiodic pattern; see Fig. VI-2c. In this regime (IV) the corresponding quasiexponential decay is found; see Section 3c in Chapter II.

Later on this quasiperiodic arrangement of reaction zones starts to dissolve, and a coarse-grained structure appears; it is built from large cluster separated by irregularly patterned reaction zones, see Fig. VI-2d. The individual eddies are now the smallest elements of the structure. In this phase of the reaction (V) we find an exponent $\alpha = 1/2$ which corresponds to a two-dimensional fluctuation-dominated decay over the whole system.

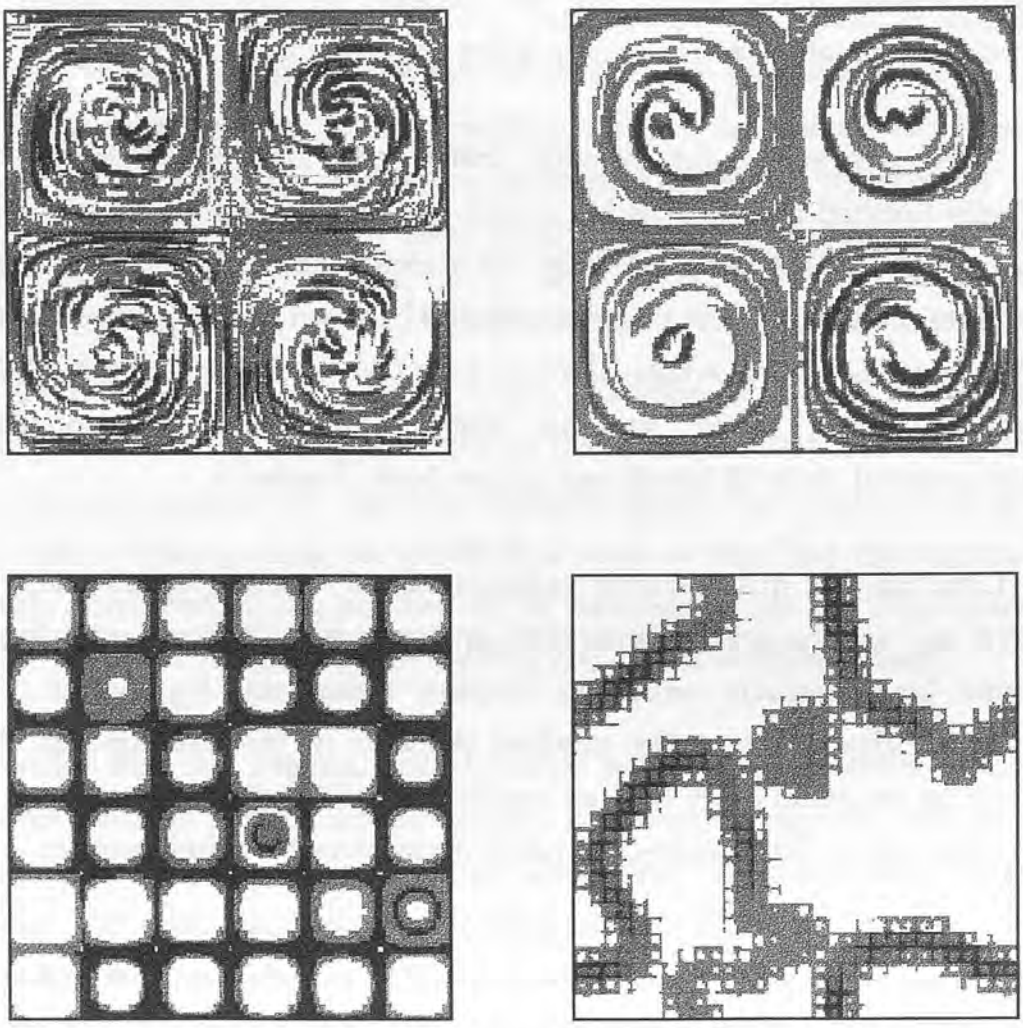

Fig. VI-2- Mosaic of patterns showing the topology of the reaction zones at three different stages of the advected reaction. For the sake of clarity two different sets of parameters were used. a) Upper left: a snapshot at t=24 of a simulation run with u_0=10, n=2 and L=150, corresponding regime II; b) upper right: the same as in a) but now at t=60 (regime III); c) lower left: a snapshot at t=300 of a simulation with u_0=10, n=6 and L=150 (regime IV); d) lower right: a snapshot at t=800 of a simulation run with the parameters of Fig. VI-1 (regime V).

Needles to say, given the diversity of kinetic behaviors just described, we were forced to use a very specific set of parameters when preparing Fig. VI-1, in order to be able to show all decay forms on the same picture. To emphasize the findings and our interpretation, we adopt in Fig. VI-3 and Fig. VI-4 other parameter values; this enables us to display in a more specific way some of the previously identified kinetic regimes. In particular, the one-dimensional Zeldovich behavior is better evidenced when dealing with high-intensity flows in large eddies. This is essentially the contents of Fig. VI-3. In this case, both the mixing regime and especially the $t^{-1/4}$-behavior start later and last longer when increasing the eddies' size. These two regimes (II and III) can be related with the reactants and reaction zones pictures shown for the case n=2 in Figs. VI-5 and VI-6 respectively.

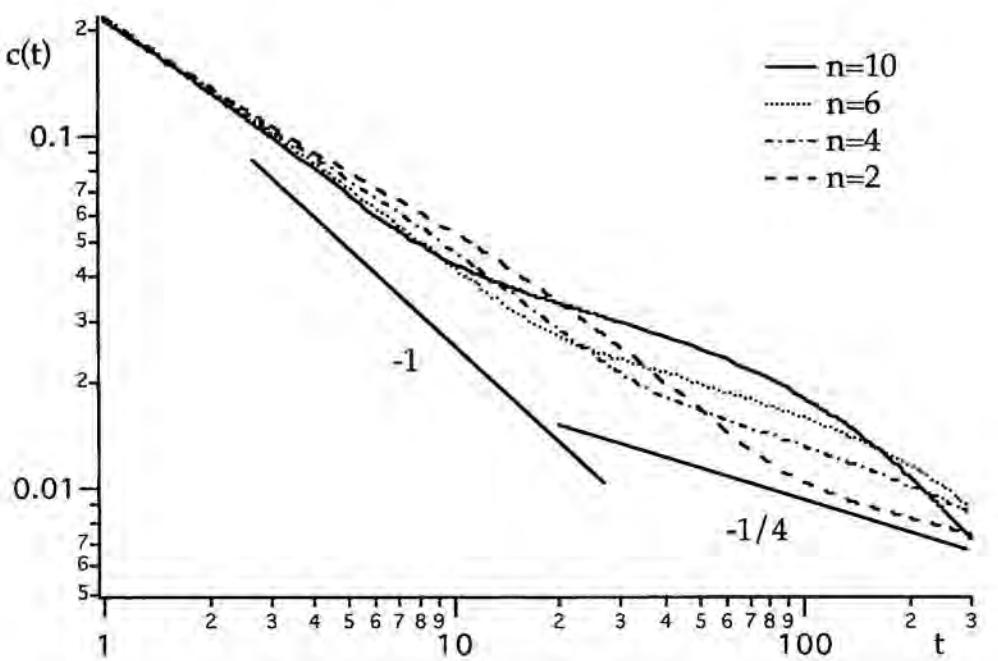

Fig. VI-3- Double-logarithmic plot of c(t) for lattices containing different number of eddies, namely n=2, 4, 6 and 10, with u_0=10.

On the other hand, Fig. VI-3 does not show the long-time kinetic behavior. We need to choose less intense velocity fields and especially to deal with larger systems, composed of smaller eddies, in order to detect to long-time $t^{-1/2}$-regime. This is precisely what is illustrated in Fig VI-4. Pattern organization for the case n=30 in Fig. VI-1 is displayed for different times in Figures VI-7 and VI-8. Figs. a) stands for the quasiperiodic arrangement and Figs. b) and c) correspond to the standard two-dimensional Zeldovich kinetic stage.

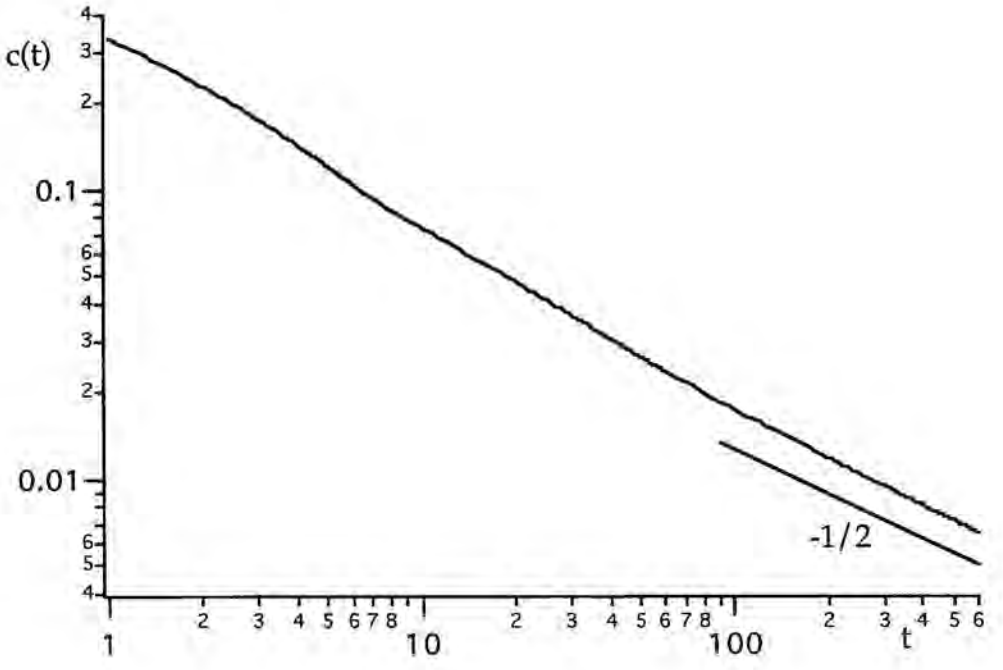

Fig. VI-4- Double-logarithmic plot of c(t) vs. t for the eddy-lattice with n=60, where the values of parameters are those of Fig. VI-1.

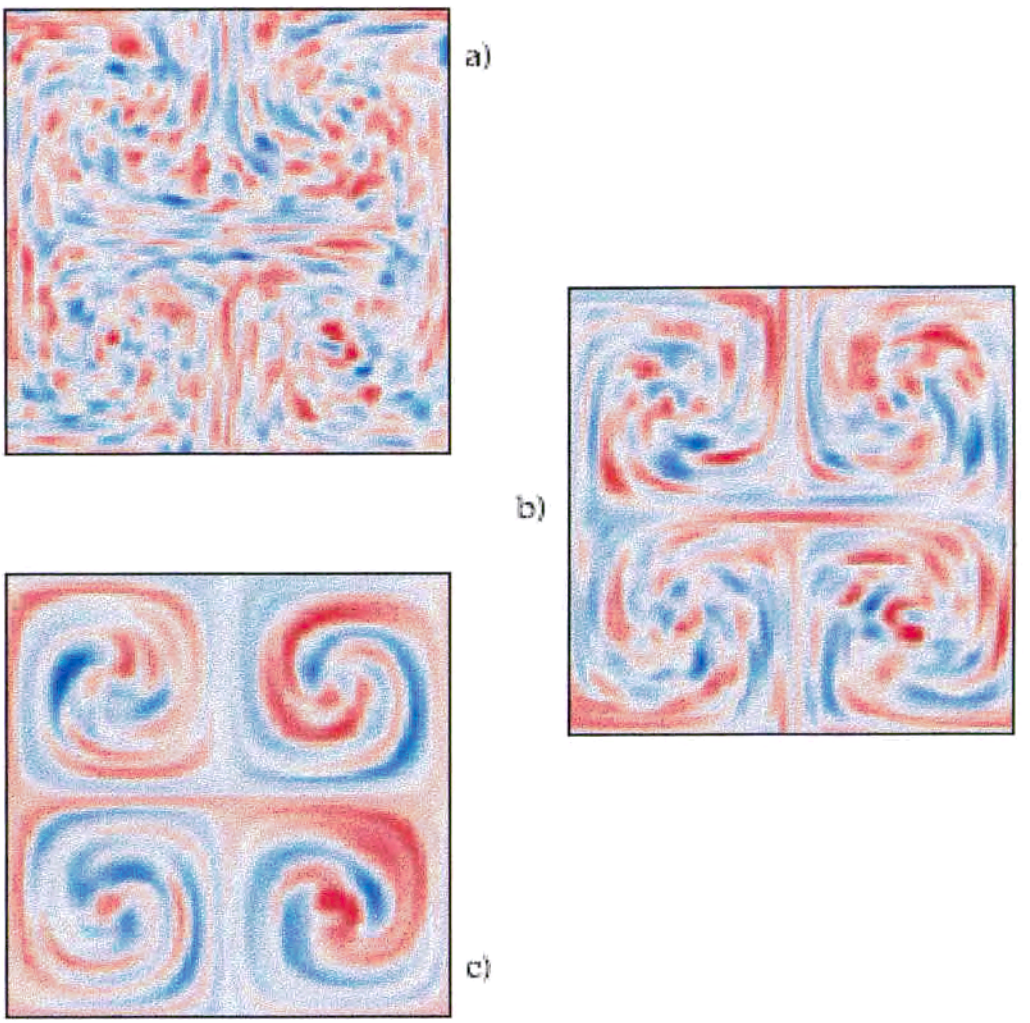

Fig. VI-5- Time evolution of the reactants pattern for the n=2 eddy-lattice flow with u_0=10. Three different times are shown: a) t=12, b) t=24 and c) t=48.

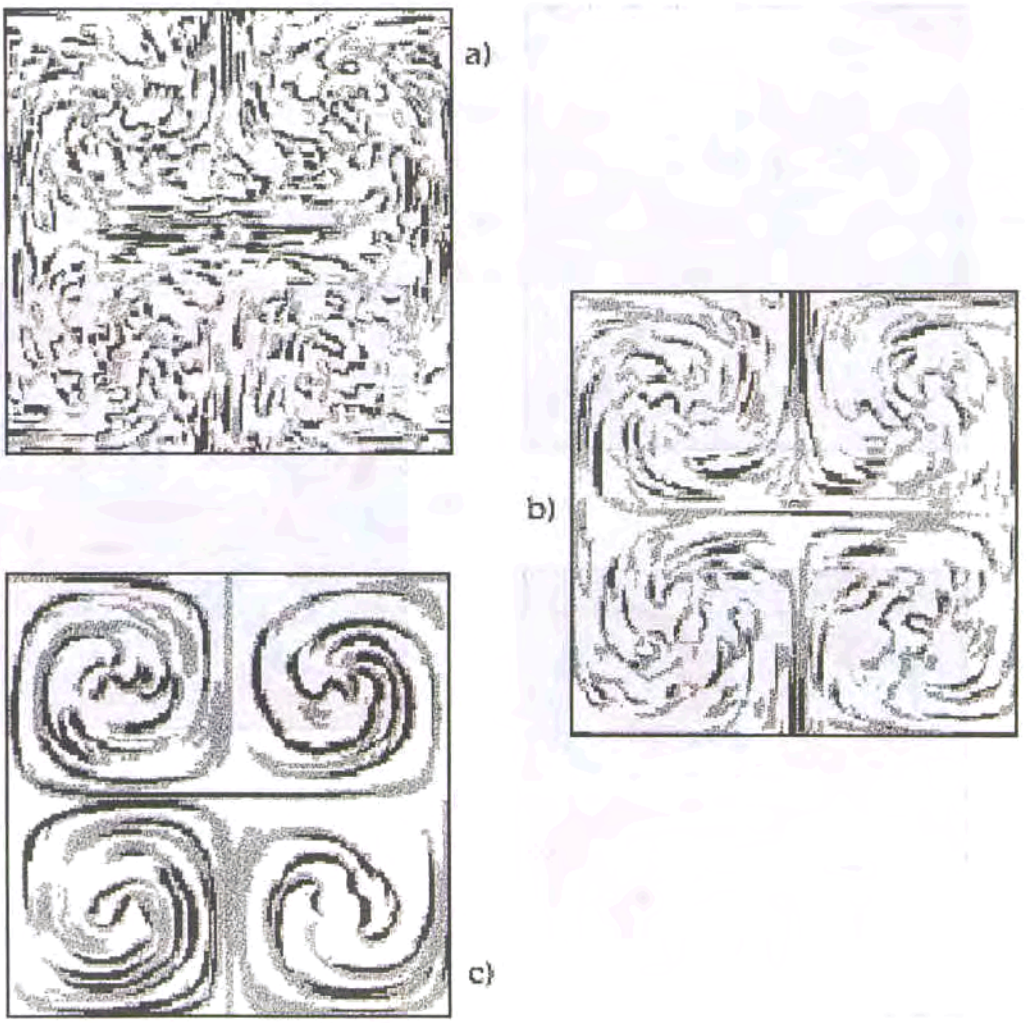

Fig. VI-6- Time evolution of the reaction zones for the case and times depicted in Fig. VI-5.

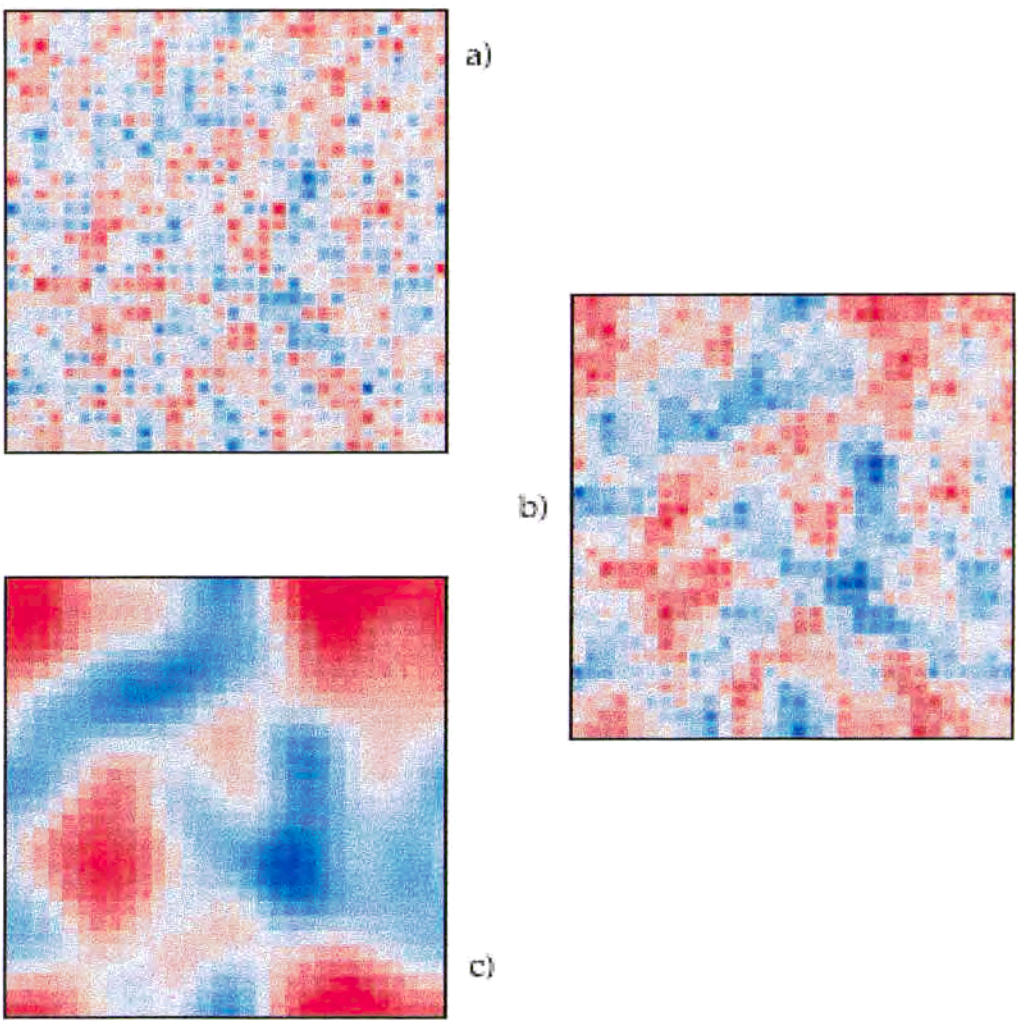

Fig. VI-7- Distribution of reactants for three different times for the case of eddy-lattice flow with n=30 and u_0=2. Three different times are shown: a) t=80, b) t=200 and c) t=1000.

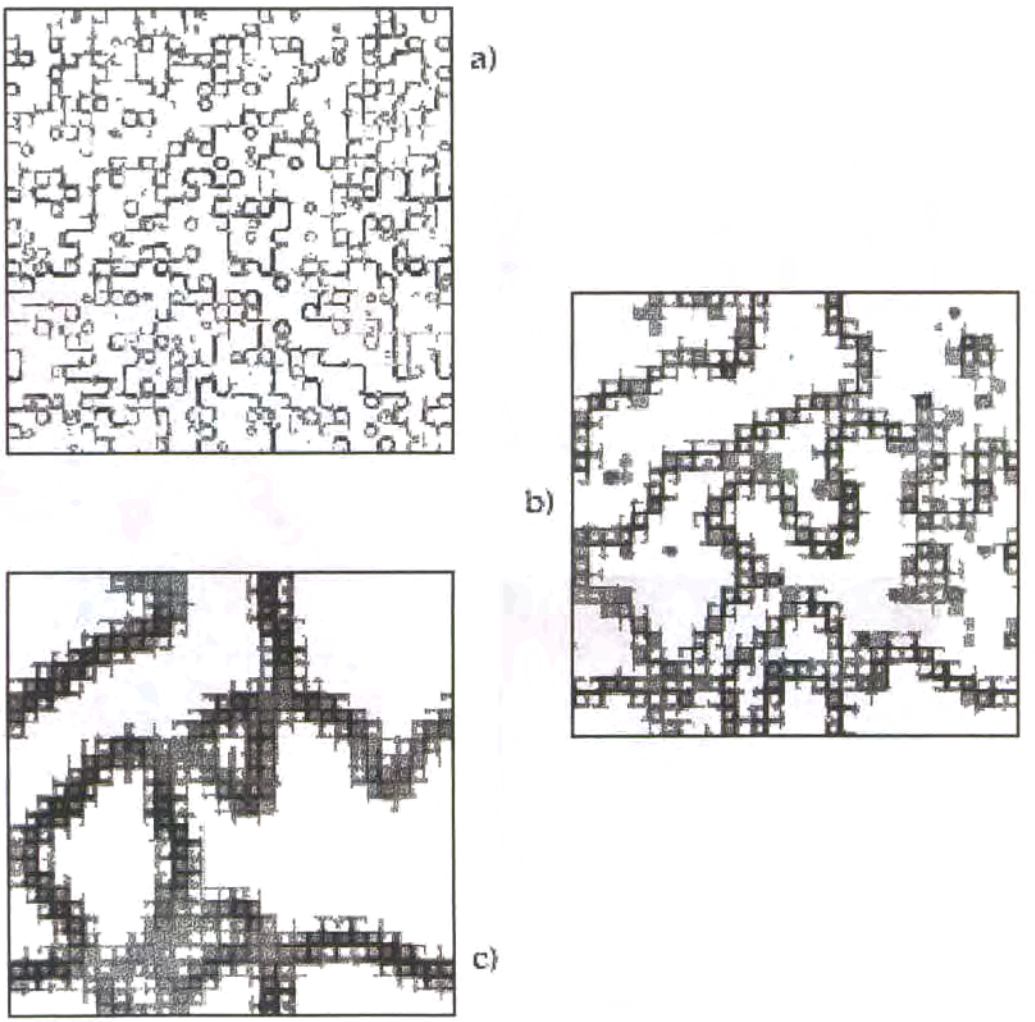

Fig. VI-8- Time evolution of the reaction zones for the case and times depicted in Fig. VI-7.

SECTION VI-2 -Turbulent Flow-

Somewhat unexpectedly, the seemingly much more complex turbulent flow leads to a simpler kinetic behavior [Rei96b, Sok96, Rei97a, Rei97b]. We concentrate in the case with the following simulation parameters: L=300, D=0.1, K=10, initial Poisson distribution, and a Kraichnan spectrum flow with ε=500, λ=2 and ν=2 (u_0^2=1.243, l_0=1.7 and t_0=2). Δx=1 and $\Delta t=2.10^{-3}$ are fixed to assure the numerical convergence.

Figures VI-9, VI-10 and VI-11 depict the main results: Figure VI-9 refers to the global kinetic behavior, whereas Figs. VI-10 and VI-11 show the spatial organization of the system for four different times. After a slow transient regime, the system enters a regime of local mixing, $c(t) \sim t^{-1}$, i.e., a micromixing stage, whose length scale is dictated by the correlation length of the flow. Looking at the pictures a) of Figs. VI-10 and VI-11 one realizes that the system is still not much segregated at this stage.

Following this regime the decay crosses over a two-dimensional fluctuation-dominated situation whose hallmark is a $c(t) \sim t^{-1/2}$ power law. To emphasize this conclusion, Fig. VI-9 also shows for the sake of comparison, the kinetic behavior of two systems without flow, but with different diffusion coefficients, namely, with D, the (bare) diffusion coefficient, and with D^*, the effective turbulent diffusion coefficient, calculated for a non-reacting advected scalar immersed in such turbulent flow conditions [Car93a, Car94]. As shown in Fig. VI-9 the long-time behavior of the advected system approaches that of the nonadvected

reaction under turbulent diffusion. Furthermore, the mixing regime interpolates between the short-time behavior governed by D and the long-time behavior governed by D^*. Looking at the last three times of Figs. VI-10 and VI-11 one realizes that the system is clearly segregated at this fluctuation-dominated regime in spite of the mixing flow.

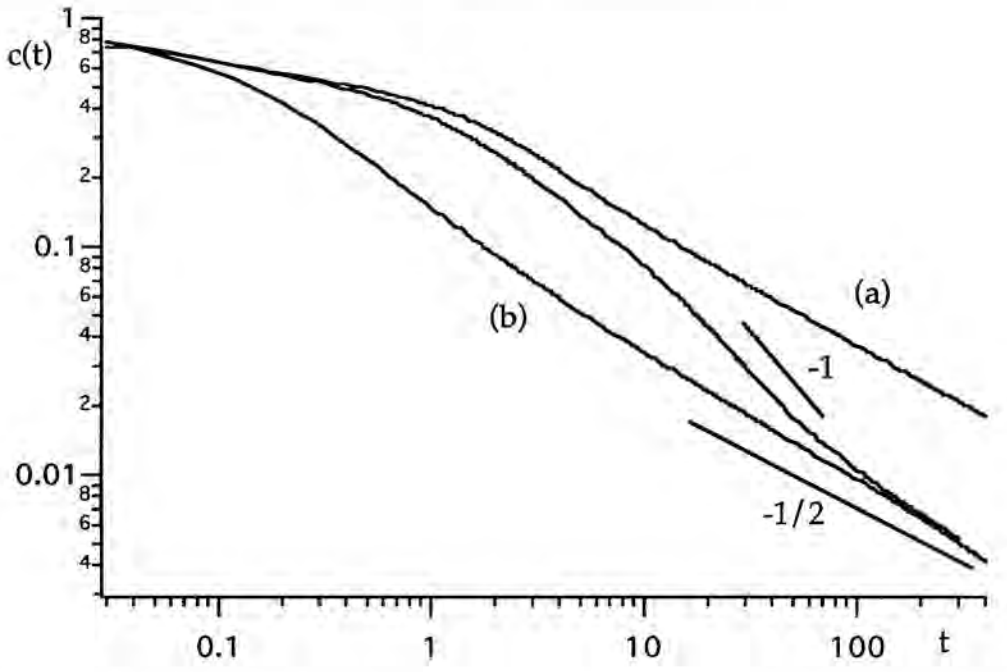

Fig. VI-9- Double-logarithmic plot of c(t) vs. t for turbulent flow. The simulation parameters are ε=500, λ=2 and ν=2, which corresponds to u_0^2=1.243, l_0=1.7 and t_0=2. For the sake of comparison two additional curves are provided: a) c(t) for the nonadvected reactive system with the diffusion coefficient D=0.1 and b) c(t) for a nonadvected reactive system with the corresponding effective turbulent diffusion coefficient D^*=1.529.

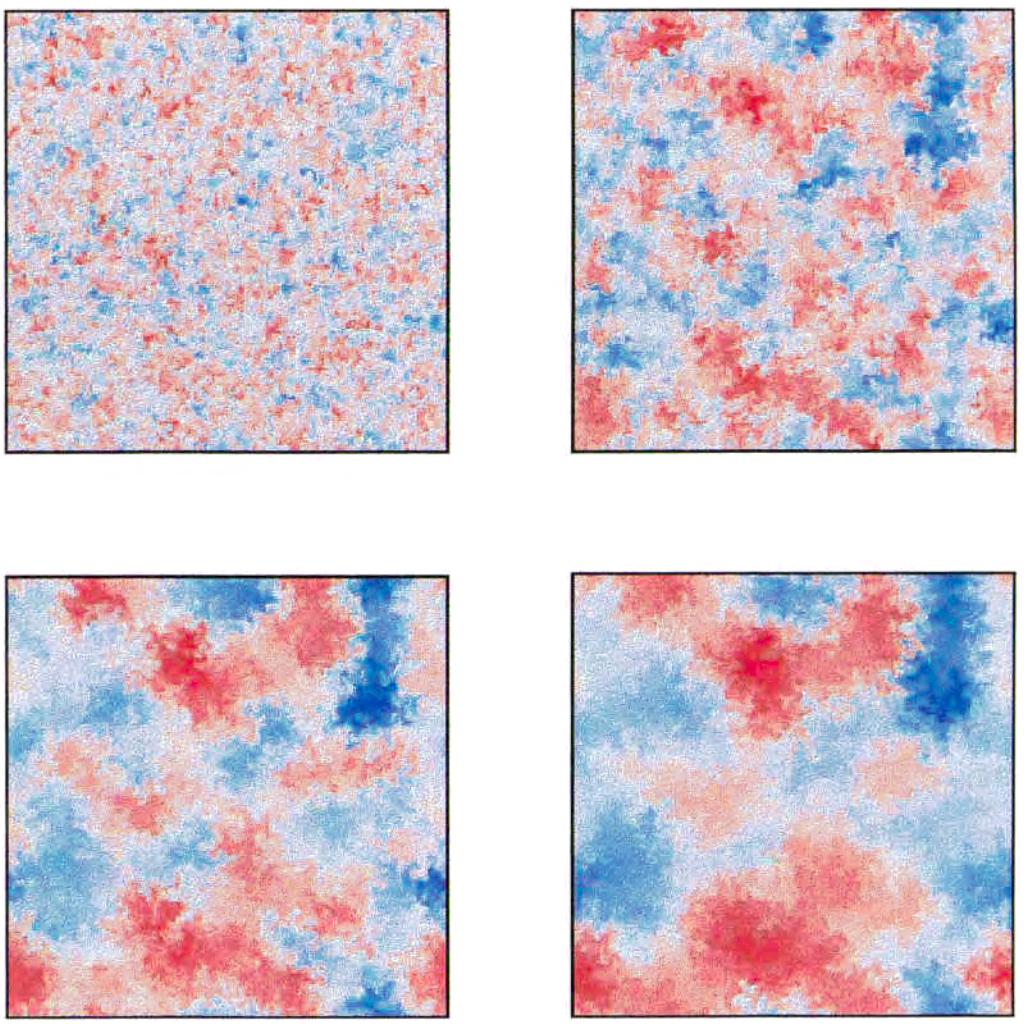

Fig. VI-10- Reactants distribution of one realization of the advected system studied in Fig. VI-9. Four times are displayed: t=50, 100, 200 and 300.

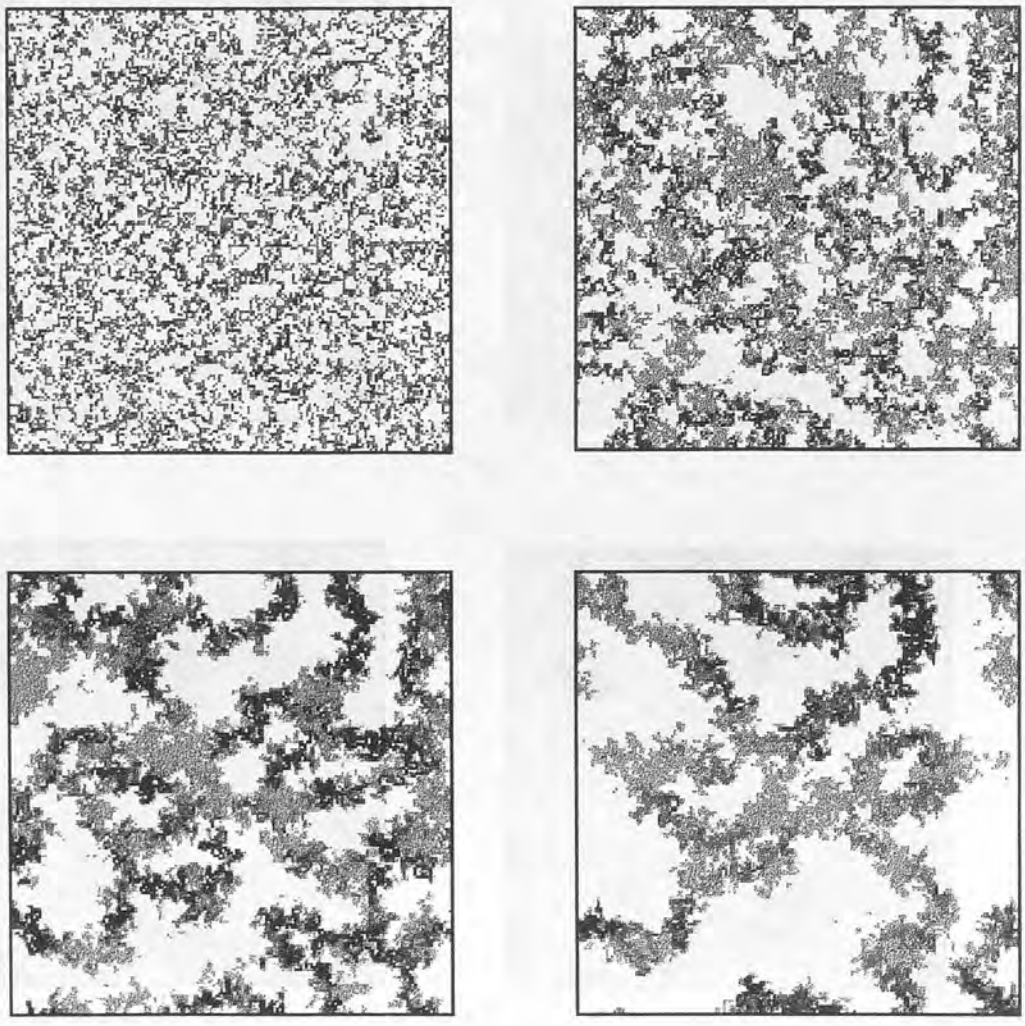

Fig. VI-11- Time evolution of the reaction zones for the case and times depicted in Fig. VI-10.

A qualitative study of the influence of the different flow parameters has been done in Figure VI-12. We have simulated under the same conditions (L, D, K,...) of the previous case (u_0^2=1.243, l_0=1.7 and t_0=2) three additional situations changing the intensity, the correlation time and the correlation length. In all these new cases, the effective turbulent diffusion coefficient have been calculated and nonadvected reacting systems with these new D^* have been simulated.

In the first case we fix ε=1000, thus u_0^2=2.486, and the scalar-dispersion simulation leads to a value D^*=2.5. The corresponding results are plotted in dotted lines in Fig. VI-12. It is clearly shown that the mixing stage starts earlier than in the reference case because a stronger flow affects the kinetics of the system more rapidly than a weaker one.

In the case plotted in dashed lines the value of the correlation length is l_0=3.4 (by fixing ε=8000, λ=4 and ν=8) and its corresponding D^* is equal to 3.56. One easily observes that in this case the flow needs more time to enter the mixing stage but this regime is sustained during a longer time, so that the fluctuation-dominated regime is only achieved at very late times. This is due to the fact that the flow only mixes at length scales of the order of l_0.

Finally we decrease the correlation time to t_0=1 by setting ε=500, λ=2 and ν=4. The corresponding scalar-dispersion simulation leads to D^*=1.08 and the results are plotted in dotted-dashed lines in Fig. VI-12. In this case the fluctuation-dominated regime is achieved earlier than in the reference case even though the flow needs more time to enter the mixing stage.

From all these results shown in Fig. VI-12 we finish with the following conclusion: the mixing of reactants is favoured for strong (large u_0^2) flows with large correlation times and large correlation lengths. Contrarily the weaker flows with small correlation lengths and small correlation times lead to the effective diffusion regime at earlier times.

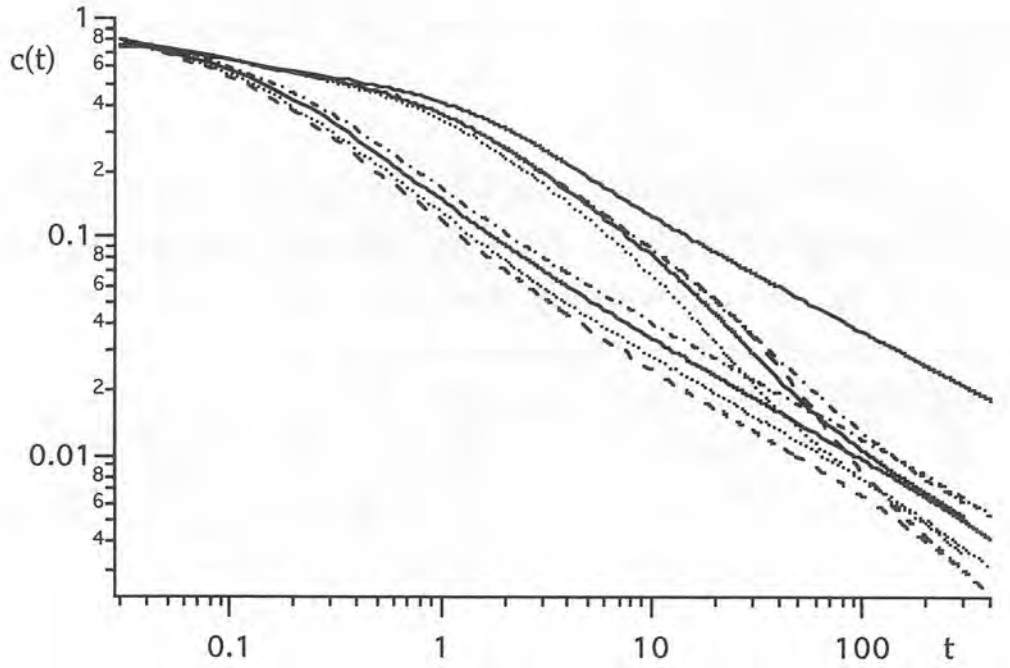

Fig. VI-12- The same representation of Fig. VI-9 but for different flow parameters. The case of Fig. VI-9 corresponds to the solid line. In dotted lines the case with a higher intensity flow u_0^2=2.486, in dashed lines the case with a larger correlation length l_0=3.4 and finally with dotted-dashed lines the case with a smaller correlation time t_0=1.

SECTION VI-3 -Shear-flow on a Cylindrical Surface-

In Section VI-1 we have suggested that the slow intermediate-time decay observed for the eddy-lattice flow is due to an essentially one-dimensional diffusion across flow lines. Therefore, it is interesting to consider here an analytically tractable model of reaction under flow with closed flow lines. This allows us to gain a better insight into the problem of reactions under mixing trying to validate our suggestion. We note that already the simple diffusion equation under planar flows represented by arrays of eddies is very complex, so that no analytical solutions for it are known, see [Cri91] and references therein. We choose thus a model with closed flow lines which is simple enough to allow for an analytical treatment: we focus thus on reactions under shear flows on cylindrical surfaces [Sok92b, How96].

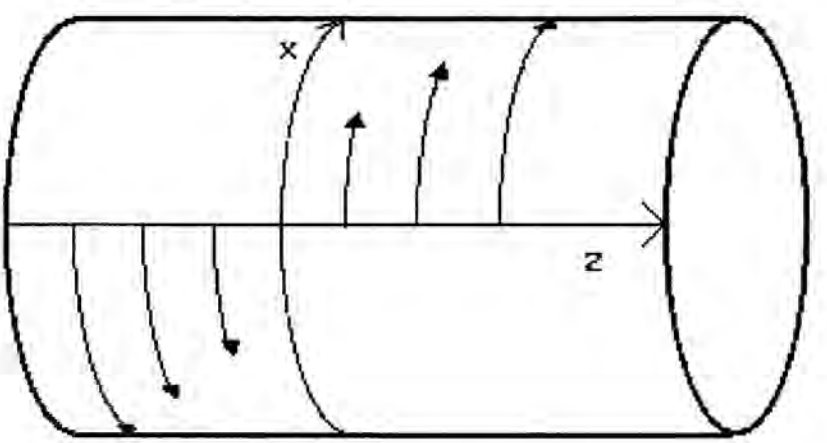

Fig. VI-13- Geometry of the shear flow on the surface of the cylinder used in the analytical calculations.

The flow situation and the coordinates used are presented in Fig. VI-13. We consider a cylinder parallel to the z-axis and take x to denote the coordinate along its circular cross section ($0 \le x < L$). The velocity field is given by $v_x = \alpha z$ and $v_z = 0$. To start, we show in Fig. VI-14 the time dependence of the reactants' concentration as it follows from numerical simulations. The simulations indeed display a short-time decay regime $c(t) \sim t^{-1/2}$ (I), an intermediate-time decay which goes as t^{-1} (II) and a $t^{-1/4}$ long-time behavior (III). The corresponding pattern evolution is depicted in Fig. VI-15 for one realization with the same simulation parameters of Fig. VI-14. As we proceed to show, these kinetic findings can be understood based on an analytical treatment.

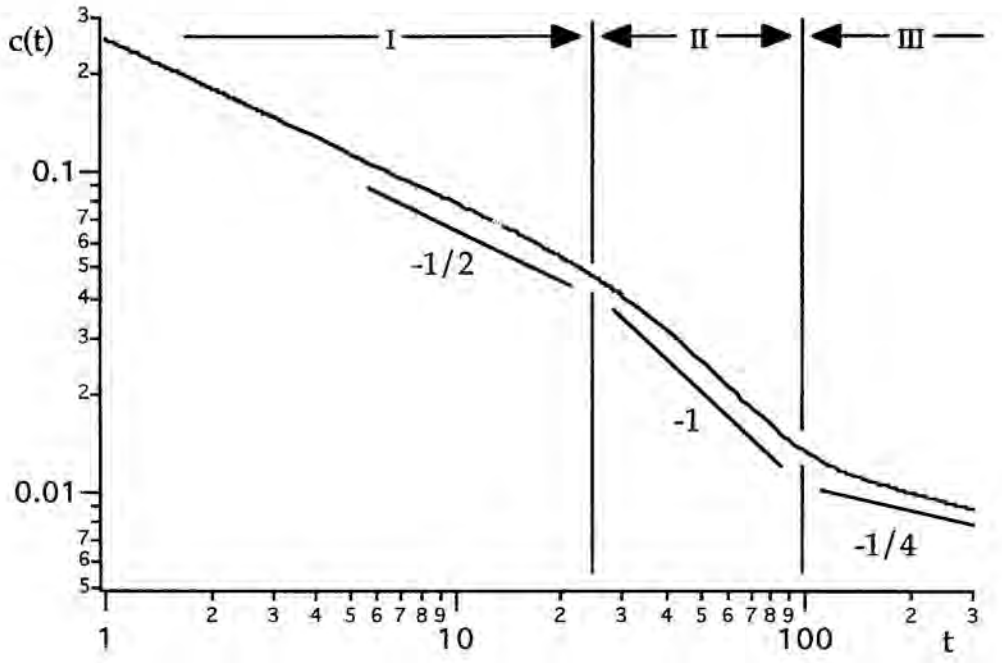

Fig. VI-14- Double-logarithmic plot of c(t) vs. t corresponding to the shear flow considered in Fig. VI-13 with α=0.32.

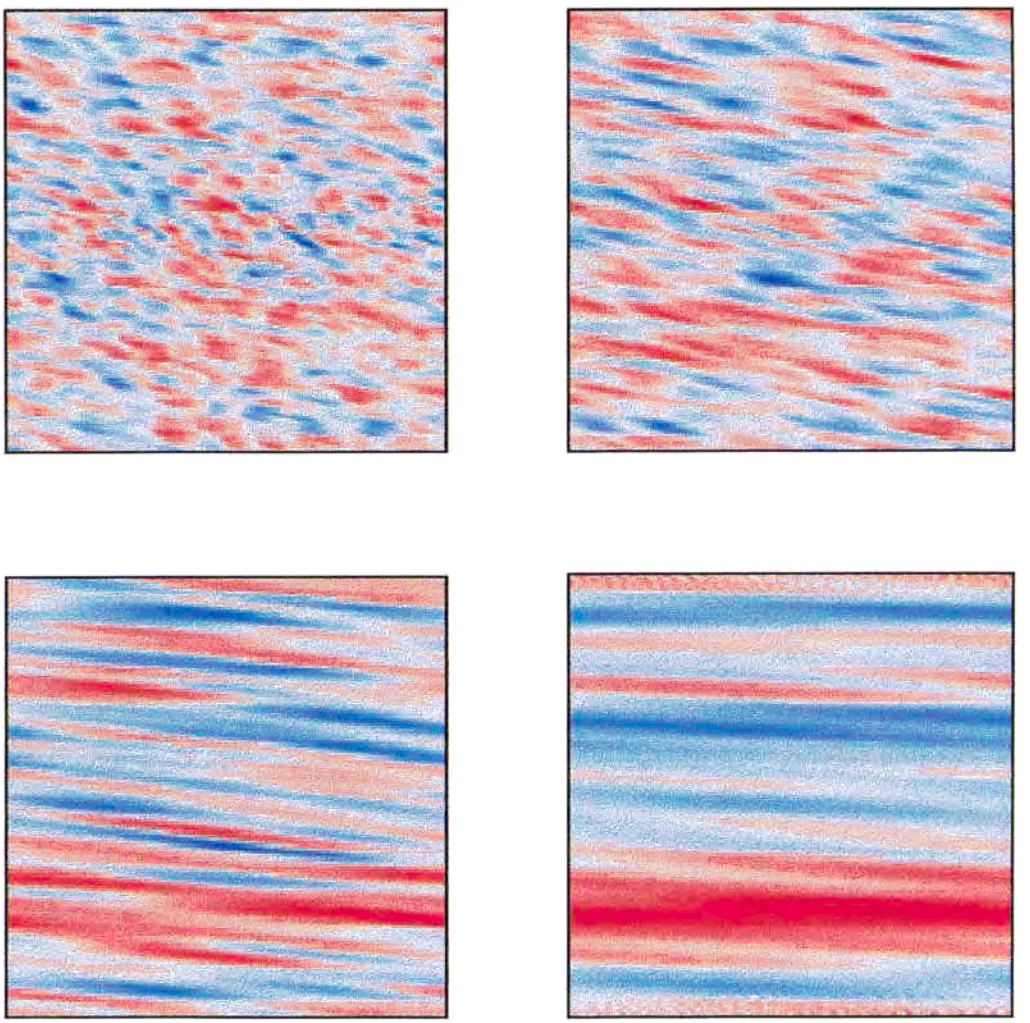

Fig. VI-15- Reactants picture of a system with shear flow corresponding to one realization of Fig. VI-14. Four times are displayed: a) t=10, b) t=30, c) t=100 and d) t=200.

The reaction-diffusion-advection system is modeled in terms of the mean-field reaction-diffusion equations, Eqs. (I-1) and (I-2), introducing the velocity field [Rei96b]. Then one has

$$\frac{\partial c_A(\vec{r},t)}{\partial t}+\vec{v}\cdot\vec{\nabla}c_A(\vec{r},t)=D\nabla^2 c_A(\vec{r},t)-Kc_A(\vec{r},t)c_B(\vec{r},t) \qquad \text{(VI–1)}$$

and

$$\frac{\partial c_B(\vec{r},t)}{\partial t}+\vec{v}\cdot\vec{\nabla}c_B(\vec{r},t)=D\nabla^2 c_B(\vec{r},t)-Kc_A(\vec{r},t)c_B(\vec{r},t) \qquad \text{(VI–2)}$$

where the drift term $\vec{v}\cdot\vec{\nabla}c$ describes the transport of reactants by an incompressible fluid whose velocity field is $\vec{v}$. Besides the restrictions of this scheme reported in Chapter I the addition of the drift term also supposes that the velocity does not change considerably on a cell length scale.

The analytical procedure will be more or less the same than what was used for the purely reaction-diffusion scheme. As we did in Section I-2, the semi-sum and semi-difference functions are introduced, obtaining

$$\frac{\partial q(\vec{r},t)}{\partial t}+\vec{v}\cdot\vec{\nabla}q(\vec{r},t)= D\nabla^2 q(\vec{r},t) \qquad \text{(VI–3)}$$

and

$$\frac{\partial s(\vec{r},t)}{\partial t}+\vec{v}\cdot\vec{\nabla}s(\vec{r},t)= D\nabla^2 s(\vec{r},t)-K(s^2(\vec{r},t)-q^2(\vec{r},t)) \qquad \text{(VI–4)}$$

Parallel to the analytical study developed in Section I-2 with Eqs. (I-3) and (I-4) we solve Eq. (VI-3) and approximate the spatial average of Eq. (VI-4) leading to

$$\frac{\partial\langle s(\vec{r},t)\rangle}{\partial t} = -K(\langle s^2(\vec{r},t)\rangle - \langle q^2(\vec{r},t)\rangle) \qquad \text{(VI–5)}$$

where $\nabla^2\langle s(\vec{r},t)\rangle = 0$ and $\langle \vec{v}\cdot\vec{\nabla}s(\vec{r},t)\rangle = 0$ since $\langle s(\vec{r},t)\rangle$ does not depend on $\vec{r}$. Therefore, for very fast reactions ($K\to\infty$), the solution of Eq. (VI-5) also holds locally $s(\vec{r},t) \approx |q(\vec{r},t)|$ and $c_A(t) = c_B(t) = \langle s(\vec{r},t)\rangle = \langle |q(\vec{r},t)| \rangle$ as in the non-advected stoichiometric systems.

The formal solution of Eq. (VI-3) for the $q(\vec{r},t)$ variable can be developed exactly as we did in Section I-2 (Eqs. (I-7) and (I-8)) and in Section II-1 for random initial distributions (Eq. (II-2)), but now the Green's function is not the solution of the simple diffusion equation (Eq. (I-9)). The Green's function for diffusion in a two-dimensional shear flow on a cylindrical surface can be built up from the corresponding function for an unbounded shear flow [Sok92b, Rei96b, Rei97a]. The last function can be obtained from Novikov's solution for dispersion under shear, see [Mon75] and references therein. This function is the solution of the equation

$$\frac{\partial G}{\partial t} + \partial z\,\frac{\partial G}{\partial x} = D\left(\frac{\partial^2 G}{\partial x^2} + \frac{\partial^2 G}{\partial z^2}\right) \qquad \text{(VI–6)}$$

under the initial condition $G(x,z,x_0,z_0,0) = \delta(x-x_0)\delta(z-z_0)$. This solution reads

$$G(x,z,x_0,z_0,t) = \frac{\sqrt{3}}{2\pi Dt\sqrt{\alpha^2t^2+12}} \times \exp\left\{-\frac{3\left[x-x_0-\frac{\alpha t}{2}(z+z_0)\right]^2}{Dt(\alpha^2t^2+12)} - \frac{(z-z_0)^2}{4Dt}\right\} \qquad \text{(VI–7)}$$

For the shear flow on a cylinder, the closed geometry in the x direction requires that the Green's function is periodic, i.e.,

$$G(x,z,x_0,z_0,t) = G(x+L,z,x_0,z_0,t) \qquad \text{(VI–8)}$$

The solution of Eq. (VI-6) which fulfills the boundary condition Eq. (VI-8) can be built from the solution in an infinite space using the standard 'reflection' procedure: one sums over functions with different values of the argument $x_{0,n} = x_0 + nL$. This results in

$$G(x,z,x_0,z_0,t) = \frac{\sqrt{3}}{2\pi Dt\sqrt{\alpha^2t^2+12}} \times \sum_{n=-\infty}^{\infty} \exp\left\{ -\frac{3\left[x-x_0+nL-\frac{\alpha t}{2}(z+z_0)\right]^2}{Dt(\alpha^2t^2+12)} - \frac{(z-z_0)^2}{4Dt} \right\} \qquad \text{(VI–9)}$$

We proceed now to the evaluation of Eq. (II-2). The integral in Eq. (II-2) is a convolution of three functions and can therefore be readily expressed in terms of Fourier transforms. Since G is periodic in x and is well defined for all real z values, its Fourier transform is

$$G(k_x,k_z,t) = \int_0^L dx \int_{-\infty}^{\infty} dz\, G(0,0,x,z,t) \exp(ik_x x + ik_z z) \qquad \text{(VI–10)}$$

where k_z is continuous and k_x is discrete, $k_x = (\pi n/L)$. The inverse transform then reads

$$G(0,0,x,z,t) = \frac{1}{\pi L} \sum_{n=-\infty}^{\infty} \int_{-\infty}^{\infty} dk_z e^{-i(\frac{\pi n x}{L} + k_z z)} G(\frac{\pi n x}{L}, k_z, t) \qquad \text{(VI–11)}$$

Substitution of Eq. (VI-11) into Eq. (II-2) gives then

$$\langle q^2(t)\rangle = \frac{c_0}{\pi L}\sum_{n=-\infty}^{\infty}\int_{-\infty}^{\infty} dk_z\, G^2(\frac{\pi n x}{L}, k_z, t) \qquad \text{(VI–12)}$$

The structure of the Green's function, Eq. (VI-7), is a two-variable Gaussian,

$$G(0,0,x_\alpha,x_\beta,t) = \frac{\sqrt{\det \mathbb{A}}}{2\pi}\exp\left(-\frac{1}{2}\sum_{i,j=\alpha,\beta} A_{ij}x_i x_j\right) \qquad \text{(VI–13)}$$

where the matrix $\mathbb{A}$ has the form

$$\mathbb{A} = \frac{1}{2Dt(1+\alpha^2t^2/12)}\begin{pmatrix} 1 & \alpha t/2 \\ \alpha t/2 & 1+\alpha^2t^2/3 \end{pmatrix} \qquad \text{(VI–14)}$$

The Fourier transform of $G(0,0,x_\alpha,x_\beta,t)$ is a Gaussian in $\vec{k}$

$$G(k_\alpha,k_\beta,t) = \exp\left(-\frac{1}{2}\sum_{i,j=\alpha,\beta}(A^{-1})_{ij}k_i k_j\right) \qquad \text{(VI–15)}$$

with $\mathbb{A}^{-1}$ denoting the inverse to $\mathbb{A}$. The integral in Eq. (VI-12) reads therefore

$$\langle q^2(t)\rangle = \frac{c_0}{\pi L}\sum_{k_x}\int_{-\infty}^{\infty} dk_z \exp\left(-\sum_{i,j=\alpha,\beta}(A^{-1})_{ij}k_i k_j\right) \qquad \text{(VI–16)}$$

with i,j being x or z and $k_x = (\pi n/L)$. The inversion of the matrix $\mathbb{A}$, Eq. (VI-14), gives

$$\mathbb{A}^{-1} = 2Dt\begin{pmatrix} 1+\alpha^2t^2/3 & -\alpha t/2 \\ -\alpha t/2 & 1 \end{pmatrix} \qquad \text{(VI–17)}$$

A further step is the integration over k_z in Eq. (VI-16), which leads to the

following expression for $\langle q^2(t)\rangle$:

$$\langle q^2(t)\rangle = \frac{c_0}{\pi L}\sqrt{\frac{\pi}{2Dt}}\sum_{n=-\infty}^{\infty}\exp\left(-2Dt(1+\alpha^2t^2/12)\frac{\pi^2}{L^2}n^2\right) \qquad \text{(VI-18)}$$

Even in the advected scheme, for very fast reactions, the Gaussian nature of the q variable can also be assumed and therefore Eq. (I-13) still holds here. This Eq. (I-13) allows us to obtain c(t) as a function of $\sigma(t) = \langle q^2(t)\rangle^{1/2}$. As we proceed to show based on Eq. (VI-18), $\sigma(t)$ displays under moderate mixing in large systems three different power laws: at first one has a $\sigma(t) \sim t^{-1/2}$ short-time behavior, which changes to $\sigma(t) \sim t^{-1}$ at intermediate times, followed by a much slower $\sigma(t) \sim t^{-1/4}$ pattern at long times. To establish this we analyze now carefully the behavior of Eq. (VI-18).

For small t one can replace the summation in Eq. (VI-18) by an integration, obtaining

$$\langle q^2(t)\rangle = c_0\frac{\sqrt{3}}{\pi Dt\sqrt{\alpha^2t^2+12}} \qquad \text{(VI-19)}$$

We note that Eq. (VI-19) is identical to the expression for reaction on an unbounded 2D-surface under shear flow [Sok92b]. For very short times ($\alpha^2t^2/12 \ll 1$) we hence find $\sigma(t) \sim t^{-1/2}$, i.e., the standard two-dimensional fluctuation-dominated kinetic pattern. In this time window corresponding to regime (I) of Fig.VI-1, the effects of mixing are not yet pronounced. The next stage starts when $\alpha^2t^2/12$ gets to be larger than unity. From Eq. (VI-19) we expect then $\sigma(t) \sim t^{-1}$ to hold. The concentration thus reproduces the classical t^{-1}-pattern, but now with an effective reaction rate which depends on the shear rate α (regime (II)). The crossover from the first to the second regime occurs for times around $t_{c1} \sim \alpha^{-1}$.

For very long times in Eq. (VI-18) only the term with n=0 in Eq. (VI-13) is relevant, so that $\langle q^2(t)\rangle$ goes as $\langle q^2(t)\rangle \sim t^{-1/2}$, from which $\sigma(t) \sim t^{-1/4}$ follows; this is the one-dimensional asymptotic form (regime (III)). The transition between the previous, $\sigma(t) \sim t^{-1}$ regime and the asymptotic one takes place when $2Dt(1+\alpha^2t^2/12)(\pi^2/L^2)$ gets to be comparable to unity, which, for large L, corresponds to a crossover time of the order of

$$t_{c2} \approx \left(\frac{6L^2}{\pi^2 D\alpha^2}\right)^{1/3}$$

For L large t_{c2} is much larger than t_{c1}. The qualitative explanation for this change of regime and for the magnitude of t_{c2} is as follows: during the time t the diffusion mixes the inhomogeneities in the z-direction up to the length scale $l_D \sim \sqrt{Dt}$. Full mixing in the x-direction can take place only if the fluid elements moving along two flow lines separated by a distance l_D have made during t at least one full revolution with respect to each other, so that inhomogeneities situated on different places of the flow lines can be only mixed by diffusion. This corresponds to the requirement that $(\partial v_x/\partial z)l_D t = \alpha l_D t \sim L$, from which $t_{c2} \sim (L^2/D\alpha^2)^{1/3}$ follows, i.e., a similar expression to the above. The formation of clusters along the closed flow lines is clearly observed looking at the pattern evolution in Figs. VI-15. From $\sigma(t)$ the time dependence of the concentrations c(t) follows; these mirror the findings of Fig. VI-14.

In a infinite system, for example inside one eddy of the eddy lattice considered in Section VI-1, an effective mixing in the z-direction, i.e. perpendicular to the flow lines, can take place only when the diffusion length in the direction perpendicular to the flow is of the order of $\Lambda = L/n$, the size of the eddy. In such systems an additional (third) crossover time

shows up, for which we have $t_{c3} \sim \Lambda^2/D$. Now the hierarchy of crossover times ($t_{c1}<t_{c2}<t_{c3}$) determines the reaction's behavior under mixing. The long-time stage, for $t>t_{c3}$ involves the diffusion between different eddies. For a fixed shear rate α and for a characteristic eddy size Λ one has $t_{c2} \sim (t_{c1}^2 t_{c3})^{1/3}$, so that if the system is not very small and if the mixing is not very slow a low-dimensional diffusion-controlled regime shows up.

CHAPTER VII

-Spatial Organization Under Turbulent Mixing-

In the last chapter we concentrated on two different advection mechanisms: the eddy-lattice and the stochastic turbulent flows. Both cases show an intermediate, rather than asymptotic, classical ($c \sim t^{-1}$) decay which is unavoidably followed by a segregation stage. In short what we are recognizing is the low efficiency of these two-dimensional mixing procedures. In Section VI-1 we reported that the formation of ring-clusters along the closed flow lines slowed down strongly the reaction rate and in Section VI-2 we observed that even the stochastic turbulent mixing showed at enough long times the fluctuation-dominated regime due to the clusterization process.

In the present chapter we concentrate on the reactants spatial organization under turbulent mixing flows during the different kinetic regimes [Rei97b]. The properties of the clusters and of the reaction zones are discussed and we focus on the interplay between the kinetic patterns and the spatial organization of the system. The key question to be analyzed here is whether the transient t^{-1} behavior is a signature of the homogenization of the system or contrarily if such a classical behavior might be compatible with some degree of spatial segregation. The results are compared to situations in the absence of mixing. For all the simulations that are shown in this chapter we fix L=300, $D_A=D_B=D=1$, $\Delta x=1$, $\Delta t=2.10^{-3}$ and $c_0=1$. The numerical results are obtained by averaging over five different initial Poisson distributions of reactants. Different K values are used. Moreover, for the simulations with turbulent flow we take the Kraichnan's spectrum with $\varepsilon=500$, $\lambda=2$ and $\nu=2$, that implies $u_0^2=1.243$, $l_0=1.7$ and $t_0=2$.

The kinetic regimes appearing in the course of the reactions were discussed in detail in Section VI-2, so that we limit ourselves here to a short overview. In Fig. VII-1 concentration decays are displayed both in presence and absence of stirring. In the first case it is worth noting that after a slow transient stage, in which the effects of mixing are not very pronounced, the system enters a mixing stage, whose duration is dictated by the correlation length of the flow. This stage is characterized by a concentration decay of the form $c \sim t^{-1}$, akin to the classical kinetic law. Following this stage the decay crosses over to a two-dimensional diffusion-controlled (fluctuation-dominated) situation, whose hallmark is a $c \sim t^{-1/2}$ power-law. In Fig. VII-1 it is also shown the behavior of the global semi-difference function $q(t) \equiv \langle\!| q(\vec{r},t) |\!\rangle/2$, which is independent of K. Four simulations are considered: two in the absence of mixing with K=0.5 and K=10, and the other two under turbulent mixing, again for K=0.5 and K=10. Note that in the case

of large K (K=10) the concentration decay follows closely q(t), whereas for K=0.5 the concentration decay deviates from q(t) for quite a while. Eventually the curves converge at very long times, but these times lay outside the range displayed in Fig. VII-1.

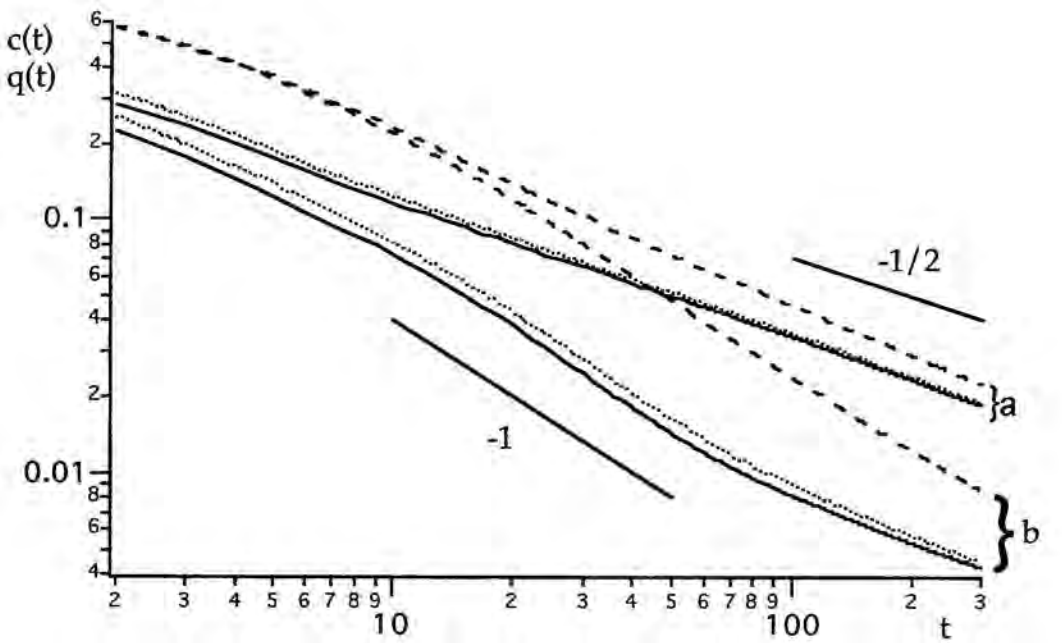

Fig. VII-1- Time dependence of the reactants' concentrations c(t) and comparison to q(t) (a) for the non-advected case and (b) under turbulent mixing. The dashed curves are for K=0.5, the dotted ones for K=10. The full curves display q(t).

The small difference between the c(t) and q(t) curves in the case with mixing and larger K (K=10) is a signature of that the system is segregated even though the kinetic behavior follows the classical $c \sim t^{-1}$ law. We will return to the discussion of these properties after analyzing the relation

between the reaction's efficiency and the spatial organization of the reactants. To do that we focus on two distinct functions, namely on the density-density correlations that are closely related to the effective reaction rate, and on the production-rate correlations that are connected to the geometry of the reaction zones.

SECTION VII-1 -Density-density Correlation Functions-

The two-point correlation functions of the concentrations are a probate means to highlight the segregation of the reactants; such functions were used for the non-stirred systems in Chapter III. These correlation functions were defined through:

$$C_{ij}(\mathbf{r}) = \frac{\langle c_i(\vec{r}'+\vec{r})c_j(\vec{r}')\rangle}{\langle c_i(\vec{r})\rangle\langle c_j(\vec{r})\rangle} \qquad \text{(VII–1)}$$

with j and i being A or B and where the averaging is taken over the volume of the system and over the orientations of the vector $\vec{r}$. Remember from Chapter III that the behavior of $C_{AB}(r)$ for small distances r shows in how far the spatial separation of the reactants is complete and allows to quantify it, while the behavior of $C_{AA}(r) = C_{BB}(r)$ measures the aggregation of similar reactants in clusters. In the presence of segregation one has for small r the relations $C_{AB}(r) < 1$ and $C_{AA}(r) = C_{BB}(r) > 1$; furthermore all these functions tend to unity as r grows. The characteristic length scale of the correlation functions (the scale on which they differ considerably from unity) is then an estimate for the cluster size. In Figs. VII-2a-c, density-density correlation functions as a function of time for different situations are displayed.

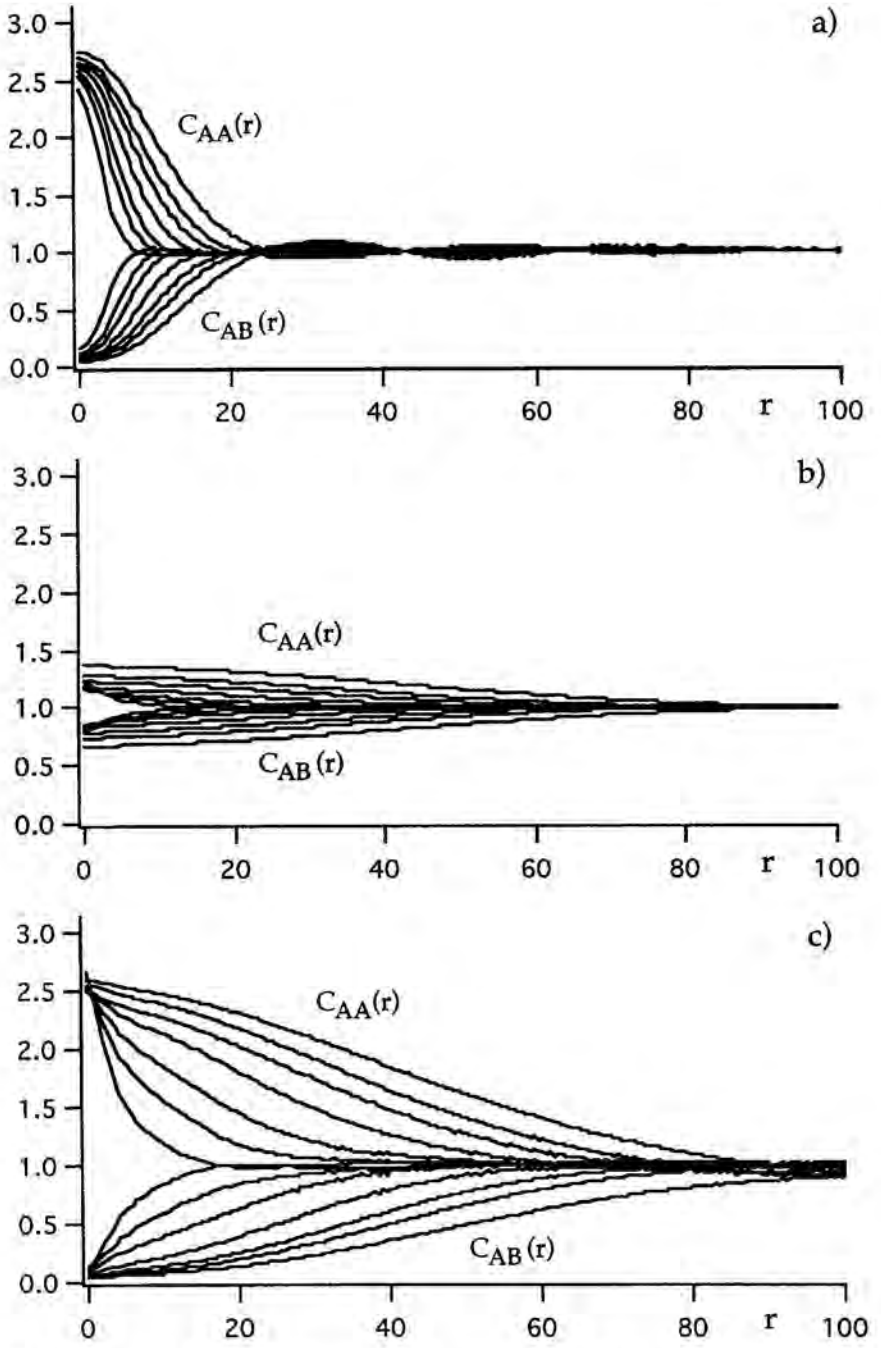

Fig. VII-2- (a) $C_{AB}(r,t)$ (lower curves) and $C_{AA}(r,t)$ (upper curves) for the nonadvected case and K=0.5 for t=20, 40, 60, 100, 150, 200 and 300 (from left to the right). (b) the same for the advected system, (c) same as in (b) but for K=10.

Just for the sake of comparison we plot in Fig. VII-2a the correlation functions of the concentrations corresponding to the non-advected system for a moderate reaction rate, K=0.5. Data for advected systems are plotted in Fig. VII-2b for K=0.5, and in Fig. VII-2c for K=10. For the nonadvected system one readily infers from the behavior of $C_{AB}(r)$ for small r that even at the shortest time presented the segregation is very strong. The behavior of the advected system is different: the segregation of the reactants is hampered by mixing and even destroyed for K=0.5, a fact which parallels the findings based on the difference between the c(t)- and q(t)-curves in Fig. VII-1. Nevertheless note that even here mixing does not insure the full homogeneity of the system. In fact segregation is restored by an increase of the local reaction rate K. Note that in Fig. VII-2c one observes strong segregation within the whole time range of simulations and that this range includes also a time window, where the concentrations decay in a nearly classical fashion, i.e. following the t^{-1} kinetics, a finding usually associated with very good mixing.

In the time window corresponding to a $c \sim t^{-1}$ behavior, i.e. where the empirical form $c^{-1}(t) = A+K^*t$ is fulfilled, we denote K^* as the effective reaction rate and evaluate it through a linear regression. This is the contents of Figure VII-3. In the case K=0.5, a value of $K^*=0.423$ is found for $20<t<150$, i.e. K^* is only 15% smaller than the local reaction rate K. Contrarily, in the case K=10 we find $K^*=1.247$ for $20<t<100$ so that K^* is now 8.3 times smaller than K. Thus the kinetics of the system is controlled by K when this local reaction rate is small or when mixing is intensive, while for large K or for moderate mixing the effective reaction rate K^* is strongly affected by the advection process. These findings parallel the situation under shear flow, considered analytically in detail in [Sok92b, How96], where the decay form

follows a $c(t) \sim (K^* t)^{-1}$ pattern, with an effective reaction rate K^* which depends strongly on the shear rate. Hence, for small K and/or at high flow intensities, the flow homogenizes the system to such an extent that the effective reaction rate K^* is controlled by the local reaction rate K. In the opposite case (large K and/or moderate flows) the mixing procedure is not able to prevent the reactants' segregation, so that the kinetics of the reaction, although nearly classical, depends strongly on the advection field. In this case we will talk about pseudo-classical kinetic behavior for advection-controlled reactions.

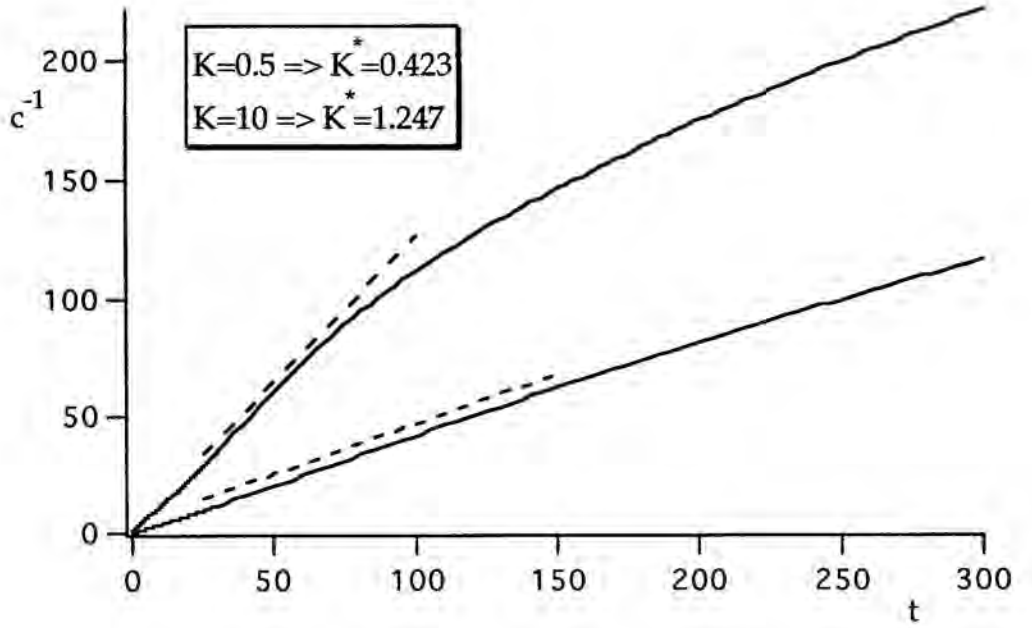

Fig. VII-3- c^{-1} vs. t plotted in the advected cases with K=10 and K=0.5. The linear regression within the classical $c \sim t^{-1}$ range gives good fitting results with K^*=0.423 for K=0.5 (K-controlled system) and K^*=1.247 for K=10 (advected-controlled).

We concentrate now on $C_{AB}(0)$, which is a characteristic measure of segregation [Rei97b]. This will allow us to focus on the relation between the slowing-down of the reaction and the segregation of the reactants. Let's consider a thermodynamically large system and calculate $\langle c_A(\vec{r})c_B(\vec{r})\rangle$. To do this one can start from the reaction-diffusion equation, Eq. (I-1) and integrate over the whole reaction volume. This leads to:

$$V\frac{dc_A(t)}{dt} = -K\int_V c_A(\vec{r},t)c_B(\vec{r},t)d\vec{r} \qquad \text{(VII–2)}$$

since the two terms containing the Laplacian and the gradient of the concentration vanish due to their mass-conserving nature. From Eq. (VII-2) it follows that under stoichiometrical conditions one has:

$$C_{AB}(0,t) = \frac{\langle c_A(\vec{r},t)c_B(\vec{r},t)\rangle}{c^2(t)} = -\frac{1}{kc^2(t)}\frac{dc(t)}{dt} \qquad \text{(VII–3)}$$

so that the value of $C_{AB}(0,t)$, which describes in how far segregation is locally (r=0) complete, is closely connected to the kinetics of the reaction. Moreover, noticing that $kc^2(t) = R_{class}$ is just the classical reaction rate for a stoichiometrical reaction, under well-mixed conditions, and that $R_{eff} = -dc(t)/dt$ is the effective reaction rate, as determined from the kinetic curve, one has $C_{AB}(0,t) = R_{eff}/R_{class}$; hence $C_{AB}(0,t)$ is a quantitative measure for the slowing down of the decay. We have verified numerically that Eq. (VII-3) holds well both for advected and for non-advected systems. In Fig. VII-4 we have plotted the values of $C_{AB}(0,t)$ as evaluated from the data of Fig. VII-2 (solid symbols) and those obtained from the kinetic curves via Eq. (VII-3). The agreement is evident. Note the nonmonotonous behaviour of $C_{AB}(0,t)$ for the advected case, showing that the effective reaction rate first grows and then starts to decay. In this case, during the the $c \sim t^{-1}$ time

window the value of $C_{AB}(0,t)$ does not decrease and even shows a small peak around t=50. This is due to the fact that at this time there exists an even faster than classical reaction kinetics but only as a very short and negligible transient regime.

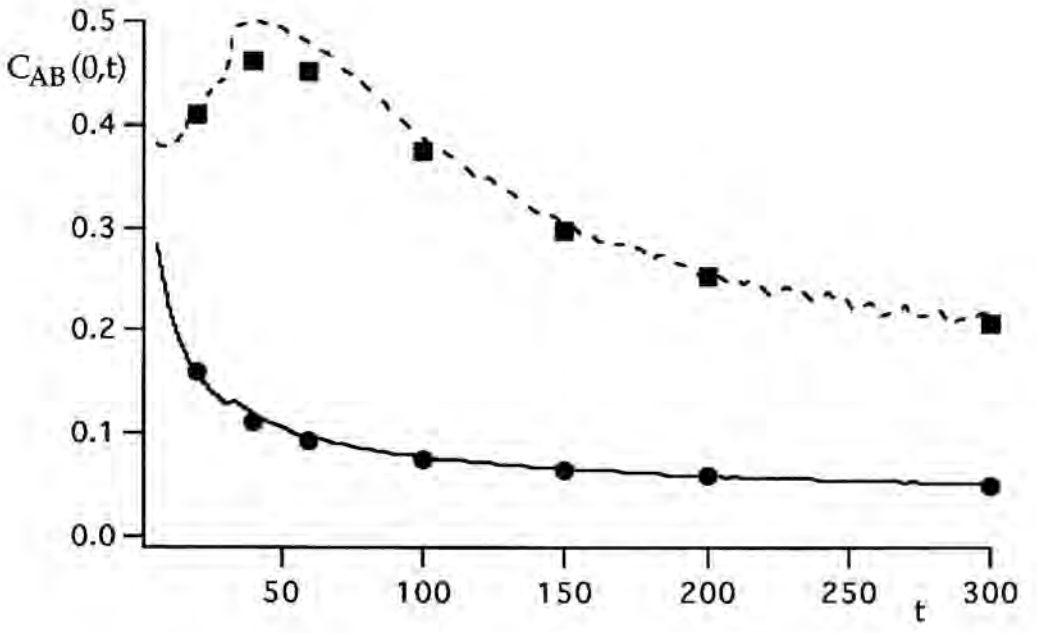

Fig. VII-4- The values for $C_{AB}(0,t)$ are shown for K=2 and t=20,40,60,100,150,200 and 300 corresponding to the advected (squares), and to the non-advected (circles) systems. For comparison the values for $C_{AB}(0,t) = R_{eff}/R_{class}$ obtained from Eq. (VII-3) are shown by the dashed line (advected) and by the full line (nonadvected) systems respectively.

SECTION VII-2 -Production-rate Correlation Functions-

As the next valuable instrument for the investigation of spatial structures in the A+B->0 reaction under mixing the quartic (production-rate) correlation functions [Rei97b] is considered here. The local reaction rate at a point $\vec{r}$ is $R(\vec{r},t) = Kc_A(\vec{r},t)c_B(\vec{r},t)$. The corresponding correlation function $\langle R(\vec{r_1},t)R(\vec{r_2},t)\rangle = K^2\langle c_A(\vec{r_1},t)c_B(\vec{r_1},t)c_A(\vec{r_2},t)c_B(\vec{r_2},t)\rangle$, contains information about the spatial organization of the reaction zones. Here we introduce

$$Q(r,t) = \frac{\langle R(\vec{r}',t)R(\vec{r}'+\vec{r},t)\rangle}{\langle R^2(\vec{r}',t)\rangle} = \frac{\langle c_A(\vec{r}',t)c_B(\vec{r}',t)c_A(\vec{r}'+\vec{r},t)c_B(\vec{r}'+\vec{r},t)\rangle}{\langle c_A^2(\vec{r},t)c_B^2(\vec{r},t)\rangle} \qquad \text{(VII–4)}$$

where the averaging should be understood in the same sense as in Eq. (VII-1). The correlation function Q is normalized in such a way that Q(0,t)=1. We display Q(r,t) at different times for K=2: in Fig. VII-5a we show the case without stirring and in Fig. VII-6a the case under synthetic turbulent flow. For all t the functions Q(r,t) have a peak at r=0; at larger distances Q(r,t) settles to a flat value. The width of the peak and the height of the flat part change with time. Figs. VII-5b and VII-6b show the same functions plotted vs. the scaled distance $r/t^{1/3}$. We turn now to the discussion of the physical meaning of the behavior of Q(r,t).

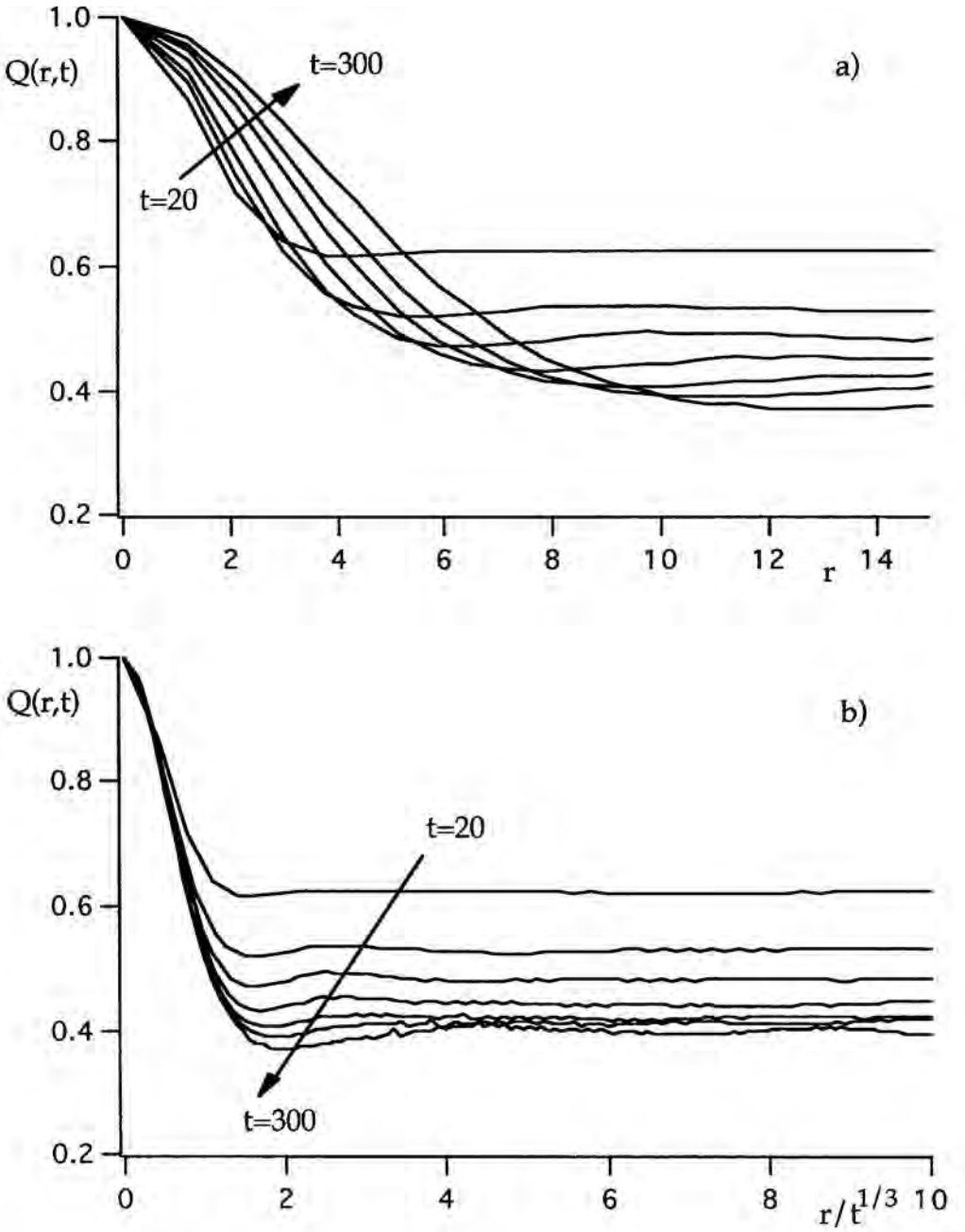

Fig. VII-5- a) Quartic correlation functions Q(r,t) for the non-advected system with K=2 at t=20,40,60,100,150,200 and 300. In (b) Q(r,t) is plotted vs. the rescaled distance $r/t^{1/3}$: Note that the initial peaks of the curves scale.

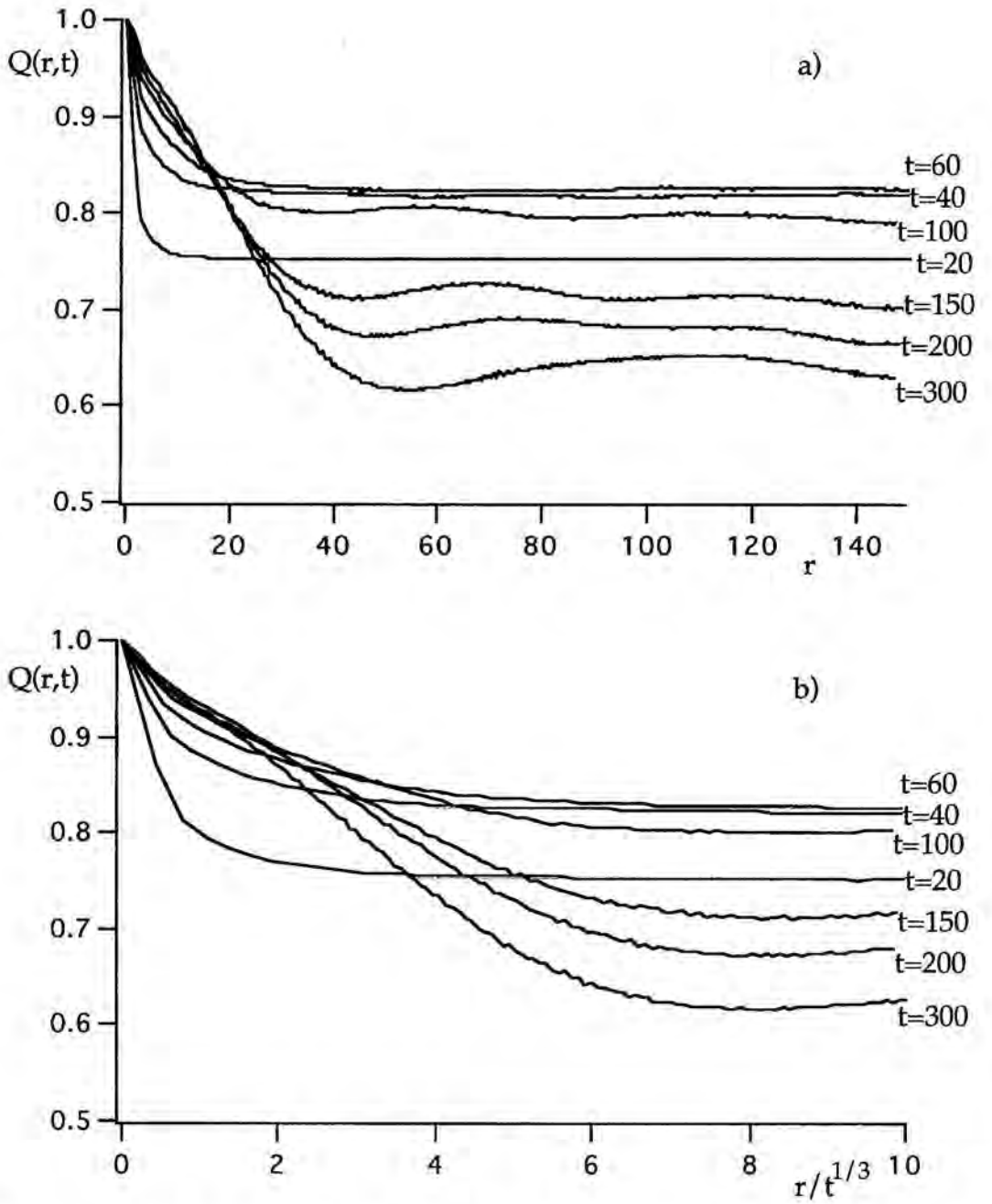

Fig. VII-6- Same as in Fig. VII-5, but now for the advected system. Note that in (b) the initial peaks do not scale at short times.

Suppose that the reaction zones, whose reaction rates are quite close in value, occupy a volume ω within the overall volume V of the system. In this case the denominator in Eq. (VII-4) is an average of a random variable which is equal to R^2 if $\vec{r} \in \omega$ and zero otherwise (as no reaction takes place outside of the reaction zones), so that $\langle R^2(\vec{r},t)\rangle = \frac{\omega}{V}R^2$. At the same time the numerator in Eq. (VII-4) is equal to R^2 if both points, $\vec{r}'$ and $\vec{r}'+\vec{r}$ belong to ω and zero otherwise. Therefore for $\vec{r}$ small the value of the numerator is $\frac{\omega}{V}R^2$, so that Q(r,t) is of the order of unity. In the opposite limit, for $r\to\infty$, when the probability that both $\vec{r}'$ and $\vec{r}'+\vec{r}$ belong to ω is clearly, $(\omega/V)^2$, the numerator's value is $\langle R(\vec{r}',t)R(\vec{r}'+\vec{r},t)\rangle = \left(\frac{\omega}{V}\right)^2 R^2$, so that the value of $Q(\infty,t)$ is proportional to ω/V, i.e. to the part of the system's volume occupied by reaction zones. The transition between these two values of Q, for small r and for large r, takes place when r is of the order of the reaction zone's width w, which gives us the characteristic width of the peak.

Let's compare now the advected and non-advected systems. We consider first the system without advection. The prediction in [Sok86] for systems described by continuum (mean-field like) equations is that the width of the reaction zone w scales as $w \sim t^{(d+2)/12}$, i.e. as $t^{1/3}$ in d=2. We show in Fig. VII-5b that this prediction is well-fulfilled, by plotting Q(r,t) as a function of the scaling variable $r/t^{1/3}$. Note in this respect the scaling of the initial peak. To explain the time-dependence of the height of the flat part of the function, we remember that the mean cluster's size $\Lambda \sim \sqrt{Dt}$ grows diffusively; the same is true for the mean cluster's perimeter $\mathcal{L}$. The mean number of clusters n per unit area of a 2D-system decays as $n = 1/\Lambda^2 \sim 1/t$. The part ω/V of the volume (area) of the system occupied by the reaction zones is then $\omega/V = n\mathcal{L}w \sim t^{-1/6}$. Therefore in d=2 and in the absence of stirring one has that the height of the reaction-rate correlation function

decreases monotonously as $Q \sim t^{-1/6}$. This finding is confirmed by the results of Fig. VII-7 where for K=2 the heights Q(∞,t), determined as the value of Q(r,t) at r=150, are displayed as a function of time in double logarithmic scales. In the case of a nonadvected system the corresponding points lay on a straight line. A linear regression leads to a slope of -0.165 with a good correlation coefficient. For the advected system this type of behavior can be seen only at long times (t>100), *vide infra*.

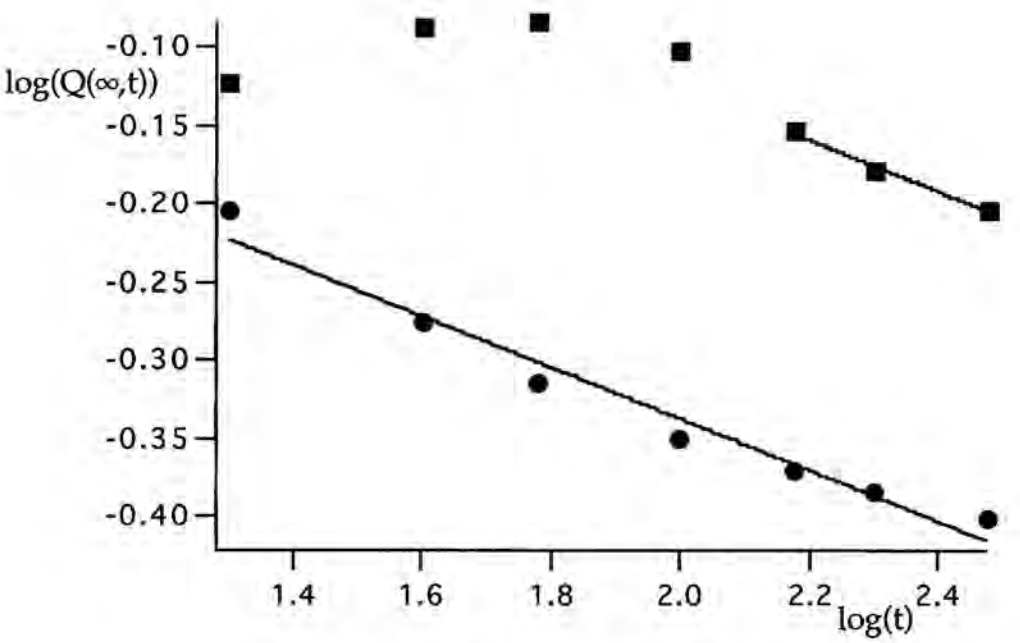

Fig. VII-7- Double logarithmic plot of Q(∞,t) vs. t for the advected (squares) and non-advected (circles) systems of Figs. 4 and 5. The straight lines have the slope 1/6.

The behavior of Q(r,t) for the advected system (Figs. VII-6) shows that the width of the reaction zones grows monotonically with time, while the value of Q(∞,t) shows a pronounced nonmonotonic behavior: it increases

until it attains its maximum, within the intermediate time domain corresponding to the $c \sim t^{-1}$ kinetic regime, and then starts to decay. Initially the reaction zones' width grows faster than $t^{1/3}$, while at longer times corresponding to the final fluctuation-dominated regime, the same $w \sim t^{1/3}$ behavior as in the non-advected case sets in. This last fact can be checked observing how the last three curves collapse if plotted against $r/t^{1/3}$ in Fig. VII-6b. The fast growth of the reaction zone's width within the $c \sim t^{-1}$ range more than compensates for the loss in perimeter of the clusters, so that the volume occupied by the reaction zones increases, leading to the observed behavior of $Q(\infty,t)$. This in turn, would explain the transient recovery of the classical kinetic law, $c \sim t^{-1}$. The growth of the reaction zone's width takes place until the width of the reaction zones gets to be of the order of the maximal mixing width in the flow; i.e. the length l_0 above which all the correlations in the flow velocities get lost, so that the behavior on larger scales is purely diffusive. After this stage the same behavior as in the case without stirring sets in, the only difference being that now rather than D, the effective diffusion coefficient D^* in the flow plays the dominant role. This can be seen from the fact that in the log-log representation of Fig. VII-7 at longer times the points for the advected system lay on a straight line which is parallel to the one obtained for the non-advected case, i.e. they also show a $Q \sim t^{-1/6}$ scaling behavior. Corresponding snapshots, showing the growth and then the shrinking of the part of the volume occupied by reaction zones are given for the advected system with K=2 in Fig. VII-8. In the first column, in spite of being in the time window corresponding to the $c \sim t^{-1}$ kinetic regime, segregation is clearly evident. Big differences can be observed during this time window with the non-advected systems on what respects to the reaction zones evolution. Comparing for example with Fig. 0b one observes that both cases show segregation but in the non-advected case the volume of the system occupied by the reaction zones does not grow, whereas it does in

the advected case. On the other hand, the patterns in the second column of Fig. VII-8 reflect a typical diffusion-controlled behavior characterized by the decrease of the reaction volume.

Turning to the discussion about K-controlled and advection-controlled reactions, the value of $Q(\infty,t)$ at times corresponding to the $c \sim t^{-1}$ kinetic time window can clarify some concepts. Our system allways will be somewhere in between these two estreme situations. For high values of $Q(\infty,t)$ (close to 1) we conclude that our system is almost homogenized and then very close to the K-controlled behavior, and therefore classical. As we reported before, this will be the case of small K and/or high flow intensities. In the other case (large K and/or moderate flows) the system will be advection-controlled, almost segregated (pseudo-classical behavior). Therefore the value of $Q(\infty,t)$ in this system during the $c \sim t^{-1}$ kinetic time window will be closer to 0 than in the other case.

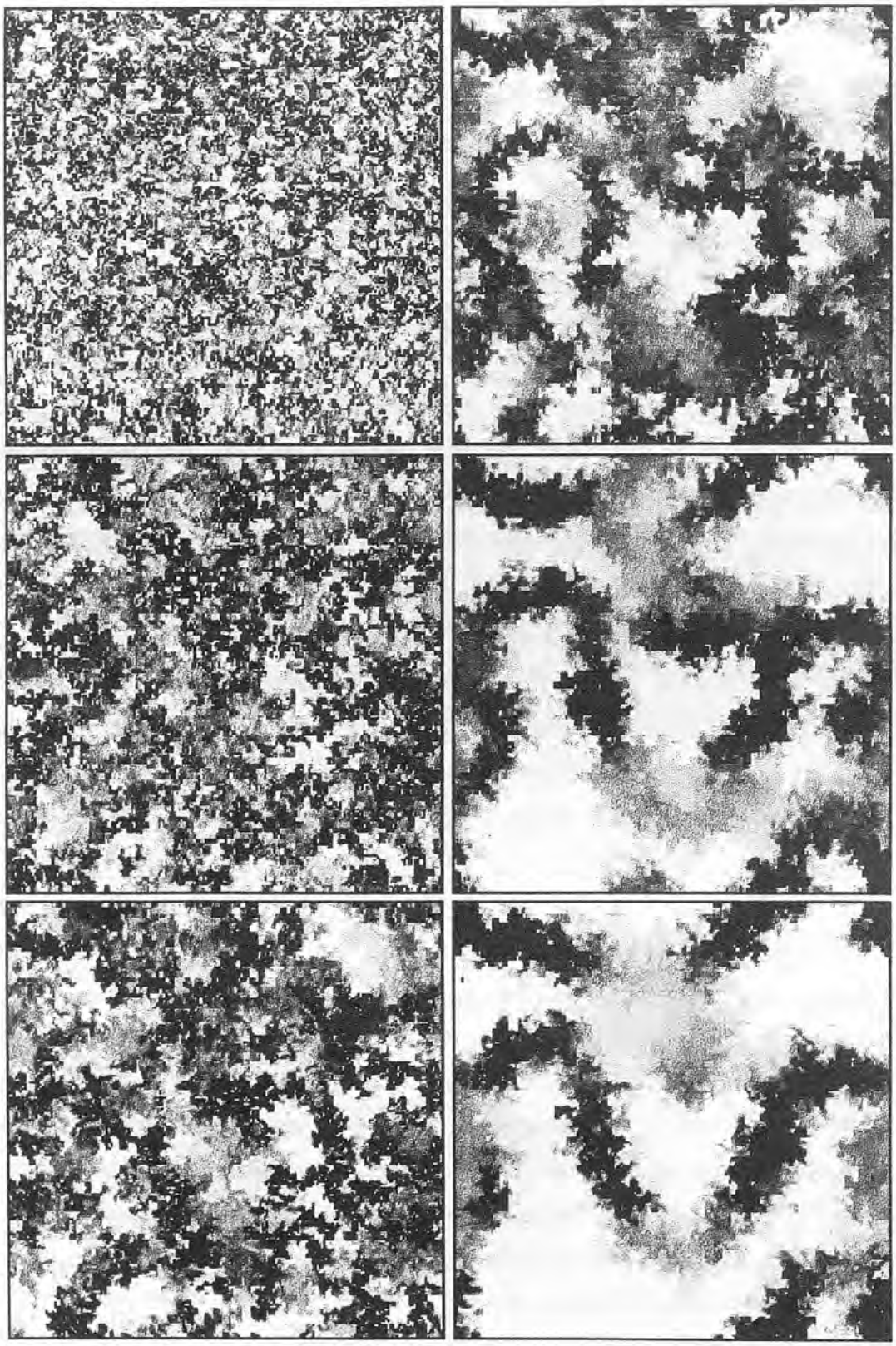

Fig. VII-8- Six snapshots of the structure of the reaction zones plotted for the advected system with K=2 at times t=20,40 and 60 (left column, from top to bottom) and t=100,200 and 300 (right column, from top to bottom).

CHAPTER VIII

-Conclusions-

In this Part II, the effect of mixing have been investigated on the A+B->0 kinetics taking place in two-dimensional spaces. Without mixing the kinetics of such reactions is dominated by fluctuations and shows at very long times a strongly nonclassical behavior, $c(t) \sim (Dt)^{-1/2}$. It is believed that mixing destroys the effect of fluctuations and restores classical kinetics. We have shown that this is not in general the case. Two mixing procedures were considered and introduced in Chapter V: the eddy-lattice flow and the turbulent flow.

In Chapter VI kinetic aspects are studied for both flows. For reactions in a random turbulent flow, we modeled the motion based on Kraichnan's energy spectrum. In this case three reaction stages occur: First a slow decay, followed by a fast intermediate stage controlled by mixing on small scales. The long-time regime is fluctuation controlled. The mixing stage interpolates between the short-time behavior governed by the diffusion coefficient D and the long-time behavior determined by an effective coefficient D^* due to the turbulent motion. In the case of a time-independent, eddy-lattice flow, the overall kinetics is much more complex, showing a very slow intermediate $t^{-1/4}$ behavior. This intermediate slowing down is due to the (closed) geometry of the flow lines in such a system. We clarified the peculiarities of reactions under closed-flow line mixing within the framework of an analytical model; we showed that reactions on a cylindrical surface under shear-flow lead to the same short- and intermediate-time behaviors as reactions under eddy-lattice flow mixing.

In Chapter VII we considered the A+B->0 reaction in the case of turbulent mixing paying special attention to the interplay of the segregation of reactants due to the reaction and to the medium's homogenization by the flow. The corresponding spatial structures were characterized by means of the density-density correlation functions $C_{AA}(r,t)$ and $C_{AB}(r,t)$ and the production-rate-production-rate correlation function $Q(r,t)$. Here $C_{AA}(r,t)$ and $C_{AB}(r,t)$ are related to the size of the clusters, and $C_{AB}(r,t)$ for $r=0$ is connected to the reaction's kinetics, and represents the relative slowing-down of the reaction compared to the classical, well-mixed case. The function $Q(r,t)$, on the other hand, highlights other aspects; its behavior at small distances represents the width of the reaction zones, while its value for r large gives the relative volume occupied by these zones. The analysis of these quantities under model turbulent mixing procedures shows the

possible coexistence of rather fast reactions with proceeding segregation and highlights the spatial organization of the system on different stages of reaction. The results presented in Chapter VII show that the effect of mixing on chemical reactions can be extremely involved, due to the complex interplay of segregation and homogenization, which take place on different length scales. Moreover we have shown that the intermediate t^{-1} behavior does not necessarily pinpoint the homogenization of the system; this is only the case for low local reaction rates K and vigorous flows where the system is controlled by the reaction process (K-controlled) and almost homogenized. For high values of K and moderate flows this classical-like kinetic behavior coexists with the presence, and even with an enhanced growth, of clusters; this is due to the fact that the fast growth of the width of the reaction zones compensates the growth of the clusters. In this case we say that the system is controlled by the advection process and that its kinetic behavior is pseudo-classical.

-BIBLIOGRAPHY-

[Ana87] L.W. Anacker and R. Kopleman. 'Steady-state chemical kinetics on fractals: segregation of reactants', Phys. Rev. Lett. **58**, 289 (1987).

[Anl84] J.K. Anlauf. 'Asymptotically exact solution of the one-dimensional trapping problem', Phys. Rev. Lett. **52**, 1845 (1984).

[Ara92] M. Araujo, S. Havlin, H. Larralde and H.E. Stanley. '"Random-force-dominated" reaction kinetics: reactants moving under random forces', Phys. Rev. Lett. **68**, 1791 (1992).

[Arg87] P. Argyrakis and R. Kopelman. 'Self-stirred vs. well-stirred reaction kinetics', J. Phys. Chem. **91**, 2699 (1987).

[Arg89] P. Argyrakis and R. Kopelman. 'Stirring in chemical reactions', J. Phys. Chem. **93**, 225 (1989).

[Arg93] P. Argyrakis, R. Kopelman and K. Lindenberg. 'Diffusion-limited binary reactions: the hierarchy of nonclassical regimes for random initial conditions', Chem. Phys. **177**, 693 (1993).

[Bal74] B.Ya. Balagurov and V.G. Vaks. 'Random walks of a particle on lattices with traps', Sov. Phys. JETP **38**, 968 (1974).

[Bat70] G.K. Batchelor, 'The theory of homogeneous turbulence'. Cambridge University, Cambridge, (1970).

[Blu86] A. Blumen, J. Klafter and G. Zumofen in 'Optical spectroscopy of glasses', pp. 199-265. Ed. by I. Zschokke (Reidel, Dordrecht, 1986).

[Blu91] A. Blumen, S. Luding and I.M. Sokolov. 'Fluctuation-dominated kinetics in the A+B->0 reaction between immobile particles', J. Stat. Phys. **65**, 849 (1991).

[Car93a] A. Careta, F. Sagues, L. Ramirez-Piscina and J.M. Sancho. 'Effective diffusion in a stochastic velocity field', J. Stat. Phys. **71**, 235 (1996).

[Car93b] A. Careta, F. Sagues and J.M. Sancho. 'Generation of homogeneous isotropic turbulence with well-defined spectra', Phys. Rev. E **48**, 2279 (1993).

[Car94] A. Careta, F. Sagues and J.M. Sancho. 'Diffusion of passive scalar under stochastic convection', Phys. Fluids **6**, 349 (1994).

[Car96] O. Cardoso, B. Gluckmann, O. Parcollet and P. Tabeling. 'Dispersion in a quasi-two-dimensional-turbulent flow: an experimental study', Phys. Fluids **8**, 209 (1996).

[Chi86] W.L. Chien, H. Rising and J.M. Ottino. 'Laminar mixing and chaotic mixing in several cavity-flows', J. Fluid Mech. **170**, 355 (1986).

[Cho94] a.J. Chorin. 'Vorticity and turbulence', Applied Mathematical Sciences v103, Ed. Springer-Verlag, NY (1994).

[Cle89] E. Clement, L.M. Sander and R. Kopelman. 'Steady-state diffusion-controlled A+B->0 reactions in two and three dimensions: rate laws and particle distributions', Phys. Rev. A **39**, 6466 (1989).

[Cle90] E. Clement, R. Kopelman and L.M. Sander. 'Bimolecular reaction A+B->0 at steady state on fractals: anomalous rate law and reactant self-organization', Chem. Phys. **146**, 343 (1990).

[Cri91] A. Crisanti, M. Falconi, G. Paladin and A. Vulpiani. 'Lagrangian chaos: transport, mixing and diffusion in fluids', Riv. Nuovo Cimento **14**, No. 12, 1 (1991).

[Don75] M.D. Donsker and S.R.S. Varadhan. 'Asymptotics for the wiener sausage', Commun. Pure and Appl. Math. **28**, 525 (1975).

[Ear93] G.D. Earle and M.C. Kelley. 'Spectral evidence for stirring scales and two-dimensional turbulence in the auroral inosphere', J. Geo. Res. **98**, 11543 (1993).

[Gar92] J. Garcia-Ojalvo, J.M. Sancho and L. Ramirez-Piscina. 'Generation of spatiotemporal colored noise', Phys. Rev. A **46**, 4670 (1992).

[Hof85] N.R.A. Hoffman and D.P. McKenzie. 'The destruction of geochemical heterogeneities by differential fluid motions during mantle convection', Geophys. J. R. Astr. Soc. **82**, 163 (1985).

[Hoo74] G. t'Hooft. 'Magnetic monopoles in unified Gauge theories', Nucl. Phys. B **79**, 276 (1974).

[How96] M.J. Howard and G.T. Barkema. 'Shear flows and segregation in the reaction A+B->0', Phys. Rev. E **53**, 5949 (1996).

[Hva80] J.M. Hvam and M.H. Brodsky. 'Dispersive transport and recombination lifetime in Phosphorus-doped hydrogenated amorphous silicon', Phys. Rev. Lett. **46**, 371 (1980).

[Isi92] M.B. Isichenko. 'Percolation, statistical topography, and transport in random media', Rev. Mod. Phys. **64**, 961 (1992).

[Isp95] I. Ispolatov, P.L. Krapivsky and S. Redner. 'Kinetics of A+B->0 with driven diffusive motion', Phys. Rev. E **52**, 2540 (1995).

[Jan95a] S.A. Janowsky. 'Asymptotic behavior of A+B->inert for particles with drift', Phys. Rev. E **51**, 1858 (1995).

[Jan95b] S.A. Janowsky. 'Spatial organization in the reaction A+B->(inert) for particles with drift', Phys. Rev. E **52**, 2535 (1995).

[Kan84] K. Kang and S. Redner. 'Scaling approach for the kinetics of recombination processes', Phys. Rev. Lett. **52**, 955 (1984).

[Kan85] K. Kang and S. Redner. 'Fluctuation-dominated kinetics in diffusion-controlled reaction', Phys. Rev. A **32**, 435 (1985).

[Kir82] P.B. Kirby, W. Paul, S. Ray and J. Tauc. 'Comparison of the dispersion parameters from time-of-flight and photo-induced midgap absorption measurements on sputtered a-Si:H', Solid State Commun. **42**, 533 (1982).

[Kla96] J. Klafter, M.F. Shlesinger and G. Zumofen. 'Beyond brownian motion', Physics Today (Feb. 1996), 33.

[Kly82] P.W. Klymko and R. Kopelman. 'Heterogeneous exciton kinetics: triplet naphthalene homofusion in an isotopic mixed crystal', J. Phys. Chem. **86**, 3686 (1982).

[Kra70] R.H. Kraichnan. 'Diffusion by a random velocity field', Phys. Fluids **13**, 22 (1970).

[Kop86] R. Kopelman. 'Rate processes on fractals: theory, simulations, and experiments', J. Stat. Phys. **42**, 185 (1986).

[Kop88a] R. Kopelman, S.J. Parus and J. Prasad. 'Exciton reactions in ultrathin molecular wires, filaments and pores: a case study of kinetics and self-ordering in low dimensions', Chem. Phys. **128**, 209 (1988).

[Kop88b] R. Kopelman. 'Fractal reaction kinetics', Science **241**, 1620 (1988).

[Kot96] E. Kotomin and V. Kuzovkov. 'Modern aspects of diffusion-controlled reactions. Cooperative phenomena in bimolecular processes'. Comprehensive Chemical Kinetics, Vol. 34. Ed. Elsevier (1996).

[Kuz84] V. Kuzovkov and E. Kotomin. 'Many-particle effects in accumulation kinetics of Frenkel defects in crystals', J. Phys. C **17**, 2283 (1984).

[Kuz88] V. Kuzovkov and E. Kotomin. 'Kinetics of bimolecular reactions in condensed media: critical phenomena and microscopic self-organisation', Rep. Progr. Phys. **51**, 1479 (1988).

[Lam96] D.J. Lamberto, F.J. Muzzio, P.D. Swanson and A.L. Tonkovich. 'Using time-dependent RPM to enhance mixing in stirred vessels', Chem. Eng. Sci. **51**, 733 (1996).

[Leo89] C.W. Leong and J.M. Ottino. 'Experiments on mixing due to chaotic advection in a cavity', J. Fluid Mech. **209**, 463 (1989).

[Ley91] F. Leyvraz and S. Redner. 'Spatial organization in the two-species annihilation reaction A+B->0', Phys. Rev. Lett. **66**, 2168 (1991).

[Ley92] F. Leyvraz and S. Redner. 'Spatial structure in diffusion-limited two-species annihilation', Phys. Rev. A **46**, 3132 (1992).

[Lin88] K. Lindenberg, B.J. West and R. Kopelman. 'Steady-state segregation in diffusion-limited reactions', Phys. Rev. Lett. **60**, 1777 (1988).

[Lin91] K. Lindenberg, W.S. Sheu and R. Kopelman. 'Scaling properties of diffusion-limited reactions on fractal and euclidean geometries', J. Stat. Phys. **65**, 1269 (1991).

[Low87] A.M. Loward. 'Fast dynamo action in a steady flow', J. Fluid. Mech. **180**, 267 (1987).

[Mac80] E.O. Macagno and J.A. Cristensen. 'Intestinal flow analysis using finite elements', Rev. Fluid Mech. **12**, 139 (1980).

[Mar97] A.C. Marti, J.M. Sancho, F. Sagues and A. Careta, 'Langevin approach to generate synthetic turbulent flows', Phys. Fluids **9**, 1078 (1997).

[McK83] D.P. McKenzie. 'The earth's mantle', Sci. Am. **249**, 50 (1983).

[Mof83] H.K. Moffatt. 'Transport effects associated with turbulence with particular attention to the influence of helicity', Rep. Prog. Phys. **46**, 621 (1983).

[Mon75] A.S. Monin and A.M. Yaglom. 'Statistical Fluids Mechanics', MIT Press, Cambridge, MA, (1975).

[Mor80] J. Mort, I. Chen, A. Troup, M. Morgan, J. Knights and R. Lujan. 'Nongeminate recombination of a-Si:H', Phys. Rev. Lett. **45**, 1348 (1980).

[Muz89a] F.J. Muzzio and J.M. Ottino. 'Evolution of a lamellar system with diffusion and reaction: a scaling approach', Phys. Rev. Lett. **63**, 47 (1989).

[Muz89b] F.J. Muzzio and J.M. Ottino. 'Dynamics of a lamellar system with diffusion and reaction: scaling analysis and global kinetics', Phys. Rev. A **40**, 7182 (1989).

[Muz91] F.J. Muzzio, P.D. Swanson and J.M. Ottino. 'The statistics of stretching and stirring in chaotic flows', Phys. Fluids A **3**, 822 (1991).

[Muz92] F.J. Muzzio, C. Meneveau, P.D. Swanson and J.M. Ottino. 'Scaling amd multifractal properties of mixing in chaotic flows', Phys. Fluids A **4**, 1439 (1992).

[Ore81] J. Orenstein and M. Kastner. 'Photocurrent transient spectroscopy: measurement of the density of localized states in a-As2Se3', Phys. Rev. Lett. **46**, 1421 (1981).

[Osh94] G. Oshanin, M. Moreau and S. Burlatsky. 'Models of chemical reactions with participation of polymers', Advances in Colloid and Interface Science **49**, 1 (1994).

[Ott88] J.M. Ottino, C.W. Leong, H. Rising and P.D. Swanson. 'Morphological structures produced by mixing in chaotic flows', Nature **333**, 419 (1988).

[Ott89] J.M. Ottino. 'The kinematic of mixing: stretching, chaos and transport'. Cambridge University Press, Cambridge (1989).

[Ott92] J.M. Ottino, F.J. Muzzio, M. Tjahjadi, J.G. Franjione, S.C. Jana and H.A. Kusch. 'Chaos, symmetry, and self-similarity: exploiting order and disorder in mixing processes', Science **257**, 754 (1992).

[Ovc78] A.A. Ovchinnikov and Ya.B. Zeldovich. 'Role of density fluctuations in bimolecular reaction kinetics', Chem. Phys. **28**, 215 (1978).

[Pre79] J.P. Preskill. 'Cosmological production of superheavy magnetic monopoles', Phys. Rev. Lett. **43**, 1365 (1979).

[Pri97] V. Privman. 'Non-equilibrium statistical mechanics in one dimension', Chapter I by R. Kopelman and A.L. Lin. Cambridge University Press, Cambridge (1997).

[Pol74] A.M. Polyakov. 'Nonhamiltonian approach to conformal quantum field theory', JETP Lett. **20**, 430 (1974).

[Ram90] R. Ramshankar, D. Berlin and J.P. Gollub. 'Transport by capillary waves. Part I. Particle trajectories', Phys. Fluids A **2**, 1955 (1990).

[Ram91] R. Ramshankar and J.P. Gollub. 'Transport by capillary waves. Part II. Scalar dispersion and structure of the concentration field', Phys. Fluids A **3**, 1344 (1991).

[Rei96a] R. Reigada, F. Sagues, I.M. Sokolov, J.M. Sancho and A. Blumen. 'Spatial correlations and cross sections of clusters in the A+B->0 reaction', Phys. Rev. E **53**, 3167 (1996).

[Rei96b] R. Reigada, F. Sagues, I.M. Sokolov, J.M. Sancho and A. Blumen. 'Kinetics of the A+B->0 reaction under steady and turbulent flows', J. Chem. Phys. **105**, 10925 (1996).

[Rei97a] R. Reigada, F. Sagues, I.M. Sokolov, J.M. Sancho and A. Blumen. 'Fluctuation-dominated kinetics under stirring', Phys. Rev. Lett. **78**, 741 (1997).

[Rei97b] R. Reigada, F. Sagues, I.M. Sokolov, J.M. Sancho and A. Blumen. 'Spatial organization in the A+B->0 reaction under confined-scale mixing', J. Chem. Phys. **107**, 843 (1997).

[Rey1894] O. Reynolds. Nature **50**, 161 (1894).

[Rhi83] P.B.A. Rhines. 'How rapidly is a passive scalar mixed within closed streamlines', Rev. Fluid. Mech. **18**, 433 (1983).

[Ric85] S.A. Rice. 'Diffusion-limited reactions' Comprehensive Chemical Kinetics, Vol. 25. Ed. Elsevier (1985).

[San96] J.M. Sancho, A.H. Romero, K. Lindenberg, F. Sagues, R. Reigada and A.M. Lacasta. 'A+B->0 reaction with different initial patterns', J. Phys. Chem. **100**, 19066 (1996).

[Sch90] H. Schnorer, I.M. Sokolov and A. Blumen. 'Fluctuation statistics in the diffusion-limited A+B->0 reaction', Phys. Rev. A **42**, 7075 (1990).

[Shl87] M.F. Shlesinger, B.J. West and J. Klafter. 'Levy dynamics of enhanced diffusion: application to turbulence', Phys. Rev. Lett. **58**, 1100 (1987).

[Shr87] B.I. Shraiman. 'Diffusive transport in a Rayleigh-Benard convection cell', Phys. Rev. A **36**, 261 (1987).

[Smi85] G.D. Smith. 'Numerical solution of partial differential equations', Clarendon Press, Oxford (1985).

[Smo17] M. Smoluchowski. 'Mathematical theory of the kinetics of the coagulation of colloidal solutions', Z. Phys. Chem. **92**, 129 (1917).

[Sok86] I.M. Sokolov. 'Spatial and temporal asymptotic behavior of annihilation reactions', JETP Lett. **44**, 67 (1986).

[Sok88] I.M. Sokolov. 'Stochastic aggregation and subsequent recombination of particles generated by pulsed excitation in fractal and homogeneous systems', Sov. Phys. JETP **67**, 1846 (1988).

[Sok89a] I.M. Sokolov. 'Steady-state chemical reaction on fractal', Phys. Lett. A **139**, 403 (1989).

[Sok89b] I.M. Sokolov. 'Kinetics of the accumulation and recombination of excitations in fractal systems', Sov. Phys. Dokl. **34**, 229 (1989).

[Sok91a] I.M. Sokolov and A. Blumen. 'Mixing in reaction-diffusion problems', Int. J. Mod. Phys. B **5**, 3127 (1991).

[Sok91b] I.M. Sokolov and A. Blumen. 'Reactions in systems with mixing', J. Phys. A **24**, 3687 (1991).

[Sok91c] I.M. Sokolov and A. Blumen. 'Mixing effects in the A+B->0 reaction-diffusion scheme', Phys. Rev. Lett. **66**, 1942 (1991).

[Sok91d] I.M. Sokolov and A. Blumen. 'Diffusion-controlled reactions in lamellar systems', Phys. Rev. A **43**, 2714 (1991).

[Sok91e] I.M. Sokolov and A. Blumen. 'Distribution of striation thicknesses in reacting lamellar systems', Phys. Rev. A **43**, 6545 (1991).

[Sok91f] I.M. Sokolov, H. Schnorer and A. Blumen. 'Diffusion-controlled reaction A+B->0 in one dimension: the role of particle mobilities and the diffusion-equation approach', Phys. Rev. A **44**, 2388 (1991).

[Sok91g] I.M. Sokolov, H. Schnorer and A. Blumen. 'Diffusion-controlled reaction A+B->0 on Peano curves', Phys. Rev. A **43**, 5698 (1991).

[Sok92a] I.M. Sokolov and A. Blumen. 'Diffusion-controlled reactions in nonstoichiometrical layered systems', Physica A **191**, 177 (1992).

[Sok92b] I.M. Sokolov and A. Blumen. 'Suppression of fluctuation-dominated kinetics by mixing' in S.M Aharony, ed. "Synthesis, characterization, and theory of polymeric networks and gels" pp. 53-65, Plenum Press, NY (1992).

[Sok93a] I.M. Sokolov and A. Blumen. 'Kinetic aspects of interacting reacting species', Europhys. Lett. **21**, 885 (1993).

[Sok93b] I.M. Sokolov and A. Blumen. 'Bimolecular reactions between passively transported species', Phys. Lett. A **178**, 364 (1993).

[Sok93c] I.M. Sokolov, P. Argyrakis and A. Blumen. 'Kinetic roughening and interacting reacting species: nonlinear aspects'. Fractals **1**, 470 (1993).

[Sok94a] I.M. Sokolov and A. Blumen. 'Memory effects in diffusion-controlled reactions', Europhys. Lett. **27**, 495 (1994).

[Sok94b] I.M. Sokolov, P. Argyrakis and A. Blumen. 'The A+B->0 reaction under short-range interactions', J. Phys. Chem. **98**, 7256 (1994).

[Sok94c] I.M. Sokolov and A. Blumen. 'Kinetics in coagulation-annihilation processes', Phys. Rev. E **50**, 2335 (1994).

[Sok96] I.M. Sokolov, R. Reigada, F. Sagues, J.M. Sancho and A. Blumen. 'Fluctuation-dominated kinetics under regular and turbulent flows' for CFIC96 Rome conference book (in press).

[Swa90] P.D. Swanson and J.M. Ottino. 'A comparative computational and experimental study of chaotic mixing of viscous fluids', J. Fluid Mech. **213**, 227 (1990).

[Tab91] P. Tabeling, S. Burkhart, O. Cardoso and H. Willaime. 'Experimental study of freely decaying two-dimensional turbulence', Phys. Rev. Lett. **67**, 3772 (1991).

[Tak70] F. Takens. 'Hamiltonian systems: generic properties of closed orbits and local perturbations', Math. Ann. **188**, 304 (1970).

[Tou83] D. Toussaint and F. Wilczek. 'Particle-antiparticle annihilation in diffusive motion', J. Chem. Phys. **78**, 2642 (1983).

[Var80] Z. Vardeny, P. O'Connor, S. Ray and J. Tauc. 'Optical studies of excess carrier recombination in A-Si:H: evidence for dispersive diffusion', Phys. Rev. Lett. **44**, 1267 (1980).

[Vic92] T. Vicsek. 'Fractal growth phenomena'. World Scientific, Singapore (1992).

[Vit88] A.G. Vitukhnovsky, B.L. Pyttel and I.M. Sokolov. 'Cluster formation in the reaction A+B=0: theory and computer simulations', Phys. Lett. A **128**, 161 (1988).

[Zel78] Y.A. Zeldovich and M.A. Khlopov. 'On the concentration of relic magnetic monopoles in the universe', Phys. Lett. B **79**, 239 (1978).

[Zum85] G. Zumofen, A. Blumen and J. Klafter. 'Concentration fluctuations in reaction kinetics', J. Chem. Phys. **82**, 3198 (1985).

[Zum91] G. Zumofen, J. Klafter and A. Blumen. 'Stochastic and deterministic analysis of reactions: the fractal case', Phys. Rev. A **44**, 8390 (1991).

[Zum93] G. Zumofen and J. Klafter. 'Scale-invariant motion in intermitent chaotic systems', Phys. Rev. E **47**, 851 (1993).

[Zum94] G. Zumofen and J. Klafter. 'Reaction dynamics controlled by enhanced diffusion', Phys. Rev. E **50**, 5119 (1994).

[Zum96a] G. Zumofen, J. Klafter and M.F. Shlesinger. 'Reactions controlled by enhanced diffusion: deterministic and stochastic approaches', Chem. Phys. **212**, 819 (1996).

[Zum96b] G. Zumofen, J. Klafter and M.F. Shlesinger. 'Breakdown of the Ovchinnikov-Zeldovich segregation in the A+B->0 reaction under Levy mixing', Phys. Rev. Lett. **77**, 2830 (1996).